LUNG INFLAMMATION ASSOCIATED WITH ACUTE NECROTIZING PANCREATITIS IN DOGS AND MICE

A Thesis Submitted to the College of Graduate Studies and Research

in Partial Fulfillment of the Requirements for the Degree of Master of Science

in the Department of Veterinary Biomedical Sciences

University of Saskatchewan

Saskatoon

By

VANESSA VROLYK

PERMISSION TO USE

In presenting this thesis in partial fulfillment of the requirements for a Postgraduate degree from the University of Saskatchewan, I agree that the Libraries of this University may make it freely available for inspection. I further agree that permission for copying of this thesis in any manner, in whole or in part, for scholarly purposes may be granted by the professor or professors who supervised my thesis work or, in their absence, by the Head of the Department or the Dean of the College in which my thesis work was done. It is understood that any copying or publication or use of this thesis or parts thereof for financial gain shall not be allowed without my written permission. It is also understood that due recognition shall be given to me and to the University of Saskatchewan in any scholarly use which may be made of any material in my thesis.

Requests for permission to copy or to make other use of material in this thesis in whole or part should be addressed to:

Head of the Department of Veterinary Biomedical Sciences,

Western College of Veterinary Medicine, University of Saskatchewan,

52 Campus Drive, Saskatoon, Saskatchewan S7N 5B4

ABSTRACT

Acute necrotizing pancreatitis (ANP) is a common gastrointestinal cause of emergency admissions in dogs and humans and can lead to a systemic inflammatory response syndrome resulting in multiple organ dysfunction syndrome. Among the various complications associated with ANP, acute lung injury (ALI) or its more severe form, acute respiratory distress syndrome (ARDS), are major contributors leading to high mortality rates associated with severe acute pancreatitis (AP) in human patients. The incidence of ALI/ARDS in ANP dogs is not well characterized. However, signs of respiratory complications have been reported clinically in dogs suffering from AP. The pathophysiology of ANP and its systemic complications in dogs and humans are not well understood. Most of the data related to AP comes from rodent models of AP, which may not always represent the true mechanisms occurring in the lungs of dogs or humans with ANP.

I decided to undertake evaluation of pancreas and lungs from dogs (N=21) that died of ANP. The cases were selected through the search of the medical records of the Veterinary Medical Center of the Western College of Veterinary Medicine (WCVM). Six healthy SPCA dogs were used as controls. The histology of pancreas was first graded to record the range of ANP severities within dog cases included in this study. Then, characterization of lung inflammation was done with histological grading and qualitative analysis of immunohistochemical staining for von Willebrand Factor (vWF), Toll-Like Receptor-4 (TLR4), interleukin-6 (IL6), and inducible nitric oxide synthase (iNOS). Quantification of the recruitment of septal macrophages in the lungs, designated as pulmonary intravascular macrophages

(PIMs), in ANP dogs was achieved by counting the number of positive cells in alveolar septa using a macrophage antibody (MAC387). The results revealed that dogs suffering from ANP have variable lung inflammation, which was characterized by a significant infiltration of mononuclear phagocyte cells in the alveolar septa of all ANP dogs (median, 138; range 31-935) compared to control dogs (median: 1.5; range 0-16; $p < 0.001$), which suggested that PIMs are induced in ANP. In addition, robust staining for vWF in alveolar septal capillaries in lungs of ANP dogs suggested a strong microvascular inflammatory response. Finally, TLR4, IL6, and iNOS expression was increased in lungs of ANP dogs compared to control dogs.

The second study was to investigate whether PIMs are induced in a mouse model of L-arginine-induced ANP. Therefore, lungs of L-arginine treated mice (n=7 per time point) were evaluated at various time points (24 hours, 72 hours and 120 hours) using histology and immunohistochemical staining for CD68 cells and vWF. Nine control mice were used. Counting of CD68-positive cells in the lungs of mice treated with L-arginine showed increased numbers of mononuclear phagocytes in alveolar septa at every time point ($p<0.001$). Also, the lung's vasculature from L-arginine-treated mice showed increased vWF staining.

Taken together, the data showed that ANP in dogs caused significant recruitment of PIMs, increased expression of vWF, TLR4, IL-6, and iNOS suggesting presence of lung inflammation. The mouse model of L-arginine-induced ANP also showed recruitment of PIMs and increased vascular expression of vWF suggesting that this model may be relevant to study the mechanisms of PIMs recruitment and their functions in lung physiology associated with ANP.

ACKNOWLEDGEMENTS

I would like to express my sincere thanks to my supervisor, Dr. Baljit Singh, for giving me the opportunity to study under his supervision. Without Dr. Singh's constant support, patience, encouragement and kind words, this journey would have been a lot harder. He gave me the strength to persevere throughout this long process and I am very grateful that he always made time in his busy schedule to listen to my struggles and reassure me when I needed it.

I would also like to thank my advisor committee members; Dr. Anthony Carr, Dr. Beverly Kidney, Dr. Jaswant Singh and Dr. Bruce Wobeser for their precious help, advice and time. Dr. Ahmad Al-Dissi and Dr. Hélène Philibert from the Department of Veterinary Pathology also deserve thanks for their generous help in evaluating histology slides.

I could not have completed my M.Sc. program without my lab mates who were always ready to help me. I especially want to thank Dr. Gurpreet Aulakh for teaching me all the different techniques required to perform the mice experiments, Dr. Julia Montgomery for helping with the SPCA dog tissue sampling, and Dr. Stacy Anderson for her generous help during my mice experiments. I also want to thank all my lab mates who also became my friends and who made my days in the lab a lot more joyful! Thank you Michelle Townsend, Kaitlin Merkowsky, Yadu Balachandran, Nicole House and Laura Johnson.

Finally but not least, I want to thank my friends in Québec, especially Mélyssa Millette and Émilie Bouchard, and my family for listening to me, believing in me and supporting me during the last 5 years.

TABLE OF CONTENTS

LIST OF FIGURES

LIST OF TABLES

LIST OF ABBREVIATIONS

ALI	Acute lung injury
AP	Acute pancreatitis
ARDS	Acute respiratory distress syndrome
CBC	Complete blood count
DIC	Disseminated intravascular coagulation
FiO_2	Fraction of inspired oxygen
H&E staining	Haematoxylin and eosin staining
IFN	Interferon
ICAM-1	Intercellular adhesion molecule 1
IL	Interleukin
iNOS	Inducible nitric oxide synthase
LPS	Lipopolysaccharide
MIP-2	Macrophage inflammatory protein-2
MPO	Myeloperoxidase
NO	Nitric oxide
NOS	Nitric oxide synthase
O_2-	Superoxide
PaO_2	Partial pressure of oxygen in arterial blood
PDS	Prairie Diagnostic Services
PRRs	Pattern recognition receptors
PIMs	Pulmonary intravascular macrophages
PLA_2	Phospholipase A_2
ROS	Reactive oxygen species
SPCA	Society for the Prevention of Cruelty to Animals
TFNα	Tumor-necrosis-factor-α
TLR	Toll-like receptor
VMC	Veterinary Medical Center
WBC	White blood cell
WCVM	Western College of Veterinary Medicine

CHAPTER 1: REVIEW OF LITERATURE

1.1. Introduction

Acute pancreatitis (AP) is an important gastrointestinal cause of hospital admissions both in humans (1) and dogs (2, 3). Mild AP is considered completely reversible with an uncomplicated recovery. However, when people and dogs suffer from severe AP, such as acute necrotizing pancreatitis (ANP), a systemic inflammatory response syndrome can occur leading to multiple organ dysfunction syndrome with high mortality rates. The reported mortality rates for dogs and people with AP are highly variable but range between 27-58% (2-5) and 30-50% respectively (6-9). Among all systemic complications that are associated with severe AP in humans, acute lung injury (ALI) or its more severe form acute respiratory distress syndrome (ARDS) are responsible for up to 60% of the mortality occurring in the first week of the disease (10, 11).

The incidence of ALI in people suffering from AP reported in different retrospective studies varies with reported incidences being 18% (12), 20% (13), 27.7% (14), and 42 % (15). In addition, a retrospective study analysing chest radiographs from people with ANP revealed that 46% of the cases had pleural effusion which correlated significantly to the mortality outcome (15-fold increase in the mortality rate) (13).There are two retrospective studies reviewing the medical records of dogs with AP which reported clinical evidence of dyspnea or tachypnea in 4/61 dogs(7%)(2) in the first study and 18/80 dogs(23%) in the second (5).These data in the literature suggest that pulmonary complications associated with AP are more common in people than in dogs.

The pathophysiology underlying systemic complications during severe AP is not well understood explaining why there is still no specific treatment for this condition. Significant efforts have been made in the past decades to attempt to further understand the mechanisms leading to development of a systemic inflammatory response syndrome and particularly ALI. However, the majority of our knowledge comes from studies using rodent models of AP and very little is known about the specific mechanisms occurring in dogs with AP. There is, to my knowledge, no study describing the histopathology of ALI in a group of clinical cases of AP (or ANP) in dogs. There is only one case report published in 1995 where the lung histology of a single dog with ANP was evaluated (16). Therefore, in this study, the lungs of 21 dogs that died or were euthanized because of ANP were evaluated to characterize the presence of lung inflammation with a particular interest for the presence of pulmonary intravascular macrophages (PIMs). Secondly, a mouse model of ANP was used to assess the induction of PIMs upon ANP.

1.2 Pancreatitis overview

1.2.1 Pancreas physiology

Before exploring the pathophysiology of AP, the basic pancreatic physiology must be understood. The pancreas is divided into an endocrine portion, involved in regulating glycaemia through the production of insulin and glucagon, and into an exocrine portion synthesizing large amounts of digestive enzymes, such as lipase, amylase, elastase, chymotrypsinogen, and trypsin, which are stored in inactive forms in zymogen granules in the cytoplasm of acinar cells (17, 18). The exocrine

pancreas is composed of pancreatic acinar cells whereas the endocrine portion consists of clusters of different cell types forming islets of Langerhans dispersed throughout the exocrine portion. Under normal circumstances, the pancreas secretes its inactive zymogens in the duodenum lumen where they become activated to participate in digestion (17). Furthermore, it is important to note that, as with other organs present in the peritoneal cavity, the venous effluent blood leaving the pancreas drains into the portal vein before reaching the systemic circulation (17).

1.2.2 Pancreatitis definition and classification

The term pancreatitis refers to the inflammation of the exocrine portion of the pancreas. Typically, the islets of Langerhans remain intact. Pancreatitis can be acute or chronic depending on the initial cause and the progression of the disease and can be classified based on either the histopathology (pathological classification) or the clinical severity of the disease (clinical classification) (3). At the moment there is no standardized, universally accepted classification for AP in human or veterinary medicine. The well-known Atlanta Classification of Acute Pancreatitis established in 1992 has now become out-dated with the improvement of our clinical ability to diagnose the disease, and several new revised classification systems have been proposed recently (2, 3, 19, 20). Nevertheless, it seems appropriate to divide AP based on the presence or absence of pancreatic necrosis (14). Currently, a mild form with absence of pancreatic necrosis called interstitial edematous pancreatitis in human medicine (14) or edematous pancreatic inflammation in veterinary medicine (2) and a severe form characterized by pancreatic necrosis named acute necrotizing

pancreatitis in veterinary medicine are recognized (3). Most cases of AP in people are interstitial edematous pancreatitis (80-90%) whereas dogs are mainly diagnosed with ANP (2, 11, 21).

1.2.3 Pancreatitis aetiology

In people, gall stones are the most common cause of AP followed by alcohol consumption. Other less common causes or risk factors include endoscopic retrograde cholangiopancreatography, some form of drugs, obesity, diet, autoimmune diseases, pancreatic duct obstruction, and hyper-triglyceridemia (1). Often, the cause of AP in dogs cannot be determined but reported aetiologies include hyperlipoproteinemia, drugs (azathioprine, chlorthiazide, potassium bromide, sulfonamides, cisplatin, L-asparaginase, clomipramine**),** zinc intoxication, hypercalcemia, pancreatic duct obstruction, abdominal surgery, duodenal/biliary reflux, trauma, ischemia-reperfusion, and more (3). There is also a controversial anecdotal association between feeding high-fat, low-protein food or unusual food to dogs and the development of AP (22, 23). In addition, hereditary pancreatitis has been characterized in humans and in Miniature Schnauzer dogs. In humans, five pancreatitis susceptibility genes have been identified and mutations in those genes are associated with increased trypsinogen activation (24-28). In Miniature Schnauzer dogs, three variations in the *SPINK1* gene have been associated with the development of AP in this breed (29). In addition, hypertriglyceridemia is suspected to be involved in the development of AP in Miniature Schnauzer dogs (30).

1.2.4. Acute pancreatitis diagnosis

Acute pancreatitis can be diagnosed with a combination of clinical assessments. However, the definitive diagnosis is confirmed by histological evaluation of the pancreas. Briefly, the clinical diagnosis of AP is based on the typical clinical signs (acute pain in the cranial abdomen, vomiting, anorexia, depression) (3), blood work and imaging methods including transabdominal ultrasonography, radiography and contrast-enhanced computed tomography (13). Serum amylase and lipase activities have been long used to assess the integrity of the pancreas. However, assessing the elevation of those enzymes is not a sensitive method and is not specific to pancreatic injury(3). There are now commercial kits measuring specifically canine pancreatic lipase (snap-cPLi or spec-cPL), which have higher specificity and sensitivity than evaluating lipase and amylase activities, but the sensitivity and specificity of those kits vary importantly between studies (31) (3). Canine trypsin-like immunoreactivity is thought to be specific for pancreatic injury but it can also increase during renal failure. It was shown to increase early in the course of AP, followed by a rapid decrease and therefore it's level is often back to normal values when the patient is presented at the clinic (32-34).

The definitive diagnosis of ANP is based on the presence of the following pancreatic lesions on histological evaluation: 1) acinar cell necrosis 2) peripancreatic fat necrosis 3) infiltration of inflammatory cells (neutrophils, mononuclear cells, lymphocytes or mixed) 4) pancreatic edema, and 5) haemorrhage (35, 36). Researchers have used various histological scoring systems to diagnose and grade the severity of AP in dogs (35-37).

1.3 Acute pancreatitis pathophysiology

The pathophysiology of ANP in dogs is not well established and our current understanding of this disease is mainly extrapolated from rodent models of AP. There are various rat and mouse models of AP and all of them are associated with varying degrees of severity, induction pathophysiology, and pathways leading to systemic complications. Unfortunately, we do not know which experimental model resembles most closely to the mechanisms naturally occurring in dogs suffering from ANP. The review of literature also reveals the challenges of comparing results from various models of ANP. There have been a few studies using dog models of AP for diagnosis or treatment purposes but not to describe the pathophysiology of the disease in dogs (38).

The most common and important rodent models of AP include: 1) administration of cholecystokinin (CCK) analog (cerulein) resulting in a mild pancreatitis 2) a dietary model with a choline-deficient diet causing ANP 3) administration of L-arginine intraperitoneally (IP) inducing ANP and 4) retrograde injection of sodium taurocholate in the bileopancreatic duct causing severe hemorrhagic necrotizing pancreatitis (39, 40). Many other models exist but are less commonly used (39, 40).

The development of ANP is the result of various mechanisms including premature activation of digestive enzymes within pancreatic acinar cells, activation of inflammatory pathways, altered pancreatic microcirculation, oxidative stress, activation of the complement system, and potentially the kallin-kallikrein and renin-

angiotensin systems (28). A description of the main mechanisms involved in ANP is described here.

1.3.1 Trypsin-centered theory

In 1896, *Chiari* proposed the trypsin-centered theory of pancreatitis stipulating that pancreatitis is initiated by intra-acinar premature activation of trypsinogen into trypsin leading to autodigestion of the pancreas. It is well accepted that during pancreatitis, zymogen granules containing trypsinogen are not normally secreted into the duodenum lumen but instead are fused with lysozymes containing lysosomal proteases such as cathepsin B, which activates trypsinogen into trypsin (41-49). It is believed that a secretory block occurs on the apical surface of acinar cells preventing zymogen granules from exiting the cells (50). The activated trypsin can then cause the activation of other digestive enzymes present in acinar cells leading to further pancreatic injury. To protect themselves against activated trypsin, acinar cells are equipped with protective mechanisms including pancreatic secretory trypsin inhibitors (PSTI) and the induction of rapid cell death through zymophagy (17, 41). However, those mechanisms become quickly overwhelmed during AP resulting in the accumulation of trypsin causing acinar cell death through apoptosis or necrosis. According to this theory, the autodigestion of acinar cells causes the release of the cytoplasmic content of necrotic cells and activates inflammatory pathways in the pancreas promoting local inflammation (17, 18).

The trypsin-centered theory has been the basis of our understanding of AP for the last century (18). However, in the last decades, studies using genetically

modified rodents lacking trypsinogen or cathepsin B have suggested that trypsin-independent mechanisms can lead to acinar cell necrosis and to the development of AP (42, 51). Therefore, the biological significance of the premature activation of pancreatic digestive enzymes is being questioned. Some studies even suggest that intra-acinar premature activation of trypsinogen may be a protective defense mechanism in the early stage of pancreatitis in order to limit the activation of more digestive enzymes (44, 52-55).

1.3.2 Pancreatic inflammation

During AP, a substantial amount of pro-inflammatory mediators are released into the systemic circulation from the injured pancreas. Both pancreatic acinar cells and inflammatory cells are involved in the inflammation component of AP. Activation of NF-κB signalling pathways in pancreatic acinar cells has been shown to be one of the earlier events to occur during the initiation of AP in various experimental models (56, 57). The activation of NF-κB leads to the production of Tumor-necrosis-factor-α (TFNα) and interleukin (IL)-1β, which are the first pro-inflammatory cytokines to increase during AP (58, 59). Together, TNFα and IL-1β promote pancreatic inflammation by increasing the expression of ICAM-1 on endothelial cells and stimulating the production of interleukin-8 (IL-8), which leads to the recruitment and migration of neutrophils into the pancreas (60, 61). IL-6, another important pro-inflammatory cytokine, is also increased during AP and this cytokine, along with IL-8, is correlated to the severity of AP (62, 63). Other pro-inflammatory cytokines investigated during AP include IL-2, IL-4, IL-11, and IL-18.

Neutrophils are the first inflammatory cells to be recruited into the pancreas during AP and their depletion decreases the severity of the disease confirming their role in causing pancreatic injury (64, 65). In addition to being recruited via NF-κB signalling pathways, pancreatic enzymes such as trypsin, elastase, and chymotrypsin are able to regulate the migration of neutrophils during AP by increasing the expression of ICAM-1 on neutrophils and endothelial cells (66, 67). Neutrophils can then cause pancreatic injury through the release of their granules containing reactive oxygen species (ROS) such as superoxide (O_2-), hydrogen peroxide (H_2O_2), and hydroxyl ions (OH-) (66). Neutrophils could also have modulatory roles during AP as they cause a shift from acinar cell apoptosis to necrosis during AP (64, 68). Monocytes are also recruited to the pancreas during AP via MCP-1 and the administration of an MCP-1 blocker reduced the severity of AP (69). The question whether the activation of NF-κB and development of inflammation is a consequence of trypsinogen activation or whether inflammation in the pancreas occurs independently of the activation of trypsin is not settled as contradictory results have been obtained (42, 70, 71).

1.3.3 Nitric oxide and oxidative stress

The role of nitric oxide (NO) and oxidative stress in AP is controversial. NO is known to participate in pancreatic physiology by regulating pancreatic exocrine secretion, promoting capillary integrity, inhibiting leukocyte adhesion, and modulating the pancreatic microvascular blood flow (72, 73). However, in experimental pancreatitis, contradictory roles for NO have been shown as it

increased oxidative stress causing hypotension (74, 75) or had protective effects via increasing the blood flow (76). ANP and high mortality rate have been associated with vasoconstriction in pancreas in animals and humans (77-79). It was also suggested that the vascular endothelium nitric oxide synthase would be protective during AP but the inducible nitric oxide synthase (iNOS) expressed by macrophages is associated with more severe AP. A recent study showed that the severity of AP was correlated to plasma NO and that oxidative stress was greater in people developing systemic complications (80).

1.4 Acute lung injury and acute respiratory distress syndrome

Acute inflammation is typically characterized by vasodilation, increased blood flow, increased vascular permeability leading to accumulation of fluid exudates and migration of leukocytes, and the activation of nociceptors. These physiological events lead to the classical cardinal signs of inflammation: pain, swelling, redness, heat, and loss of function. The fundamental role of inflammation is to protect the body against various threats such as pathogens (virus, bacteria, fungi, parasite), tissue injuries (burns, trauma, necrosis), toxic substances and foreign bodies. In most of the cases, inflammation is beneficial and allows the restoration of homeostasis. However, in some conditions, the inflammatory response can become excessive or prolonged resulting in more tissue damage and loss of physiological functions. Examples of conditions where the inflammation itself becomes detrimental for the host include, among others, ALI, allergic reactions, autoimmune diseases, intestinal bowel disease, organ transplantation, and cancer.

ALI and its more severe form ARDS are two common and devastating syndromes associated with high mortality and morbidity, both in human and veterinary patients. In 1993, the American-European Consensus Committee (AECC) established criteria to diagnose ALI and ARDS in human patients providing consistent definitions and nomenclature. The AECC defines ALI as follow: 1) acute onset 2) presence of hypoxemia (PaO_2/FiO_2 < 300mm Hg) 3) diffuse bilateral pulmonary edema seen on frontal radiographs, and 4) pulmonary artery occlusion pressure ≤ 18mm Hg, or no evidence of left atrial hypertension (81). ARDS is characterized by the same criteria but with more severe hypoxemia (PaO_2/FiO_2 < 200mm Hg). In 2007, more appropriate definitions of ALI and ARDS for veterinary medicine were established dividing ALI into 3 main definitions: 1) Neonatal equine respiratory distress syndrome (NERDS), 2) veterinary ALI and ARDS (VetALI/ VetARDS) and 3) equine neonatal ALI/ARDS (EqNALI/ EqNARDS)(225).

The pathophysiology of ALI is complex and involves two main responses: a vascular and a cellular response. ALI can be direct (or primary) when the aggressor enters the lungs via the airways such as in microbial pneumonia, aspiration pneumonia and smoke/toxic gas inhalation. ALI can also be indirect (or secondary) when the inflammatory stimuli reach the lungs via the blood circulation as in AP, sepsis, endotoxemia, severe burns, blood poisoning, and disseminated intravascular coagulation (DIC) (82). Indirect ALI is initiated by a vascular response where structural changes in the microvasculature of the lungs are induced by inflammatory stimuli present in the blood circulation. This leads to increased vascular permeability, expression of adhesion molecules on endothelial cells and production of

chemokines resulting in the recruitment and migration of leukocytes into the lungs (83). Neutrophils are typically the first inflammatory cells to be recruited in the lungs during ALI and are highly efficient in clearing pathogens (83). However, excessive infiltration of neutrophils in the lungs can be harmful as they cause further tissue injury via release of their granules content, such as reactive oxygen species (ROS) and proteases (78). Histologically, those changes result in interstitial and alveolar edema, vascular congestion, infiltration of inflammatory cells typically neutrophils into the lung parenchyma and alveolar spaces, thickening of alveolar septa, and, in some cases, haemorrhages (84, 85).

The cellular response during ALI is strongly modulated by resident lung macrophages including alveolar macrophages, interstitial macrophages and in some cases pulmonary intravascular macrophages (PIMs). Alveolar macrophages reside in the alveoli and constitute the first line of defense against inhaled threats reaching the alveoli whereas interstitial macrophages are present in the interstitial space between the alveolar epithelium and the vascular endothelium (86). In some species, monocytes present in the microvasculature of the lungs have been shown to adhere to the endothelium and differentiate in a third population of macrophages called PIMs (87). The potential roles of PIMs in lung inflammation will be discussed later in section 1.4.1.

Macrophages are highly versatile cells and can adopt pro-inflammatory (M1 or classically activated) or anti-inflammatory phenotypes (M2 or alternatively activated) (88). M2 macrophages can be further divided into wound-healing (M2a) or regulatory (M2b) macrophages.(89). The development of one phenotype over the

other depends on the balance between activating and repressing signals present in the local environment. Alveolar macrophages have been assigned both pro-inflammatory (M1) and regulatory (M2) phenotypes during inflammatory settings (90). The induction of a pro-inflammatory (M1) phenotype is mediated by inflammatory cytokines including interleukin (IL)-1, interferon (IFN), TNFα and through activation of pattern recognition receptors (PRRs), such as Toll-like receptor-4 (TLR4) by lipopolysaccharide (LPS) (91). Pro-inflammatory macrophages have essential roles in the host defense against pathogens via enhanced phagocytosis of microorganisms and antigen-presentation. However, they are also associated with enhanced production of matrix metalloproteinases and upregulation of iNOS leading to the production of NO and ROS, which can have detrimental consequences for the host in addition to killing microbes (89, 92). Also, M1 macrophages produce pro-inflammatory cytokines and chemokines including TNFα, IL1β, IL6, IL8, IFNγ, and IL12, which induce neutrophil and monocyte recruitment (93). Interstitial macrophages would have a regulatory phenotype (M2b) by producing anti-inflammatory cytokines such as IL-10, which inhibit immune response and inflammatory processes (94, 95).

1.4.1 Pulmonary intravascular macrophages (PIMs)

There are now various studies showing that lungs from some species possess a third type of constitutive macrophages called pulmonary intravascular macrophages (PIMs). As the name suggests, PIMs are mature macrophages rather than monocytes and are located in the microvasculature of the lungs, mainly in the

thick portions of alveolar septa. In sheep, PIMs were shown to cover up to 20% of the lung endothelium surface (96, 97). Briefly, PIMs are highly phagocytic large cells (20-80 μm diameter) proven to be firmly attached to lung endothelial cells and are believed to have pro-inflammatory functions.

Species in the orders *Artiodactyla* (cattle, water buffalos, sheep, goats and pigs) (97-104), *Perissodactyla* (horses) (105-107), *Odontoceti cetacean* (toothed whales) (108) and some strains of domestic cat (109) have been shown to have constitutive PIMs, which colonize the lungs early after birth (96, 97). Species included in the order *Rodentia* (rats, mice, guinea pigs, hamsters) (101, 110) do not have constitutive PIMs. However, studies using rats have shown that PIMs can be induced (induced PIMs) upon physiological stress such as endotoxemia and liver dysfunction (111, 112). Although the mechanisms by which PIMs are induced remain to be understood, it is suggested that their induction is mediated through altered pulmonary endothelium leading to the production of chemokines and adhesion molecules.

Few studies have been conducted to evaluate the extent of PIMs in humans and dogs. Only one ultrastructural report has been published showing very few PIMs in the human lung leading to the suggestion that human lungs do not normally have PIMs (113). In addition, older publications have indirectly shown that PIMs could be induced during liver dysfunction in humans, resembling to what was observed in other species devoid of constitutive PIMs (114-117). Two studies assessed the presence of PIMs in normal dogs but none succeeded to prove their existence leading to the proposition that dogs normally do not contain constitutive PIMs (118).

Furthermore, in a fairly recent study (2008), the presence of PIMs in 2 normal dogs and 2 dogs receiving a transplant of dead *Dirofilaria immitis* was evaluated and the results revealed an absence of constitutive or induced PIMs in those dogs (119). Furthermore, a recent (2011) immunohistochemical study using 2 dogs was performed previously in our laboratory and showed presence of few mononuclear phagocytes in alveolar septa (120). To my knowledge there are no studies that have assessed the induction of PIMs in a larger group of dogs suffering from lung injury.

PIMs have a robust and very efficient phagocytic capacity for particles present in the blood circulation, including viruses, bacteria, LPS, cellular debris, and effete erythrocytes (112, 121-125). As the pulmonary circulation receives the entire cardiac output, PIMs are thought to play a physiological role in the clearance of blood particles, similar to the liver and spleen intravascular macrophage system (126, 127). However, because of their ability to clear and process microorganisms and antigens, PIMs may constitute a potential reservoir of infectious agent in the lungs with a potential detrimental impact on the lung health.

Our knowledge of PIMs' contribution to lung inflammation mainly comes from *in vivo* studies where PIMs were either induced in species that lacked these cells or were depleted with gadolinium chloride or clodronate lipososmes in species with constitutive PIMs (111, 112, 128-132). Protective effects of PIMs' depletion were noted in various models of ALI in species with constitutive PIMs such as in endotoxin-mediated lung injury in sheep (131) and horses (106), and in calves infected with *Mannheimia hemolytica* (130), thus attributing a pro-inflammatory role to PIMs. Overall, depletion of PIMs in those species resulted into reduced lung

levels of pro-inflammatory cytokines and chemokines, improved lung histology and reduced migration of inflammatory cells. Also, recent data show that depletion of PIMs in horses with spontaneous heaves led to a reduction in clinical signs and reduction in migration of neutrophils into the lungs(87).

It has been observed that species with constitutive PIMs, such as horses (128), sheep (131) or cattle (130) develop more severe lung inflammation following endotoxemia compared to species without constitutive PIMs, such as rats, where higher doses of LPS are needed to induce ALI (101, 111, 130, 133). However, lungs from rats with induced PIMs, including the bile duct-ligated rat model (111), the rat *E. coli* sepsis model (112), the rat hepatopulmonary syndrome model (111, 132), become sensitive to very low dosages of LPS (dose in μg/kg instead of mg/kg) (111) and the lung inflammatory response thus induced is more intense compared to control rats receiving their first LPS challenge. However, when PIMs are depleted after their induction in rats, the lung inflammatory response is reduced (111).

Pro-inflammatory signalling pathways in PIMs are suggested to occur through TLRs, such as TLR-4, TLR-9, and TLR-2 during sepsis and endotoxemia (111, 134-136). Following activation of TLRs, PIMs produce large amounts of pro-inflammatory mediators such as TNF-α (137), IL-1β and iNOS products (111) (130, 138), which can stimulate local endothelial cells or cross alveolar septa and stimulate alveolar macrophages (111, 134-136). Histologically, PIMs' stimulation is associated with vascular congestion and recruitment of inflammatory cells (137). PIMs' activation was also linked to aggregation of IL-8-rich platelets in the lungs in calves challenged

with intra-tracheal *Mannheimia hemolytica*, which may promote the recruitment of neutrophils (130).

Taken together, studies on PIMs suggest that they are pro-inflammatory and that their stimulation or induction enhances the lung susceptibility for the development of an enhanced inflammatory response to microbial challenges, which could lead to respiratory distress and have detrimental consequences for the host. However, the contribution of induced PIMs in lung physiology and in pathologic settings remains to be further characterized and accepted.

1.5 ALI associated with acute pancreatitis

Significant efforts have been made in the last decades to attempt to describe the mechanisms initiating and maintaining lung inflammation during AP. But there are still significant gaps in our comprehension of AP-associated lung pathophysiology. ALI is multifactorial and results from a complex combination of the release of pancreatic-specific proteins, activation of Kupffer cells and peritoneal macrophages, gut barrier dysfunction and the activation of alveolar macrophages in the lungs. A summary of the pathophysiology of AP-associated ALI follows.

1.5.1 Extra-pulmonary mechanisms involved in ALI associated with acute pancreatitis

1.5.1.1 Kupffer cells

It has been clinically observed that people suffering from pancreatitis associated with pancreatic transplantation demonstrate reduced (or absent) signs of systemic complications, including ALI, as opposite to what is seen during naïve pancreatitis (139, 140). During pancreatic grafting, the pancreatic venous effluent blood is drained into the iliac veins (systemic circulation) instead of into the portal vein, therefore, by-passing the liver. This led to the hypothesis that the liver plays a key role in the pathophysiology of systemic inflammatory response syndrome and ALI during acute pancreatitis.

Similar protective effects on ALI were noted in rodent models where a porto-caval shunting to prevent the passage of blood from the pancreas to the liver was performed or when gadolinium chloride was used to deplete Kupffer cells before the induction of AP (141). Kupffer cells are mononuclear phagocytes present in the microvasculature of liver and therefore get exposed to various pro-inflammatory mediators, including pancreatic enzymes such as elastase, released by the inflamed pancreas during AP (142). Either the porto-caval shunting or depletion of Kupffer cells abolished the rise of systemic pro-inflammatory molecules such as IL-6, TNFα, IL-1β and HSP-72 and protected against ALI (143-146). Reduction of ALI following those procedures was characterized by reduced recruitment of neutrophils in the lung assessed by myeloperoxidase (MPO) activity, lower histology scores, decrease of NF-kB activation in alveolar macrophages and lower production of NO, TNFα and

MIP-2 by alveolar macrophages (143, 146, 147). It is important to note that gadolinium chloride may deplete other macrophages such as those in the spleen in the host, which makes it challenging to directly assess the contributions of Kupffer cells in ALI associated with AP.

1.5.1.2 Peritoneal macrophages

The peritoneal cavity possesses inflammatory cells mainly macrophages and neutrophils, as a major line of defense against infection of the abdominal cavity. There are data to show an increase in the numbers of peritoneal macrophages during AP, and these macrophages contribute to the development of systemic inflammatory response syndrome and ALI upon activation by trypsin (148). People suffering from AP have been shown to have leakage of trypsin (149) and trypsin activation peptide (150) into their peritoneal cavity. Indeed, activated pancreatic enzymes can leak through the basolateral membrane of acinar cells accumulating in the pancreatic interstitium and peri-pancreatic tissue and then access the peritoneal cavity (150).

Using *in vitro* culture techniques, activation of peritoneal macrophages by trypsin led to the production of TNFα and IL-1β in a dose-dependent manner (151). TNFα and IL-1β are both found to be elevated in ascitic fluid of various rodent models of severe pancreatitis (148). The injection of trypsin into the peritoneal cavity of rats increased levels of ascites TNFα in conjunction with lung inflammation (151) suggesting that the activation of peritoneal macrophages by trypsin may contribute to the development of ALI. Furthermore, performing peritoneal lavages with

protease inhibitors in AP rats decreased the level of lung injury (152) or had no effect (153). Similarly, depletion of peritoneal macrophages by intravenous injection of liposome-encapsulated dichloromethylene bisphosphonate (Cl_2MBP liposomes) in ANP rats decreased the levels of pro-inflammatory cytokines in the peritoneal lavage (TNFα and IL-1β) and in the serum (IL-6 and IL-8), and protected against lung inflammation shown by reduced infiltration of neutrophils and edema on histological evaluation and reduced MPO activity (154). However, the intravenous treatment to deplete peritoneal macrophages may have also affected Kupffer cells. Peritoneal macrophages isolated from AP rats also expressed increased levels of iNOS, which suggests their role in raising the level of NO in the systemic circulation during AP(155).

1.5.1.3 Pancreatic enzymes

During AP, trypsin, elastase and phospholipase A_2 (PLA_2) are released in the blood circulation from the injured pancreas (149). Trypsin has been shown to cause vascular injury to various organs during AP including the lungs (156, 157). In addition, PLA_2 can cause surfactant degradation as well as increased vascular permeability via cell membrane phospholipid hydrolysis (158). Elastase can cause degradation of elastin in blood vessel walls and chymotrypsin activates xanthine oxidase leading to oxidative damage. Therefore, the release of pancreatic enzymes into the systemic circulation during AP can potentially cause vascular injury in the lungs promoting inflammation.

1.5.2 Lung mechanisms involved in ALI associated with AP

1.5.2.1 Neutrophils

Neutrophil recruitment occurs early in the course of lung inflammation during experimental AP and is associated with tissue damage such as vascular injury leading to increased vascular permeability (64, 156, 159). Depletion of circulating neutrophils with specific antibodies in various experimental AP studies prevented lung vascular permeability, decreased lung weight, improved histological scores, and increased the survival rate (64, 159, 160). However, in some models of AP, the severity of pancreatitis was also reduced when circulating neutrophils were depleted, which could therefore indirectly have a protective effect on lung injury (64, 159).

Neutrophil recruitment in the lungs seems to depend on the expression of intercellular adhesion molecule 1(ICAM-1) (67, 161). Humans suffering from ANP had higher levels of ICAM-1 in their plasma, which was correlated with the severity of AP (162). In addition, pulmonary expression of ICAM-1 is increased during experimental pancreatitis and was associated with the infiltration of neutrophils into the lungs (67, 163). Other mechanisms believed to be involved in ALI mediated by neutrophils include the activation of complement (159) and injury via hydrogen peroxide (H_2O_2) released from neutrophil granules.

It is not clear whether neutrophils are previously activated in the inflamed pancreas and then reach the lungs via the systemic circulation or if they are being recruited to the lung by activated endothelial cells or alveolar macrophages.

1.5.2.2 Pulmonary alveolar and interstitial macrophages

Many studies have focused on the role of alveolar macrophages in ALI associated with AP. As mentioned previously, pro-inflammatory mediators released by activated peritoneal macrophages and Kupffer cells in the early course of AP can lead to the activation of AM. In addition, there is some evidence that alveolar macrophages can also be activated by pancreatic-specific proteins such as PLA_2, which is found to be elevated in the serum and BAL fluid of humans with AP complicated with ALI (164-169).

Activated alveolar macrophages during AP have been shown to acquire a pro-inflammatory phenotype (M1) producing pro-inflammatory mediators such as TNFα, IL-1β, and MIP-2 resulting in the recruitment neutrophils into the lungs (147, 164, 170-172). In addition, a great amount of work has been done regarding the induction of iNOS in alveolar macrophages and the production of NO in the lungs during AP. Alveolar macrophages have been shown to express high levels of iNOS in various experimental AP studies resulting in increased levels of NO in the lungs (164, 171, 173). iNOS in alveolar macrophages was reported to be induced by pancreatic PLA2 both in *in vitro* and *in vivo* experiments (147, 164, 171, 172). The role of NO during ALI associated with AP is controversial as in some studies the increase in NO has been associated with more lung injury (164, 173) whereas in other studies NO was protective and reduced the severity of ALI (174). In one of the AP studies, interstitial macrophages were characterized by an inhibitory phenotype (M2b) as they produced anti-inflammatory cytokine IL-10 through PPARgama activation (170).

1.5.2.3 Innate immunity: Lung TLRs

TLRs are part of the pattern recognition receptors (PRRs) family and have critical roles in the host defense against invading microorganism via the recognition of pathogen-associated molecular pattern (PAMP) of viruses, bacteria and fungi by immune cells (175). Activation of TLRs leads to a series of signalling pathways causing an acute response necessary to kill pathogens. TLR4 is a well-known receptor for LPS and is involved in bacterial infections and septicemia caused by Gram-negative bacteria (176, 177). However, it has been shown that TLR4 can also be activated in settings other than LPS or other bacterial products by recognizing damage associated molecular pattern molecules (DAMPs) such as heat shock protein 60 and 70, extra domain A of fibronectin, oligosaccharides of hyaluronic acid and fibrinogen (178, 179). Although TLR4 is involved in protecting the host against various infections, over-expression of this receptor can lead to the production of an excessive amount of pro-inflammatory cytokines and subsequently to undesirable tissue damage. TLR4 could be involved in ALI associated with AP since sepsis and endotoxemia are potential complications.

It has been shown in rats that acute hemorrhagic necrotizing pancreatitis leads to an increased expression of TLR4 in the lungs assessed by mRNA and protein expression and was associated with lung injury (174). The increased TLR4 in the lungs of those rats was associated with the production of increased level of IL6 and TNFα and with histological signs of lung injury. Therefore, it was suggested that TLR4 may have a role in the development of ALI associated with severe AP. However, the identity of cells contributing to increased TLR4 in the lungs and

whether this increase is mediated via endotoxemia are not fully understood.

1.6. L-arginine-induced mouse ANP model

In 1984, it was observed that a high dose of L-arginine injected intraperitoneally induces changes in the pancreas consistent with acute pancreatitis (180). Since then, intraperitoneal injections of an L-arginine solution have been used in rats to induce ANP while sparing the islets of Langerhans and without causing injury to other abdominal organs (180-182). However, it is only since 2007 that the L-arginine procedure to induce ANP has been standardized in mice (181). The pancreatitis induced in mice with L-arginine is characterized histologically by changes in the pancreatic acinar cells as early as 6 hours with disappearance of zymogen granules from some areas after 24 hours followed by the appearance of inflammatory cells and acinar cell necrosis at 72 hours and with only small areas of intact acinar cells remaining after 96-120 hours (181). In addition, plasma amylase levels rise within 24-48 hours, peak at 72 hours and return to normal values within 96-120 hours following L-arginine treatments (181, 183). This non-invasive model is associated with a low mortality rate and is considered a physiologically good model to study the progression of AP as well as its systemic complications including ALI. In mice, ALI is characterised histologically by alveolar thickening, infiltration of inflammatory cells mainly neutrophils and pulmonary hemorrhage at 72 hours after the L-arginine challenge, and this is associated with increased lung MPO activity (181, 184, 185). In addition, interestingly, there has been a case report of a 16 years old boy diagnosed with acute pancreatitis which was associated to the boy's daily

intake of L-arginine supplements (500 mg/day) over a period of 5 months for the purpose of body building (227).

1.6.1 L-arginine-induced ANP model mechanisms

The pathophysiology of the L-arginine-induced ANP model is not fully understood. L-arginine is classified as a conditionally essential amino acid and can be metabolised by two main enzymes: arginase and nitric oxide synthase. It is mostly accepted that the arginase metabolism pathway is involved to some degree in the pathophysiology of this model. However, discrepancy exists regarding the role of nitric oxide synthase and NO in the induction of pancreatitis.

Arginase is mainly present in the liver and is a key enzyme in the urea cycle as it hydrolyses L-arginine into L-ornithine and urea. Because very little arginase is present in the pancreas, kidneys and lung, most of L-arginine is believed to be metabolized in the liver (186). A pharmacokinetic study of L-arginine administered intraperitoneally suggested that the half-life of L-arginine is between 1-2 hours, indicating that L-arginine is rapidly metabolized (180). It was shown that, after intraperitoneal injections of L-arginine, the levels of L-ornithine increased by a 54-fold indicating the importance of this pathway in metabolising L-arginine in this model (187). The role of the arginase pathway in the development of pancreatitis was demonstrated by the inhibition of this enzyme prior to L-arginine injections, which reduced pancreatitis severity by decreasing trypsin level, pancreatic MPO activity, and histology scores (186). Furthermore, it is L-arginine's metabolite L-ornithine, rather than L-arginine itself, that is believed to induce pancreatic injury.

Intraperitoneal injections of L-ornithine create ANP at lower doses than L-arginine (187). More specifically, L-ornithine would generate free radicals such as superoxide and thus have toxic effects via oxidative stress (188, 189).

Nitric oxide synthase, which is present in pancreatic acinar cells (190), metabolises L-arginine into L-citrulline and NO. An increase in iNOS has been observed 24 and 48 hours following the injection of L-arginine (191). Some studies suggest that the combination of NO with superoxide (O_2-) produced in the arginase pathway leads to the production of reactive nitrogen species, which would contribute to the oxidative stress causing pancreatitis in the L-arginine model (73, 188, 189, 192). In addition, neuronal and endothelial cells present in close proximity to pancreatic acinar cells may also contribute to the increase in reactive oxygen and nitrogen species (193). Studies using NOS inhibitors, such as L-NAME, or antioxidants reported both protective effects and no improvement in severity of pancreatitis. (187, 191, 194-196). Furthermore, intraperitoneal administration of NO donor sodium nitroprusside or L-citrulline, the NO liberating metabolite, failed to induce pancreatitis (187). Thus, the role of iNOS in the induction of pancreatitis in the L-arginine model is still remains. Some studies even suggest a protective role for NO during acute pancreatitis by increasing the pancreatic microvascular blood flow, inhibiting leukocyte activation, and protecting against trypsinogen activation and acinar cell necrosis (189, 195, 197).

It is not well understood why only the pancreas and not other abdominal organs is affected in the L-arginine model (180-182). It was suggested that this could be due to the high turnover of proteins in pancreatic acinar cells, which would

cause them to import large quantity of L-arginine more rapidly than in other organs. In addition, the presence of large amount of digestive enzymes in pancreatic acinar cells could be an explanation for the specific effect of L-arginine on the pancreas.

CHAPTER 2: HYPOTHESES AND OBJECTIVES

2.1 Hypotheses:

1) Acute necrotizing pancreatitis (ANP) in dogs is accompanied by acute lung injury (ALI) and is associated with the induction of pulmonary intravascular macrophages (PIMs).
2) PIMs are recruited in the L-arginine ANP mouse model.

2.2 Objectives:

A. To characterize lung inflammation in clinical cases of ANP in dogs using histological evaluation and immunohistochemical staining with special focus on the recruitment of mononuclear phagocytes.
B. To induce ANP in mice using the L-arginine model and to assess lung inflammation including the induction of PIMs.

2.3 Rationale:

Dogs suffering from ANP often develop a systemic inflammatory response syndrome leading to multiple organ dysfunction syndrome with high mortality rates. Among all systemic complications that are associated with severe acute pancreatitis (AP) in humans, ALI or its more severe form acute respiratory distress syndrome (ARDS) are responsible for up to 60% of the mortality (11). The incidence of pulmonary complications in dogs with AP is not well established. However, signs of respiratory distress in those dogs are reported as a cause of death or euthanasia clinically and in the literature (2). The pathophysiology leading to ALI is not well

understood and the majority of our knowledge comes from studies using rodent models of AP. Very little is known about the specific mechanisms such as the recruitment and functions of pulmonary intravascular macrophages (PIMs) in the lungs of dogs with AP. Because there has not been any detailed study of the lung histology in dogs that have died due to AP (or ANP), I propose to fill this gap with a special focus on the characterization of recruitment of PIMs and expression of selected inflammatory molecules. Following this, I will investigate lung inflammation including recruitment of PIMs in a mouse model of L-arginine-induced ANP. While data from the lungs of spontaneous cases of ANP in dogs provides valuable insights into the potential contributions of lung inflammation to mortality, the mouse model will provide a platform to dissect specific mechanisms contributing to the development of lung injury observed in AP.

CHAPTER 3: LUNG INFLAMAMTION IN CLINICAL CASES OF ANP IN DOGS

3.1 Introduction

AP in dogs is one of the most common gastrointestinal causes of emergency admissions in small animal veterinary clinics (2, 3). While AP can occur in a mild form with low morbidity, the severe form of AP, acute necrotizing pancreatitis (ANP), is associated with systemic inflammatory response syndrome and multiple organ dysfunction syndrome with high mortality rates. When suffering from this disease, the risk of mortality can increase up to 27-58% (2-4) and this significant mortality rate is mainly associated with the various systemic complications associated with ANP. In human patients suffering from severe AP, acute lung injury (ALI) or its more severe form acute respiratory distress syndrome (ARDS) are responsible for up to 60% of the mortality occurring in the first week of the disease (10, 11). Furthermore, the incidence of ALI in people with AP varies form 18%-46% (12-15) depending on the severity of AP. There are two retrospective studies that reviewed the medical records of dogs with AP, which reported clinical evidence of dyspnea or tachypnea in 4/61 dogs (7%)(2) in the first study and 18/80 dogs (23%) in the second (5).

ALI or ARDS are common devastating conditions associated with high morbidity and mortality in humans and animals. The pathophysiology of ALI is complex and involves a vascular and cellular response. During indirect ALI, the vascular endothelial cells constitute the first cells to be exposed to inflammatory mediators. Activation of those cells can lead to structural changes of the lung microvasculature leading to increased vascular permeability, expression of adhesion molecules on endothelial cells and production of chemokines resulting in the

recruitment and migration of leukocytes into the lungs. Neutrophils are typically the first inflammatory cells to be recruited into the lungs during ALI and play an important role in clearing pathogens (83). However, excessive recruitment of neutrophils through various adhesion molecules including selectins and integrins can cause further lung injury through the release of their granules content, such as ROS and proteases (83).

The cellular response during ALI is strongly modulated by the pulmonary resident macrophages including alveolar macrophages, interstitial macrophages and, in some species, pulmonary intravascular macrophages (PIMs). PIMs are highly phagocytic large cells (20-80μm diameter) with characteristics of mature macrophages and are believed to have pro-inflammatory functions. Some species in the orders *Artiodactyla* (cattle, water buffalos, sheep, goats and pigs) (97-104), *Perissodactyla* (horses) (105-107), *Odontoceti* cetacean (toothed whales) (108) and some strains of domestic cat (109) have been shown to have constitutive PIMs. Furthermore, PIMs can be induced with physiological stress such as endotoxemia and liver dysfunction (111, 112) in species that do not normally have them including *Rodentia* (rats, mice, guinea pigs, hamsters) (110) (101) and *Lagomorpha* (rabbits) (111, 112). To my knowledge there are no studies that have assessed the induction of PIMs in dogs suffering from ANP-associated lung injury. Although the mechanisms are not well known, PIMs stimulation or induction would enhance the host susceptibility to lung injury during subsequent microbial challenges(111).

ALI associated with AP would be multifactorial resulting from the complex combination of the release into the blood circulation of pancreatic-specific proteins

(147, 156, 157, 164, 171, 172), activation of Kupffer cells (143-146) and peritoneal macrophages (148, 151, 152), gut barrier dysfunction(198, 199), and the activation of alveolar macrophages (AM) in the lungs. Most studies assessing ALI in experimental AP studies using rodent models have focussed on the role of AM, which have been shown to be activated during AP by various mechanisms leading to the acquirement of a pro-inflammatory phenotype. (164-169). Following their activation, alveolar macrophages cause lung injury producing pro-inflammatory mediators such as of TNFα, IL-1β, and MIP-2 resulting in the recruitment of neutrophils into the lungs and in lung injury (147, 164, 170-172). In addition, alveolar macrophages have been shown to express high levels of inducible nitric oxide synthase (iNOS) in various experimental AP studies resulting in increased levels of nitric oxide (NO) in the lungs. (164, 171) (173). The role of NO during ALI associated with AP is controversial because in some studies the increase in NO has been associated with more lung injury (164, 173) (140) whereas in others NO was protective and reduced the severity of ALI (174). Although significant progress has been made to characterize the role of alveolar macrophages during ALI in rodent models of AP, no study has assessed the recruitment and role of PIMs during this disease.

The majority of our knowledge on ALI associated with AP comes from studies using rodent models of AP and very little is known about the specific mechanisms occurring in dogs with ANP. Therefore, in this study, the lungs of 21 dogs that died or were euthanized because of ANP were evaluated to characterize the presence of ALI with a particular interest for the presence of PIMs. In addition,

immunohistochemistry for TLR4 and IL6 was performed to further characterize pro-inflammatory mechanisms in the lungs of ANP dogs. iNOS expression was also assessed by immunohistochemistry since NO seams to be involved in ALI associated with AP in rodent models. Lastly, von Willebrand Factor (vWF) was previously shown in our laboratory to be increased in inflamed lungs, therefore its expression in lungs of ANP dogs was also described with immunohistochemistry.

3.2 Materials and Methods

3.2.1 Selection of canine ANP cases

Cases of dogs that died or were euthanized from ANP were selected by searching the medical records of the Veterinary Medical Center (VMC) of the Western College of Veterinary Medicine (WCVM) between the years of 2000 to 2013 and using the keywords ‘necrotizing pancreatitis’ and ‘pancreas necrosis’. A search was also made in the Prairie Diagnostic Services Inc. (PDS) electronic system to identify external cases of ANP dogs that were sent to PDS for the post-mortem evaluation and that may not have been included in the VMC database. Then, the necropsy reports from the identified cases were reviewed to confirm the post-mortem diagnosis of ANP and to select cases where both lung and pancreas were collected during necropsy for paraffin embedding. Cases with a mention of significant post-mortem/autolysis on the necropsy reports or cases where the carcass had been frozen were excluded because of the importance of the tissue quality for immunohistochemistry. Finally, two American College of Veterinary Pathologists (ACVP) board-certified veterinary pathologists reviewed the haematoxylin and eosin staining (H&E staining) slides of the pancreas from all

selected cases to confirm the diagnosis of ANP (described bellow). After this selection process, 21 ANP dog cases remained, including 4 external cases and 17 VMC cases.

3.2.2 Control dogs

Six dogs euthanized at the Saskatoon Society for the Prevention of Cruelty to Animals (SPCA) for behaviour reasons (aggressive behaviour) were used as control dogs. Each dog was visually evaluated before being euthanized for general health status (hair quality, weight, energy level, alertness) and for signs of respiratory diseases such as coughing, nasal discharge, abnormal respiratory patterns and lethargy. All SPCA dogs appeared healthy. The signalment information was also recorded for every dog. Further clinical evaluation could not be performed under agreements made with the SPCA. The SPCA staff performed the euthanasia of the animals.

3.2.3 Review of ANP dogs medical records

Medical records for the 17 cases of ANP from the VMC were reviewed and data regarding the presence of respiratory clinical signs, leukograms, presence of DIC, and concomitant conditions were recorded. If multiple blood analyses were available, leukograms performed within 48 hours prior to death were used in order to be more consistent between cases. Blood work done at the time of presentation was not used as 3 cases were hospitalized 5-10 days before death for other reasons than ANP and use of those blood results would not have been representative of changes caused by ANP. Inflammatory leukograms when present were divided into

two categories based on severity: 1) inflammatory leukogram defined as white blood cell (WBC) count ≥ 20.0 X 10^9 cells/L or ≤ 4.0 X 10^9 cells/L, with ≤ 10% band neutrophils and 2) severe inflammatory leukogram defined as WBC count ≥ 20.0 X 10^9 cells/L or ≤ 4.0 X 10^9 cells/L, neutrophil count ≤ 1.0 X 10^9 cells/L, or ≥ 10% band neutrophils (2). The presence or absence of concomitant peritonitis and endocrine diseases was based on cytology of abdominal fluid and blood analyses, respectively. The presence of peritonitis was also confirmed with the post-mortem evaluation. Concomitant hepatic, renal and gastrointestinal diseases were recorded based on the post-mortem findings. For the 4 external cases, the histories provided with the post-mortem evaluation requests were considered detailed enough to be included into the case reviews. However, leukograms were not available for the 4 external cases and were not performed on 3 VMC cases.

3.2.4 Lung and pancreas tissue samples

Formalin-fixed and paraffin-embedded lung and pancreas from all 21 ANP cases were provided by the PDS of the WCVM. One paraffin block per animal per organ was used. Each lobe of the lungs and both right and left lobes of the pancreas from the control dogs was sampled (1cm^2) for fixation in 4% paraformaldehyde overnight at 4^oC (between 16-20h) followed by embedding in paraffin (see *Appendix I Table A* for complete protocol*).* In addition, portions of the lung and pancreas samples were snap-frozen in liquid nitrogen.

3.2.5 Canine pancreas histology grading

Two board-certified pathologists from the Department of Veterinary Pathology at the WCVM, who were blinded to the identity of the samples, independently graded the pancreatic histology to confirm the diagnosis of ANP. They also evaluated tissues from control dogs to ensure that they had normal pancreas. While H&E stained slides from the ANP cases were provided by PDS, I performed the staining on the tissues from the control dogs.

The pancreatic tissues from the ANP and control dogs were graded for the presence of 1) pancreatic necrosis 2) infiltration of inflammatory cells in the pancreas and 3) pancreatic edema. The evaluators also recorded the identity of the inflammatory cells infiltrating the pancreas. The scoring system is described in *Table B.* The summation of the scores obtained from each of the three criteria evaluated gave the histology score. An average was calculated from the histology scores obtained for each pathologist in order to generate a final pancreas histology score for each dog.

Table B: Grading system used to evaluate canine pancreas histology

Grading criteria	Score	Description
Pancreas necrosis	0	Absence of pancreas necrosis
	1	Necrosis in <10% of the pancreas parenchyma
	2	Necrosis in 10-25% of the pancreas parenchyma
	3	Necrosis in 25-50 % of the pancreas parenchyma
	4	Diffuse pancreas necrosis; >50% of the pancreas parenchyma
Pancreas edema	0	Absence of pancreas edema
	1	Focally increased space between lobules
	2	Diffusely increased space between lobules
	3	Pancreatic acini disrupted and separated
Infiltration of inflammatory cells in the pancreas	0	Absence of inflammatory cell infiltration in the pancreas
	1	Rare inflammatory cell or around ductal margins
	2	Inflammatory cell infiltration in the pancreas parenchyma (<50% of the lobules)
	3	Inflammatory cell infiltration in the pancreas parenchyma (>50% of the lobules)
Type of inflammation	Neutrophilic, monocytic, lymphocytic, mixed	

3.2.6 Canine lung histology grading

The lung histology from each dog was evaluated by the same two board-certified pathologists independently and they were blinded to the identity of the cases. The lungs of ANP and control dogs were scored for signs of inflammation based on 1) alveolar septa thickening and 2) the presence of lung edema. The type of inflammatory cells infiltrating the lungs was also recorded. The scoring system is described in *Table C.* The summation of the scores obtained from both criteria evaluated gave the histology score. An average was made with the histology scores obtained for each pathologist in order to generate a final lung histology score for each dog.

Table C: Grading system used to evaluate canine lung histology

Grading criteria	Score	Description
Lung edema	0	Absence of lung edema
	1	Mild lung edema
	2	Moderate lung edema
	3	Severe lung edema
Alveolar septa thickening	0	Absence of alveolar septa thickening
	1	Mild alveolar septa thickening
	2	Moderate alveolar septa thickening
	3	Severe alveolar septa thickening
Type of inflammation	Neutrophilic, monocytic, mixed	

3.2.7 Immunohistochemistry on canine lung tissue

To perform immunohistochemistry, paraffin sections of lungs from ANP and control dogs were de-paraffinized in xylene for 30 minutes and rehydrated in descending concentrations of ethanol (100%-95%-70%-50%) for 10 minutes each. The slides were then incubated with 0.5% H_2O_2 in methanol for 20 minutes to quench the endogenous peroxidase activity. Antigen retrieval was performed using pepsin (2 mg/ml in 0.01N HCl) for one hour (for macrophage, IL6, iNOS and vWF staining) or by heat-induced epitope retrieval (HIER) using boiling citrate buffer pH 6.0 in which slides were submerged in a staining rack for 20 minutes (for TLR4 staining). Both pepsin and HIER methods are used to break the tissue protein cross-linking caused by aldehyde-containing fixative such as formalin. This cross-linking can mask protein epitopes and prevent the binding of the primary antibody to its antigen resulting in a lack of staining. Blocking was done using bovine serum albumin (BSA) (1% in PBS) for 30 minutes at room temperature after which slides were incubated with the primary antibodies overnight (16 hours) at 4°C with antibodies against macrophages, IL6, TLR4, iNOS, and vWF (dilutions and antibody sources in *Table D).* Slides were washed 3x 5 minutes in PBS 1x to remove excess antibodies. Then, tissue sections were incubated for 30 minutes at room temperature with the appropriate horseradish peroxidase (HRP) conjugated secondary antibody. Color development was performed using a commercial kit (VECTOR VIP Peroxidase Substrate Kit; Vector laboratories, Burlingame, CA) followed by counter staining using nuclear counter stain methyl green (Vector laboratories). Slides were dehydrated using ascending concentration of ethanol

(50%-70%-95%-100%) 1 minute each then put in xylene for 5 minutes followed by mounting of coverslips.

The negative control consisted of omitting the primary antibody for every different secondary antibody used. In addition, isotype-matched controls were performed by substituting each primary antibody with the appropriate immunoglobulin isotype. vWF staining was used as a marker of inflammation but also as a control for the immunohistohemical protocol as it is normally present in Weibel Palade bodies (WPb) of endothelial cells.

Table D: List of antibodies used on dog lung tissues with respective dilutions and sources

Primary antibodies		
Antibody	**Dilution in BSA 1%**	**Source**
Monoclonal mouse anti-human macrophage clone MAC387 (MCA874G)	1:75	AbD Serotec
Polyclonal goat anti-mouse IL6 (sc-1265)	1:50	Santa Cruz Biotechnology
Polyclonal goat anti-mouse TLR4 (sc-12511)	1:50	Santa Cruz Biotechnology
Polyclonal rabbit anti-human iNOS (sc-651)	1:25	Santa Cruz Biotechnology
Polyclonal rabbit anti-human vWF (P0448)	1:500	DAKO
Secondary antibodies		
Horseradish peroxidase (HRP) conjugated secondary antibodies	1:100 (Except for vWF staining: 1:300)	All from DAKO

3.2.8 Quantification of MAC387 immunohistochemistry

Lung sections from ANP and control dogs were stained using the monoclonal mouse anti-human macrophage antibody (clone MAC387) as described above. This antibody binds to calprotectin (200-202), which is mainly present in macrophages, but can also be present in monocytes and neutrophils. For every ANP and control dog, positively stained macrophages/monocytes and positively stained neutrophils were counted independently in 20 fields of view at 600X following a consistent counting pattern for each slide. A field of view was considered appropriate for counting if about more than 50% of the view was covered by lung parenchyma. Fields of view where more than 50% of the area was covered with airways (bronchiole) or blood vessels were ignored moving to the next field of view. Neutrophils and macrophages/monocytes could be differentiated from each other by evaluating the cell morphology. Neutrophils showed intra-nuclear staining, therefore, making the multi-lobulated nucleus of neutrophils easy to recognize. Monocyte and macrophage reaction to the antibody was characterized by staining of the nucleus and the cytoplasm. Representative images of MAC387 staining of the different cell types are shown in *Figure 3.1.* The counts from all 20 fields of view were combined resulting in a total neutrophil count and a total macrophages/monocytes count for every dog. Those two total counts were also combined resulting in a total inflammatory cell count for every dog.

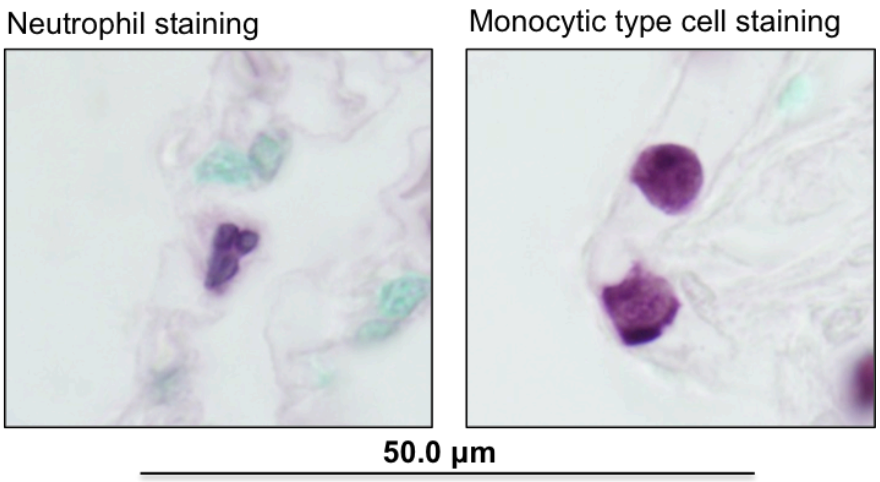

Figure 3.1. **Example of MAC387 staining.** MAC387 staining of a neutrophil (left) and mononuclear phagocytes (right) in a dog lung section.

3.2.9 Interpretation of immunohistochemical markers of inflammation

Immunohistochemistry of vWF, TLR4, IL6, and iNOS was qualitatively evaluated. For vWF staining, the presence or absence of positive staining was recorded for the following cells: 1) medium-large blood vessel endothelial cells, 2) alveolar septal capillary endothelial cells, 3) alveolar macrophages, and 4) mononuclear phagocytes in alveolar septal capillaries. For the staining of TLR4, IL6, and iNOS, the presence or absence of positive staining was recorded for the following cells: 1) airway epithelial cells (apical, cytoplasmic or basal staining) 2) medium-large blood vessel endothelial cells, 3) alveolar macrophages 4) mononuclear phagocytes in alveolar septal capillaries and 5) alveolar septa. This evaluation was performed for all dogs in the study.

3.2.10 Statistical analysis

Statistical analysis was performed using statistical software (*GraphPad Prism*, Version 5.04 for Windows, GraphPad Software, San Diego California USA). Data from the histological grading and MAC387 counting are expressed as median with the range. Comparison between control and ANP dog medians were done with the non-parametric test: Mann-Whitney U. $P < 0.05$ is considered significant.

The strength of the association between lung histology scores versus pancreas histology scores and the association between MAC387 counts and pancreas histology scores were assessed by Spearman Rank correlation coefficient. Correlation coefficients were interpreted as follows: $r = 0$, no correlation; $0 < r < 0.1$, trivial correlation; $0.1 \leq r < 0.3$, slight correlation; $0.3 \leq r < 0.5$, moderate correlation;

$0.5 \leq r < 0.7$, substantial or high correlation; and $r \geq 0.7$ very high correlation (226). Comparison of MAC387 count medians between dog cases with or without peritonitis was performed by Mann-Whitney U. $P < 0.05$ is considered significant for Mann-Whitney U test.

3.3 Results

3.3.1 Clinical description of control and ANP dogs

The signalment information for control and ANP dogs is described in *Table E*. Various breeds were represented in the ANP group with no sex predisposition. ANP dogs were generally older dogs with a median age of 8 years. All ANP dogs (except for 3 dogs) were presented to the emergency and died or were euthanized within 48 hours. The other 3 dogs were admitted 5-10 days prior to death. Clinical evidence of pulmonary complications was recorded in 4/21(19%) dogs and included pleural effusion in 3 dogs (one dog with dyspnea) and increased lung sounds only in the fourth dog. All ANP dogs that had a complete blood count (CBC) done (n=14) within the last 48 hours prior to death showed inflammatory leukograms, which was divided into two categories based on severity described earlier resulting in 3 dogs with inflammatory leukograms and 11 dogs with severe inflammatory leukograms. Concomitant conditions/complications included liver diseases, kidney diseases, peritonitis, DIC and more. The incidence of different concomitant conditions/complications is listed in *Table F.*

3.3.2 Pancreas histology grading

Representative histology of pancreas from control and ANP dogs is shown in *Figure 3.2.* The histological evaluation of pancreas of control dogs resulted in scores of ''0'' for every scoring category leading to a total pancreas histology score of ''0'' for every control dog (*n*=6), as shown in *Figure 3.3*. This confirmed that control dogs had normal histology of the pancreas and that they were suitable control animals for this study.

The results from the grading of pancreatic histology in ANP dogs are shown in *Figure 3.3* and are as follows: necrosis of pancreas (median, 2; range, 1-4), infiltration of inflammatory cells in the pancreas (median, 1.5; range, 0-3) and pancreatic edema (median, 2; range 0.5-3). The median value for the total pancreas histology scores for ANP dogs was 4.5 (range 2.5 – 9.5) indicating variation in the severity of pancreatitis among cases. The presence of pancreatic necrosis confirmed the diagnosis of ANP. The extent of pancreatic necrosis varied from <10% to > 50 % of the parenchyma. In addition, infiltration of inflammatory cells in the pancreas varied from none (4 ANP dogs) to massive infiltration in > 50 % pancreas parenchyma. The type of pancreatic inflammation when present was mainly neutrophilic (n=12), but also monocytic (n=3), mixed (n=1) and lymphocytic (n=1). Pancreatic edema varied from a focally increased space between lobules to disrupted and separated pancreatic acini. There was a moderate correlation between the severity of pancreas necrosis and the infiltration of inflammatory cells into the pancreas (Spearman Rank correlation coefficient r = 0.37).

3.3.3 Lung histology grading

Representative lung histology from control and ANP dogs is shown in *Figure 3.4.* The results from the histologic grading of lung tissue sections for signs of inflammation in ANP and control dogs are as follows: alveolar septal thickening (*control* median: 0.25; range 0-1.5, *ANP* median: 1; range 0-2.5) and lung edema (*control* median: 0.25; range 0-0.5, *ANP* median: 0.5; range 0-2). This resulted in the following total lung histology scores: control median: 0.5; range 0-2 and ANP median: 1.5; range 0-3, as shown in *Figure 3.5*. Although these results were not statistically significant, lung sections from some of the dogs suffering form ANP showed signs of lung inflammation such as moderate edema and accumulation of inflammatory cells, mostly mononuclear phagocytes, in the alveolar septa, and an increase in alveolar macrophages. The pathologists did not agree on the identity of infiltrating cells in lungs of two of the ANP dogs. One of the control dogs showed infiltration of mononuclear phagocytes corresponding to an alveolar septal thickening score of 1.5.

As for the lung edema criterion, there was an initial disagreement between pathologists regarding the true significance of the protein-rich fluid present in the alveolar spaces. Indeed, for some cases, one pathologist considered the protein-rich fluid as a real pathological edema lesion (leading to a high score for edema) and the other pathologist as an artifact (leading to a score of ‘’0’’). Therefore, a third independent pathologist evaluated the slides with lack of consensus and the scores were corrected based on the interpretation of the majority (real edema or artifact).

3.3.4 Macrophage immunohistochemical staining

Representative images of the immunohistochemical controls are shown in *Figure 3.6.* Negative control omitting the primary antibody or isotype-matched controls resulted in absence of staining in the tissues. Positive control using vWF antibody stained specifically blood vessels validating the IHC protocol. Lung sections from all ANP and control dogs were staining with monoclonal mouse anti-human macrophage antibody (clone MAC387), which recognizes the antigen calprotectin (200-202). Calprotectin is mainly expressed in macrophages but can also be present in monocytes and granulocytes. For that reason, mononuclear phagocytes (including macrophages and monocytes) and neutrophils were counted separately as described earlier. It is important to note that the MAC387 antibody did not stain alveolar macrophages; therefore, those cells were not included in the counts. Representative images of the MAC387 staining are shown in *Figure 3.7.*

The results for neutrophil counts in the lungs are as follows: for control dogs (median, 70; range 31-129) and for ANP dogs (median, 25.5; range 5-121, with one outlier at 579 cells). The decrease in the number of neutrophils in ANP dog's lung was statistically significant compared to the control dogs ($p < 0.05$) (*Figure 3.8 A)*. Neutrophils were present in alveolar septal capillaries only and not in the alveoli in both control and ANP dogs. The counts for monocytes/macrophages in the lungs are as follows: for control dogs (median:1.5; range 0-16) and for ANP dogs (median, 138; range 31-935). The increase in the number of monocytes/macrophages in lungs from ANP dogs was statistically significant compared to the control dogs ($p < 0.001$; Figure 3.8B). The total inflammatory cells (*Figure 3.8C)* in the lungs of ANP

dogs (median, 170; range 44-1100) were significantly ($p < 0.05$) more than in the control dogs (median, 71; range 33-145).

3.3.5 vWF immunohistochemical staining

Staining with a vWF antibody was used as a positive control to standardize the IHC protocol as mentioned previously. However, it was previously observed in our laboratory that the staining for vWF is increased in inflamed lungs (203). Therefore, the lungs from all the dogs in the study were stained with this antibody as a marker of inflammation.

As expected, each dog (control and ANP) showed staining of endothelial cells of larger blood vessels (*Figure 3.9 A-B)*. However, in ANP dogs, there was also robust staining of endothelial cells forming alveolar septal capillaries, which was not observed in control dogs (*Figure 3.9 C-D)*. Also, ANP dogs showed intra-cytoplasmic staining of vWF in mononuclear phagocytes infiltrating the alveolar septal capillaries (see *Figure 3.9 D-E)* and, in some cases, in the cytoplasm of alveolar macrophages (see *Figure 3.9 F)*. These two findings were not observed in control dogs. At a higher magnification, it was possible to note granular staining in the alveolar septal capillaries, which was only observed in the lungs from ANP dogs (see *Figure 3.9 D)*. A summary of the vWF staining with the frequency of each observation in the control and ANP group is described in *Table G.*

3.3.6 TLR4 immunohistochemical staining

Every control and 18 out of 21 ANP dogs showed TLR4 staining in the vascular endothelium of medium blood vessels (*Figure 3.10 A*). Only faint occasional staining was seen in mononuclear phagocytes present in alveolar septa of lungs from control dogs (*Figure 3.10 A*). Control dogs lacked staining for TLR4 in alveolar macrophages whereas half of ANP dogs showed strong TLR4 staining in the cytoplasm and nucleus of alveolar macrophages (*Figure 3.10 B*). In addition, 18/21 ANP dogs showed staining for TLR4 in inflammatory cells present in alveolar septal capillaries (mainly mononuclear phagocytes) and 4 dogs showed staining of the alveolar septal capillaries (*Figure 3.10 B*). Some staining for TLR4 was present in the airway epithelium of every control dog. The staining was granular and irregular and mainly cytoplasmic or present between epithelial cells (*Figure 3.10 C*). Interestingly, the staining pattern for TLR4 in airway epithelial cells in ANP dogs varied from cytoplasmic staining (4/21 ANP dogs), to apical staining (3/21 ANP dogs), basal staining (9/21 dogs), granular and irregular staining of the cytoplasm as in control dogs (8/21 dogs), and lack of staining on some of the epithelium (8/21 dogs) (*Figure 3.10 D*). A summary of the TLR4 staining with the frequency of each observation in the control and ANP group is described in *Table G.*

3.3.7 IL6 immunohistochemical staining

The IL6 staining was mainly observed in alveolar macrophages and mononuclear phagocytes present in alveolar septa. While nearly half of the control dogs rarely showed an alveolar macrophage positive for IL6 (*Figure 3.11 A),* 66% of

the ANP dogs showed robust staining for IL6 in alveolar macrophages and in some mononuclear phagocytes present in alveolar septa (*Figure 3.11 B)*. There was no staining of other structures of the lungs in control and ANP dogs. A summary of the IL6 staining with the frequency of each observation in the control and ANP group is described in *Table G.*

3.3.8 iNOS Immunohistochemical staining

The main finding regarding IHC staining for iNOS was the localization of iNOS in alveolar macrophages of 13/21 dogs with ANP (*Figure 3.12 B).* iNOS staining was absent in the alveolar macrophages from control dogs (*Figure 3.12 A)*. There was no staining of other structures of the lungs in control and ANP dogs. A summary of the iNOS staining with the frequency of each observation in the control and ANP group is described in *Table G.*

3.3.9 Statistical associations between lung inflammation and ANP severity

To evaluate if the severity of lung inflammation was correlated with the severity of ANP, the associations between the lung histology scores or infiltration of mononuclear phagocytes in the lungs (MAC387 counts) and the pancreas scores obtained in the different pancreatitis histology criteria were done with Spearman Rank correlation. Lung histology scores and the different pancreatitis criteria scores did not show correlation (*Table H).* However, using the counts for mononuclear phagocytes in the lungs (MAC387) instead of lung histology scores resulted in

higher correlation coefficients (*Table H).* The best correlation obtained was between the infiltration of mononuclear phagocytes in the lungs and the scores for infiltration of inflammatory cells in the pancreas with a Spearman Rank correlation coefficient of r=0.46 (or r=0.49 without the outlier value); $p < 0.05$, considered as moderate correlation. Correlation graphs are illustrated in *Figure 3.13.* As peritonitis can occur secondary to severe AP, the infiltration of mononuclear phagocytes in the lungs (MAC387 counts) was also compared between dogs with (median: 138 counts, range: 106-619) or without (median: 139 counts, range: 31-950) peritonitis but there was no statistical difference between groups (p=0.4636).

Table E: Control and ANP dogs' signalment

	Control dogs (SPCA)	**ANP dogs**
Breed	Medium-size mixed breeds: n=3 Border Collie: n=1 Dachshund: n=1 Pitbull: n=1	Terriers: n= 5 American cocker spaniel: n=3 Border Collie: n=3 Shetland sheepdog: n=3 Labrador: n=2 Toy poodle: n= 2 Pug: n= 1 Samoyed: n=1 Miniature Schnauzer: n=1
Age (y)	Median 4.5 (range 1-6)	Median 8 (range 4-12)
Sex (reproductive status)	Female: n=3 (unknown) Male: n= 3 (3C)	Female: n=9 (7S) Male: n=12 (10C)

Y: Years C: Castrated S: Spayed

Table F: Incidence of concomitant conditions/clinical findings in 21 ANP dogs

System	No of dogs (%)
From clinical assessments	
Respiratory	
• Pleural effusion (one dog with dyspnea)	3 (14%)
• Increased lung sounds only	1 (5%)
Hematopoietic (n=14 for leukograms)	
• Inflammatory leukogram*	3 (21%)
• Severe inflammatory leukogram**	11 (79%)
Peritoneum	
• Peritonitis (suppurative or necrotizing)	8 (38%)
Endocrine	
• Pre-existing diabetes mellitus	3 (14%)
• Diabetic ketoacidosis	2 (9%)
Disseminated intravascular coagulation	4 (19%)
From post-mortem diagnosis	
Hepatic	
• Chronic hepatitis	4 (19%)
• Lipidosis	5 (24%)
• Hepatic necrosis	5 (24%)
Renal	
• Glomerulonephritis	8 (38%)
• Tubular necrosis	2 (9%)
• Glomerulosclerosis	3 (14%)
• Extensive lipidosis	1 (5%)
Gastrointestinal	
• Duodenum necrosis	1 (5%)
• Enteritis (all type)	5 (24%)

* ***Inflammatory leukogram:*** *WBC count ≥ 20.0 X 10^9 cells/L or ≤ 4.0 X 10^9 cells/L, with ≤ 10% band neutrophils.* (2)

** ***Severe inflammatory leukogram:*** *WBC count ≥ 20.0 X 10^9 cells/L or ≤ 4.0 X 10^9 cells/L, neutrophil count ≤ 1.0 X 10^9 cells/L, or ≥ 10% band neutrophils* (2)

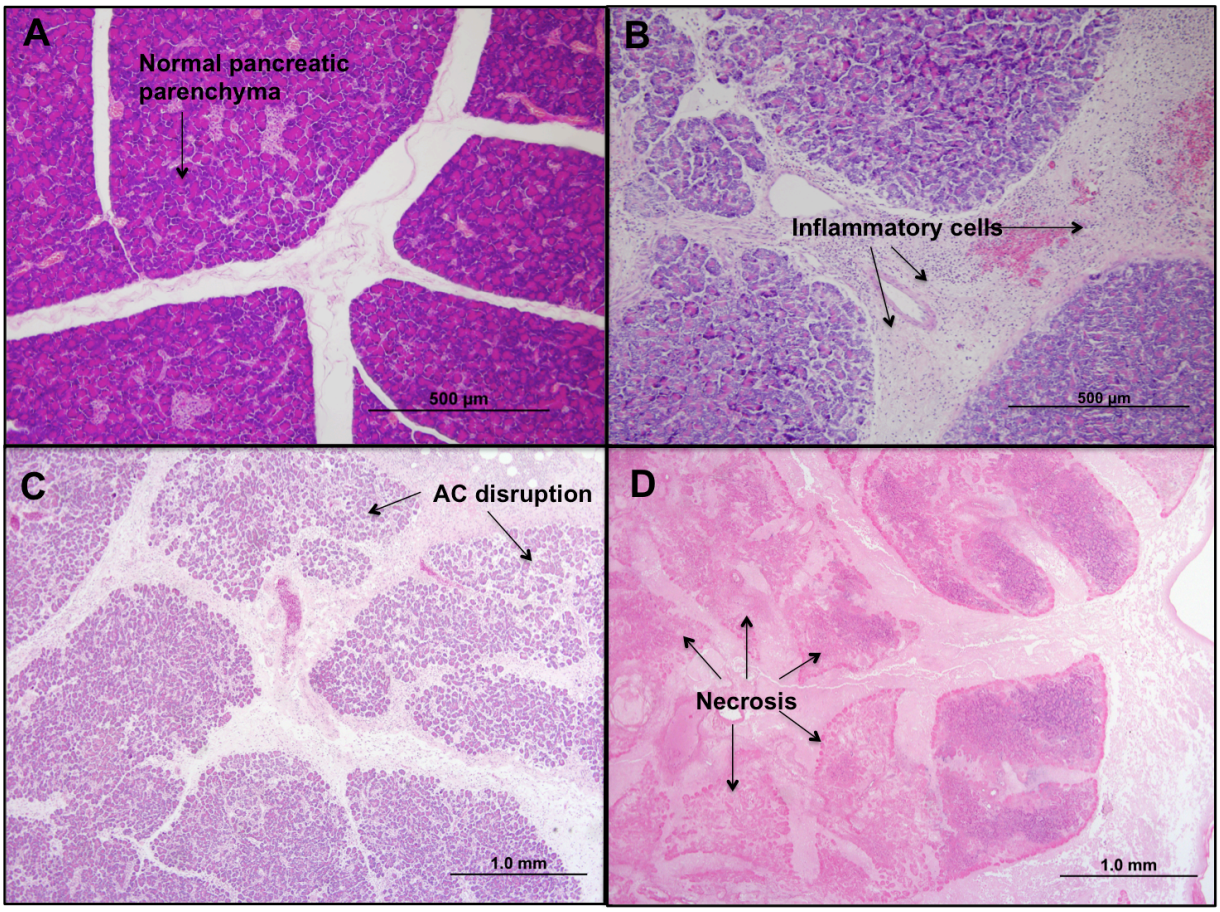

Figure 3.2. **H&E staining of dog pancreas.** (A): Pancreas histology of a control dog with normal parenchyma and clear spaces between pancreatic lobules. (B): Dog with ANP showed infiltration of inflammatory cells between pancreatic lobules, (C): acinar cell (AC) disruption and separation and (D): severe acinar cell necrosis of multiple pancreatic lobules.

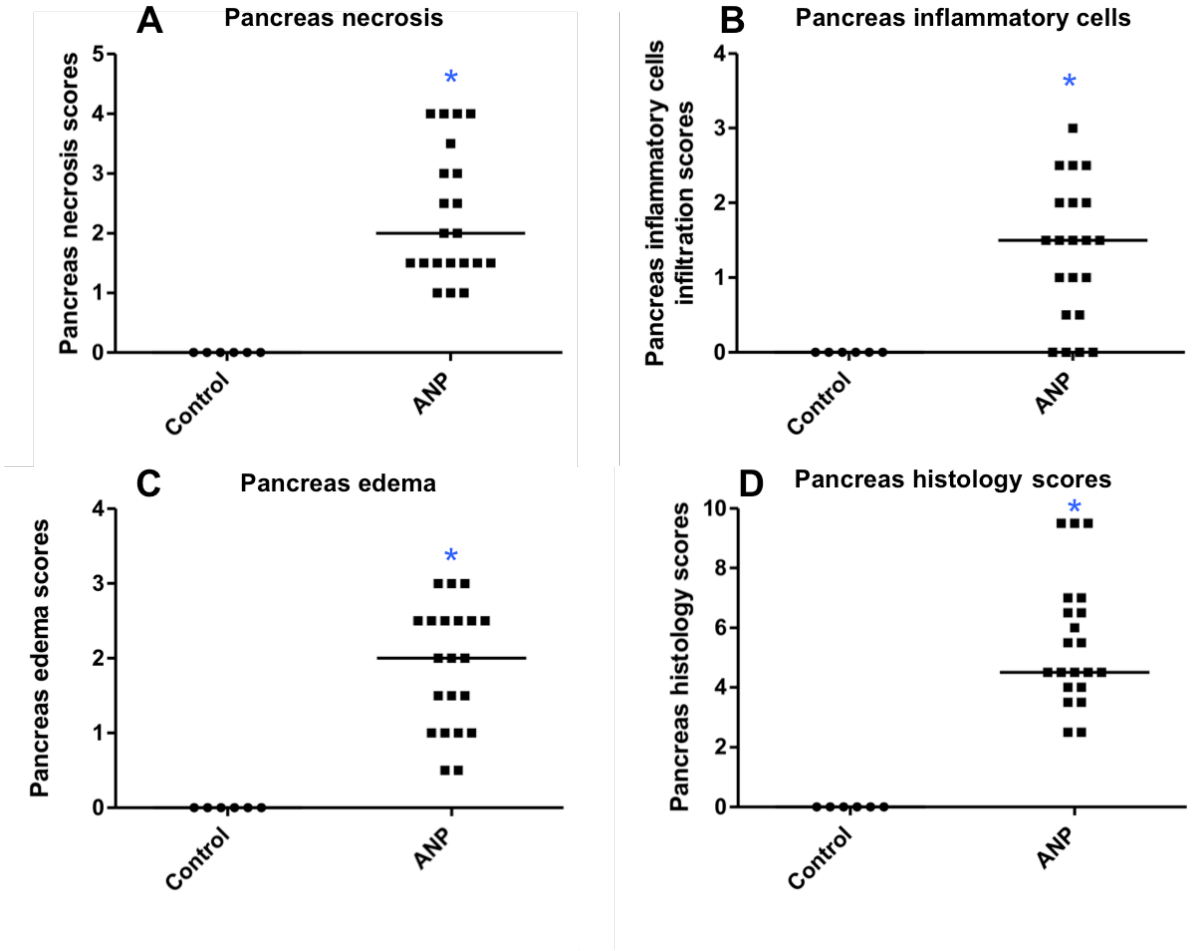

Figure 3.3. **Pancreas histology grading scores of ANP (*n*=21) and control (*n*=6) dogs.** (A): Scores for pancreas necrosis. (B): Scores for infiltration of inflammatory cells in the pancreas. (C): Scores for pancreas edema. (D): Histology scores (represent the sum of the 3 different scoring categories). Median values represented by horizontal line in graphs. Significant differences from control dogs at $p < 0.05$ denoted as asterisks (*).

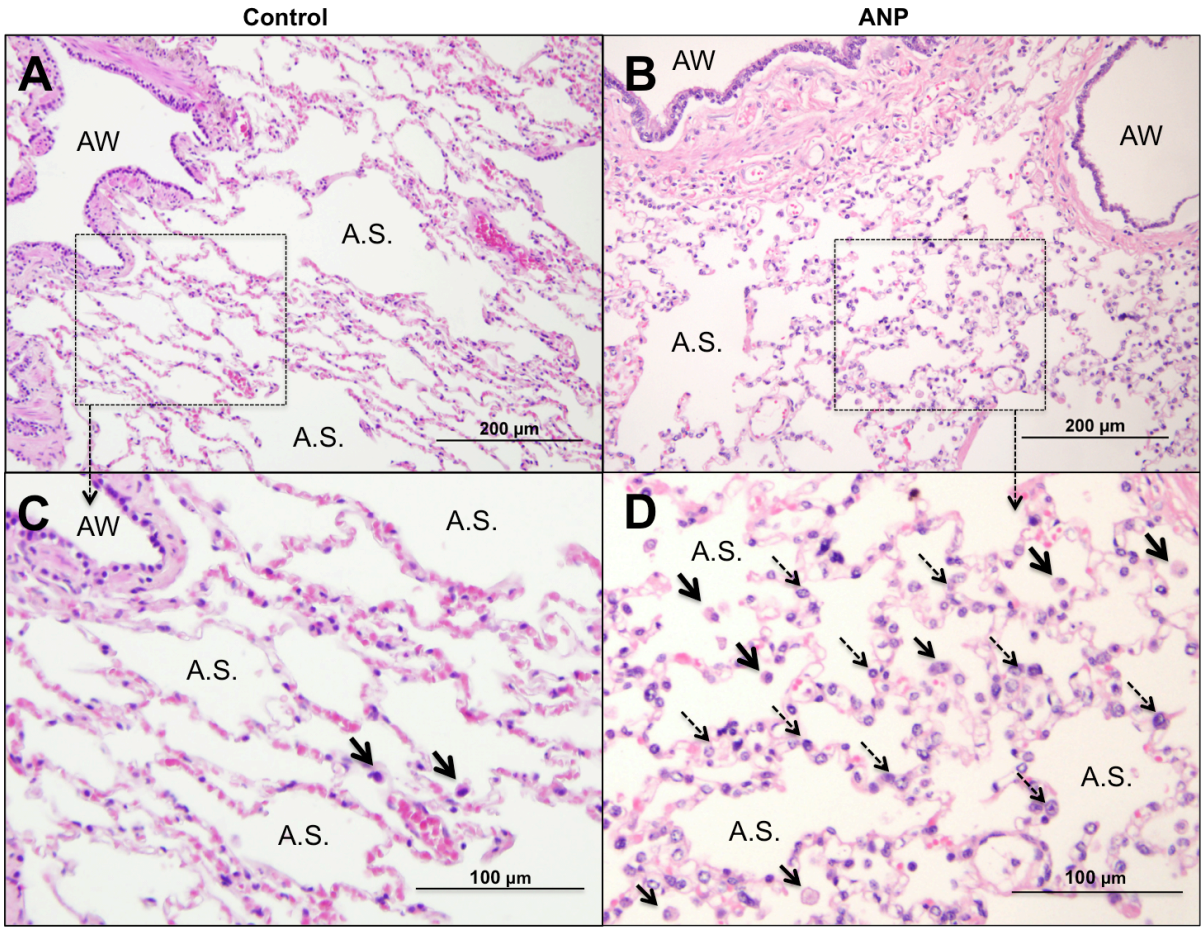

Figure 3.4. H&E staining of dog lungs. (A+C): Lungs from control dogs show normal alveolar septa with only few numbers of alveolar macrophages (arrows). (B): ANP dogs showed infiltration of inflammatory cells in alveolar septa. (D): Inflammatory cells infiltrating ANP dog's lung alveolar septa were mainly mononuclear phagocytes (dotted line arrows). In addition, increased numbers of alveolar macrophages were noted in ANP dogs (arrows). AW: Airway, A.S.: Alveolar space.

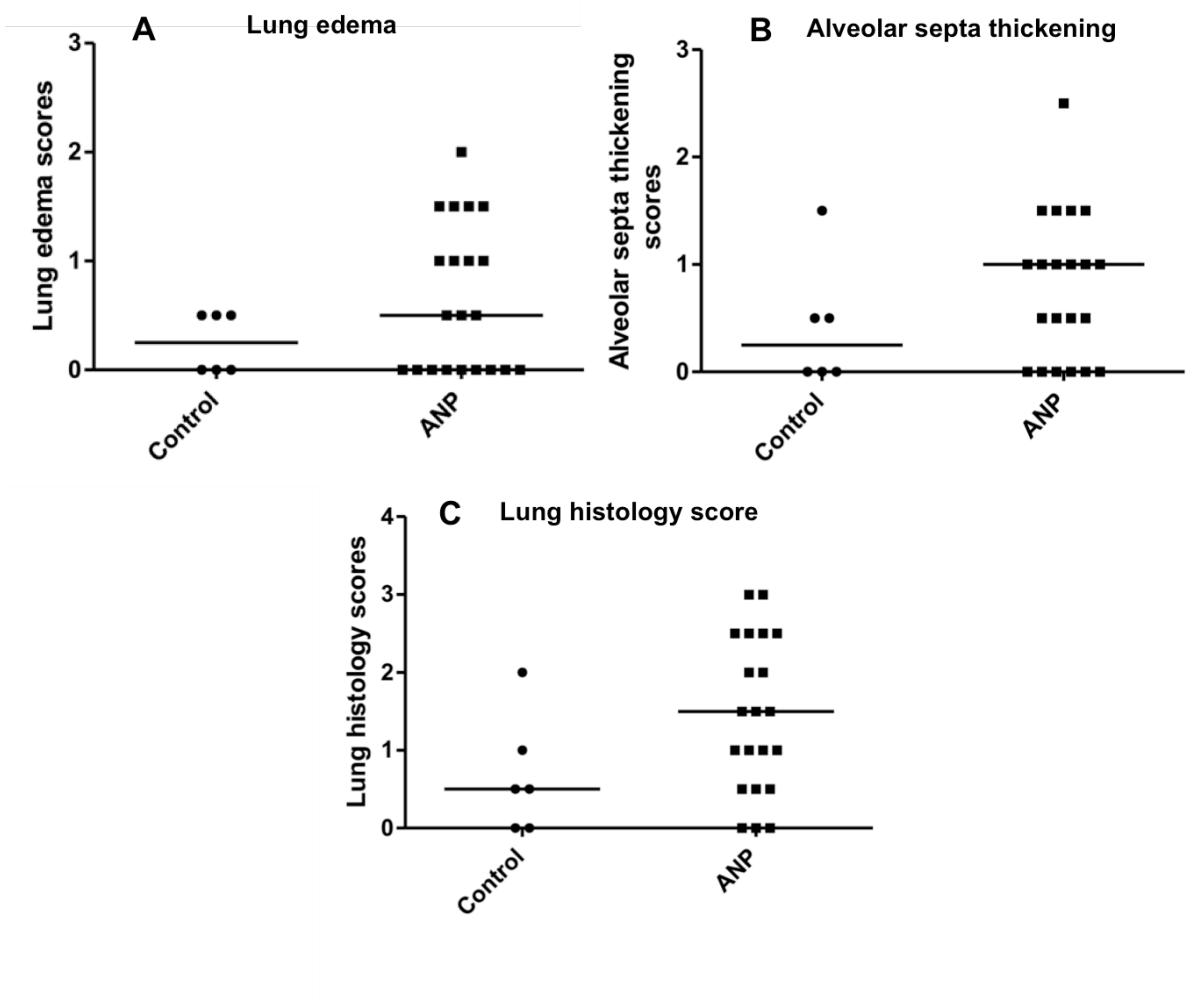

Figure 3.5. **Lung histology grading scores for ANP (n=21) and control (n=6) dogs.** (A): Lung edema scores. (B): Alveolar septal thickness scores. (C): Lung histology scores (represent the sum of the 2 different scoring categories). Median values represented by horizontal line in graphs. The scores for ANP dogs were not statistically different from control dogs.

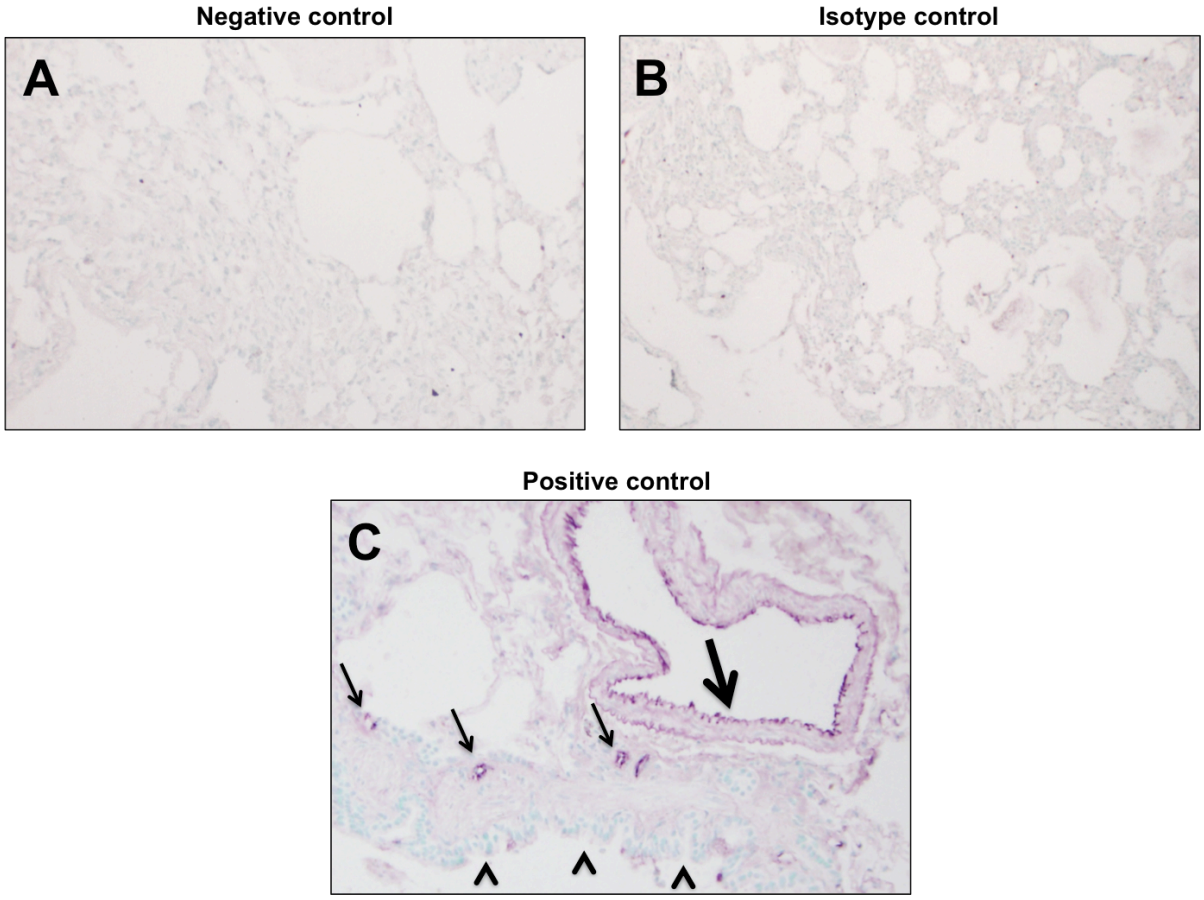

Figure 3.6. **Immunohistochemistry controls.** (A): Representative picture of the negative control omitting the primary antibody. (B): Isotype-matched control showing absence of staining. (C): Positive control using an anti-vWF antibody showing specific staining of the vascular endothelium in large blood vessel (thick arrow) and in microvessels (thin arrows). Notice that airway epithelial cells are not stained (arrowheads).

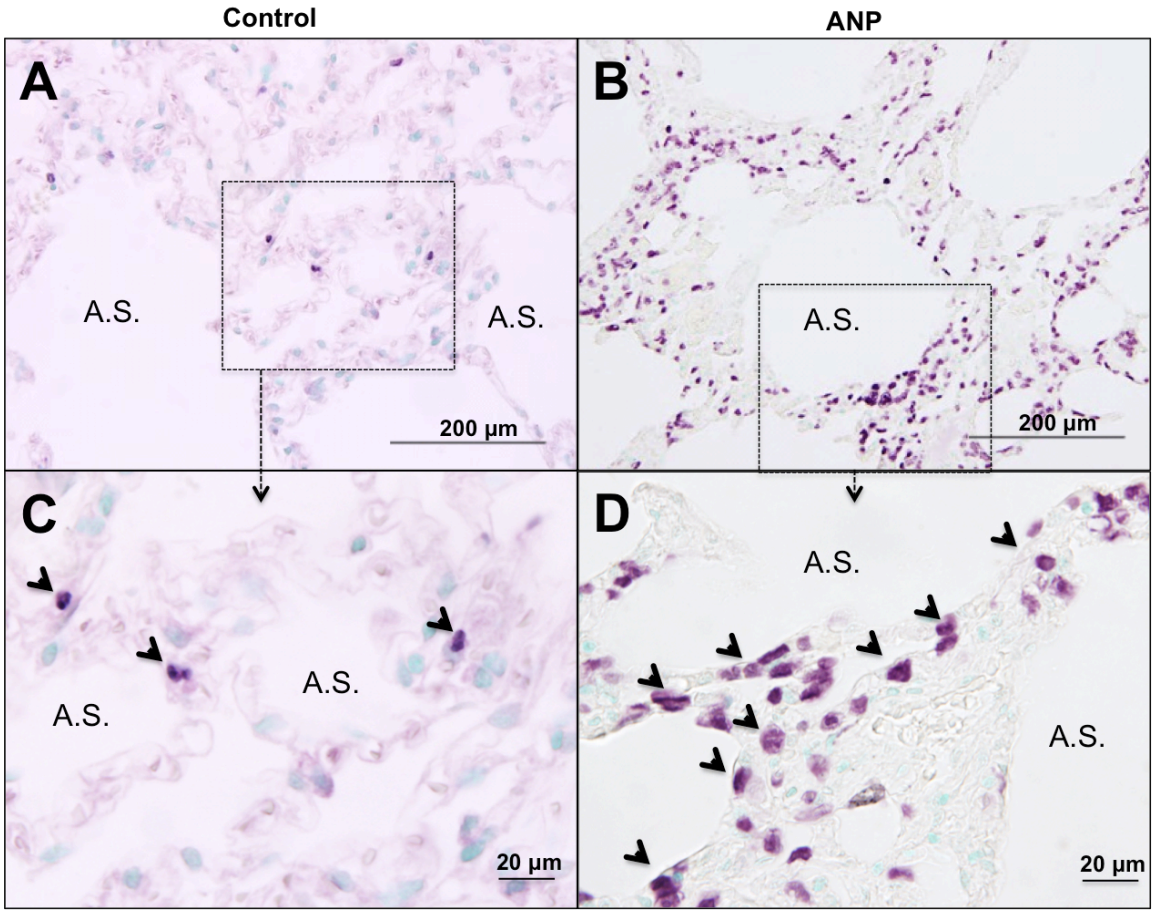

***Figure 3.7* MAC387 immunohistochemical staining in dog's lungs.** (A+C): Rare MAC387-positive cells (arrow heads) present in control dog lungs, which are mainly neutrophils. (B+D): Massive infiltration of MAC387-positive cells in alveolar septa of ANP dog lungs including neutrophils and mononuclear phagocytes.

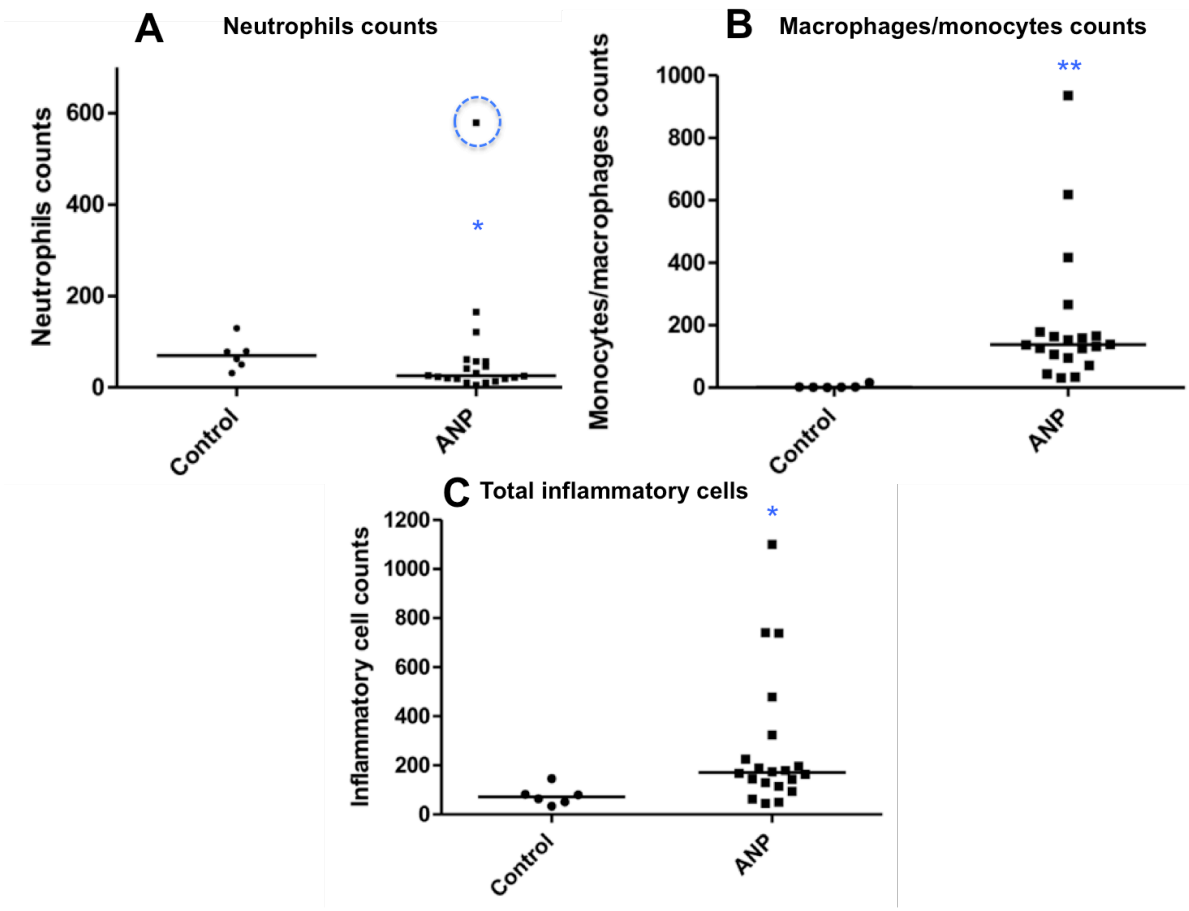

Figure 3.8 **MAC387-positive cell counts in dog lungs** (A): Neutrophils counts for controls and ANP dogs lungs. Except for one outlier case, ANP dogs had less neutrophils in their lungs compared to controls. (B): There was a significant increase of macrophages/monocytes in lungs of ANP dogs compared to control dogs. (C): Taken together, ANP dogs have more inflammatory cells infiltrating their lungs compared to the controls. Median values represented by horizontal line in graphs. One asterisk (*) denotes significant differences from control dogs at $p < 0.05$. Two asterisks (**) denotes a significant difference from control dogs at $p < 0.001$.

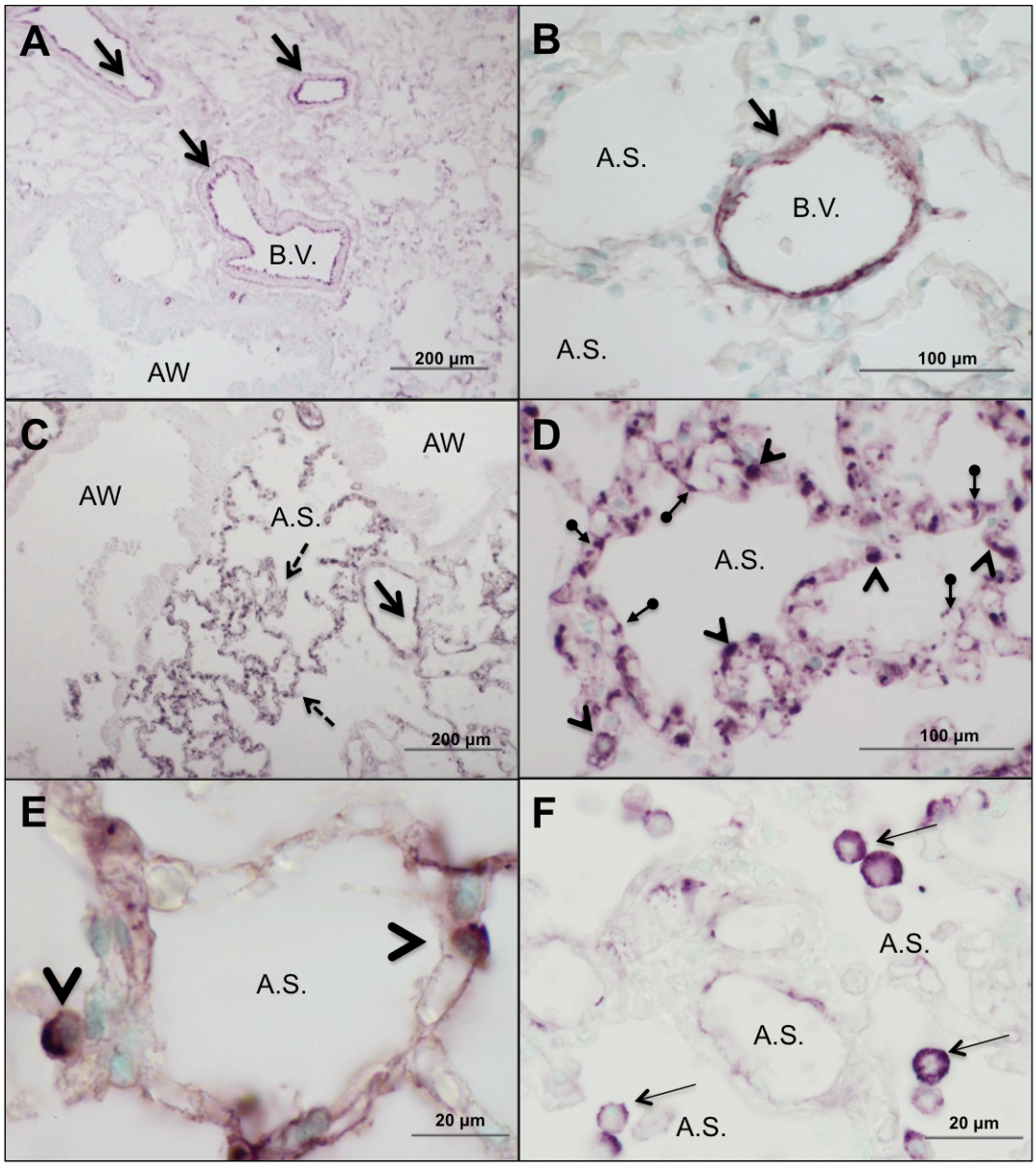

Figure 3.9. **Immunohistochemical staining for vWF in dog lungs.** (A+B): Lungs of control dogs showed staining for vWF only in endothelial cells of medium-large blood vessels (arrows). There was no staining for vWF in alveolar septa, as shown in (B). (C): As for the control dogs, ANP dogs showed staining of medium-large blood vessels (arrows) but also of alveolar septa (dotted line arrow). (D): At higher magnification, staining of mononuclear phagocytes infiltrating alveolar septa is seen (arrowheads). There is also presence of granular staining in alveolar septal capillaries (arrow with circle) of unknown nature. (E): Positively stained mononuclear phagocytes (arrowheads) with strong staining of the cytoplasm. (F): Positively stained alveolar macrophages (thin arrows) with strong staining of the cytoplasm. AW: Airway, A.S.: Alveolar space, B.V.: Blood vessel.

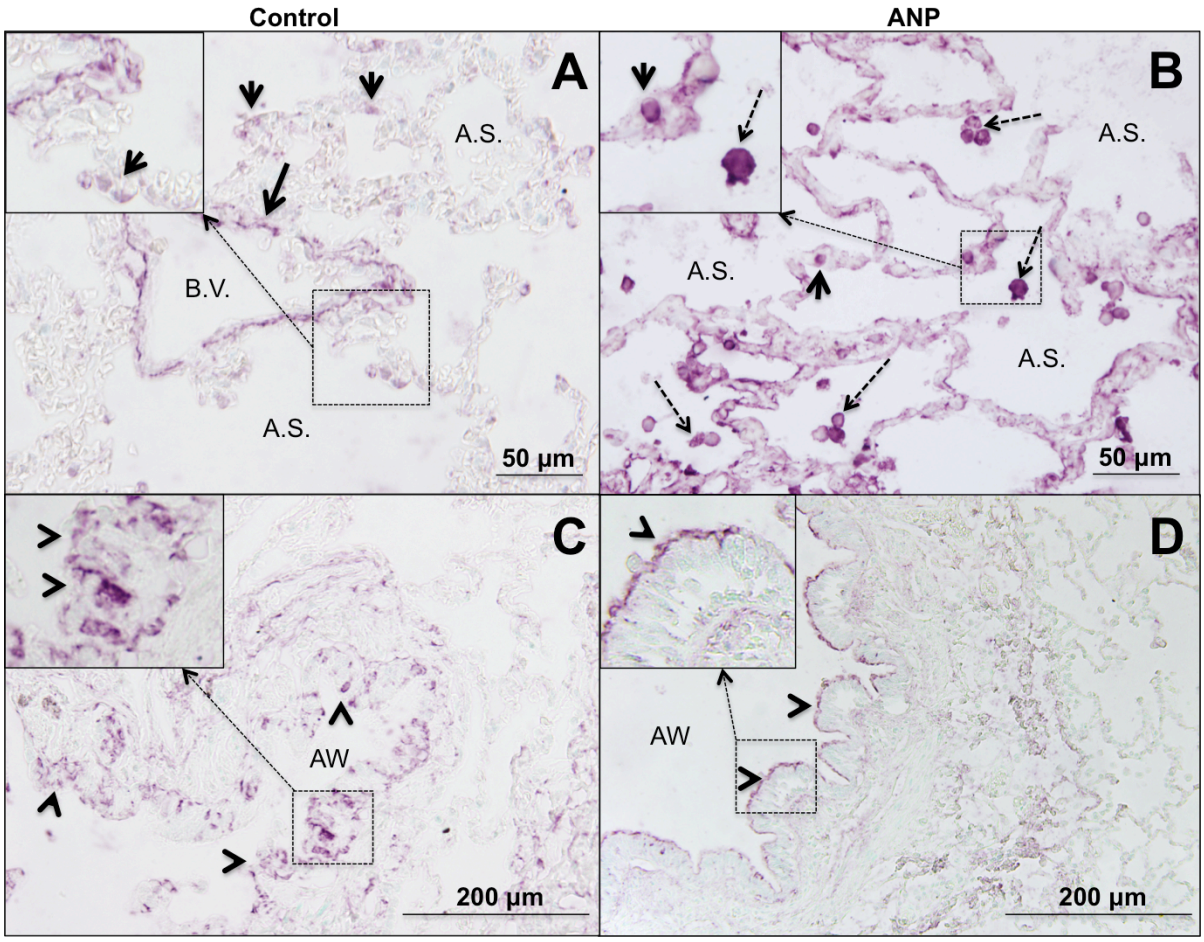

Figure 3.10. **Immunohistochemical staining for TLR4 in dog lungs.** (A): Control dogs showed TLR4 staining of the vascular endothelium (arrows) and occasional pale staining of inflammatory cells in alveolar septal capillaries (small arrows). (B): ANP dogs showed strong TLR4 staining in the cytoplasm and nucleus of alveolar macrophages (dotted line arrow). There are also positive inflammatory cells in alveolar septal capillaries (small arrows)(C): Airway epithelial cells in control dogs showed a granular and irregular TLR4 staining whereas airway epithelial cells in ANP dogs showed different staining pattern of TLR4 such as apical staining as shown in (D)(airway staining indicated by arrow heads).

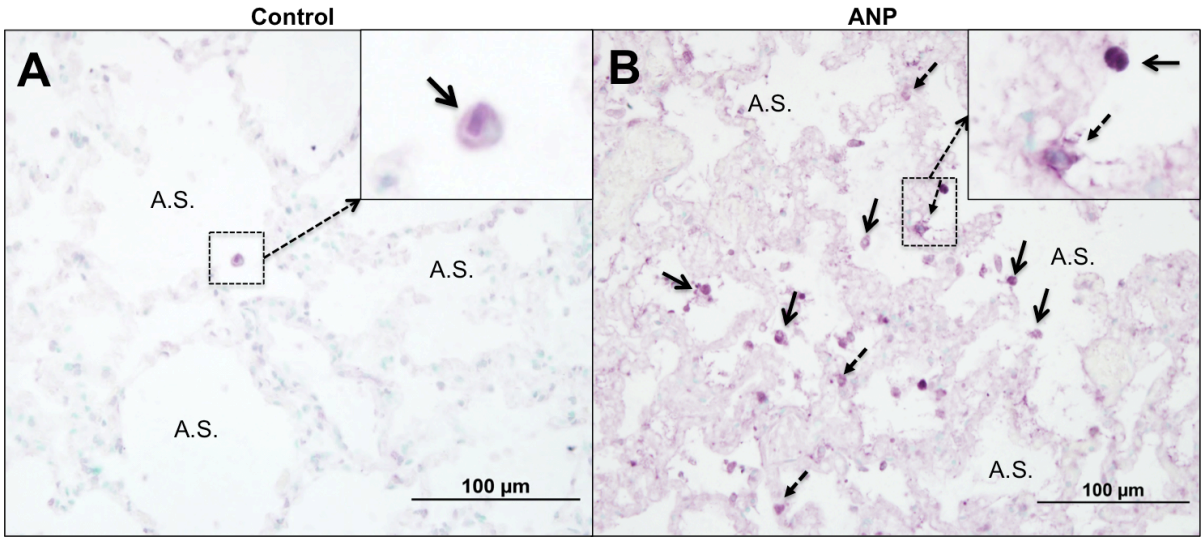

***Figure 3.11.*Immunohistochemical staining for IL6 in dog lungs.** (A): Occasionally, alveolar macrophages were observed with nuclear staining (arrow) for IL6 in some of the control dogs (B): In half of ANP dogs, strong intracytoplasmic and intranuclear staining for IL6 was noted in numerous alveolar macrophages (arrows) and in mononuclear phagocytes in alveolar septa (dotted line arrows).

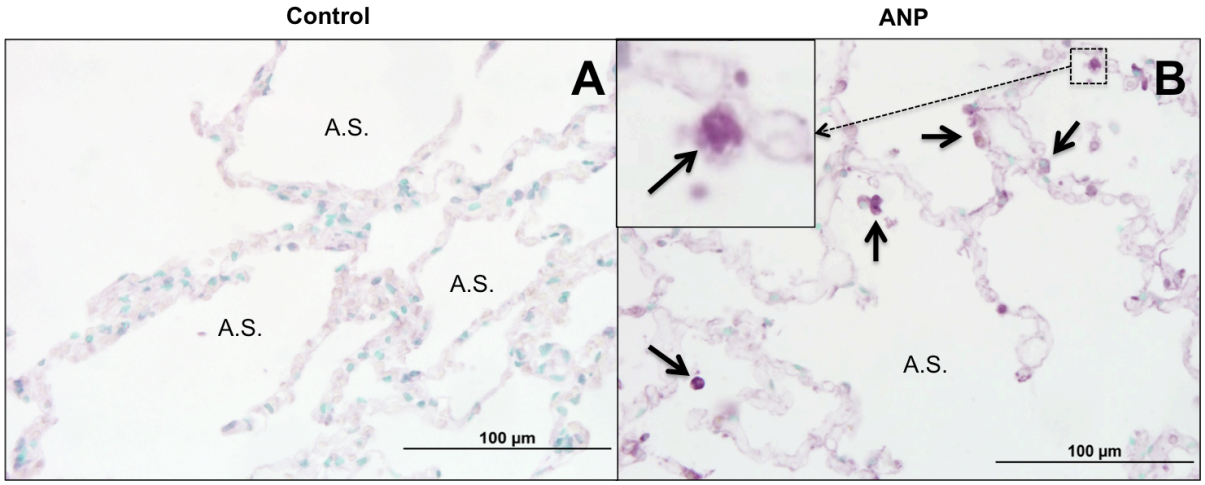

***Figure 3.12.*Immunohistochemical staining for iNOS in dog lungs.** (A): Control dogs did not show any iNOS staining. (B): ANP dogs showed iNOS staining in the nucleus, cytoplasm or both in alveolar macrophages in some cases (arrows in B indicate stained alveolar macrophages)

Table G: Summary of immunohistochemistry for inflammatory markers in ANP and control dog's lung

	vWF	**TLR4**	**IL6**	**iNOS**
Alveolar macrophages	**Ctl :** 0 % (0/6) **ANP:** 48% (10/21)	**ctl** : 0 % (0/6) **ANP:** 48% (10/21)	**ctl:** 50% (3/6) ** **ANP:** 66% (14/21) **	**ctl :** 0 % (0/6) **ANP:** 62% (13/21)
Mononuclear phagocytes in septa	**Ctl :** 0 % (0/6) **ANP:** 76% (16/21)	**ctl** : 0 % (0/6) **ANP:** 86% (18/21)	**ctl :** 0 % (0/6) **ANP:** 62% (13/21)	**ctl :** 0 % (0/6) **ANP:** 0% (0/21)
Vascular endothelial cells (med-large b.v.)	**Ctl :** 100% (6/6) **ANP:** 100% (21/21)	**ctl :** 100% (6/6) **ANP:** 86% (18/21)	**ctl :** 0 % (0/6) **ANP:** 0% (0/21)	**ctl :** 0 % (0/6) **ANP:** 0% (0/21)
Vascular endothelial cells (capillary)	**Ctl :** 0 % (0/6) **ANP:** 95% (20/21)	**ctl :** 0 % (0/6) **ANP:** 19% (4/21)	**ctl :** 0 % (0/6) **ANP:** 0% (0/21)	**ctl :** 0 % (0/6) **ANP:** 0% (0/21)
Airway epithelial cells	**ctl :** 0 % (0/6) **ANP:** 0% (0/21)	**ctl :** 100% (6/6) * **ANP:** 76% (16/21) *	**ctl :** 0 % (0/6) **ANP:** 0% (0/21)	**ctl :** 0 % (0/6) **ANP:** 0% (0/21)

The percentage (%) refers to the percentage of dogs showing staining for each inflammatory marker. The numbers in parenthesis ( ) represent the absolute number of dogs showing staining over the total n number (n=6 for control dogs, n=21 for ANP dogs)

** Indicated results for TLR4 staining of airway epithelial cells corresponds to the total number of dogs showing any pattern of epithelial cell staining. Refer to the text for the frequency of each type of epithelial staining (apical, basal, cytoplasmic)*

*** Even if the % do not illustrate it, the IL6 staining of alveolar macrophages differed between control and ANP dogs in the nature of the staining and the number of positively staining alveolar macrophages.*

B.v.: blood vessels

Table H: Spearman rank correlation coefficients for different associations between the lungs and pancreas in ANP dogs.

Lung variable (Dependant variable)	**Independent variable**	***Spearman coefficient r (p value)***
Lung histology scores	Pancreas histology scores	0.18 (p=0.45)
Lung histology scores	Pancreas necrosis scores	0.16 (p=0.49)
Lung histology scores	Pancreas inflammatory cell scores	0.05 (p=0.81)
Lung mononuclear phagocytes (MAC387) *(Without outlier)*	Pancreas histology scores	0.34 (p=0.13) *(0.41, p=0.07)*
Lung mononuclear phagocytes (MAC387) *(Without outlier)*	Pancreas necrosis scores	0.17 (p=0.48) *(0.35, p=0.13)*
Lung mononuclear phagocytes (MAC387) *(Without outlier)*	Pancreas infiltration of inflammatory cells scores	0.46 ($p < 0.05$) *(0.49,* $p<0.05$)

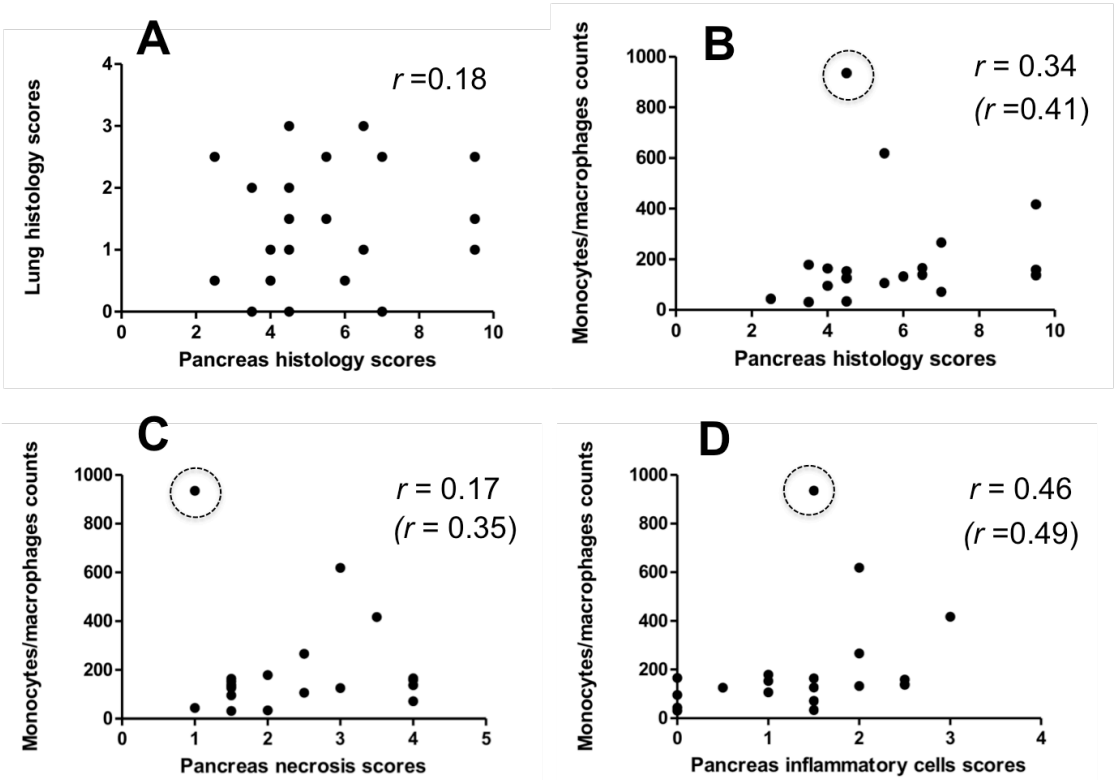

Figure 3.13. **Spearman Rank correlations between lung inflammation and pancreatitis scores in ANP dogs.** (A): Association between lung histology scores and pancreas histology scores. (B): Correlation between macrophages/monocytes positive with MAC387 antibody and pancreas histology scores. (C): Correlation between macrophages/monocytes positive with MAC387 antibody and pancreas necrosis scores and (D): Correlation between macrophages/monocytes positive with MAC387 antibody and pancreas inflammatory cell scores. The coefficient *r* value in parenthesis represents the *r* value after excluding the outlier value (indicated with the pointed circle).

3.4 DISCUSSION

Until now, there was only a single case report published in 1995 describing lung histology of a 3 year old dyspneic miniature poodle dog with ANP (16). To my knowledge, I present the first evaluation of the lung histopathology of a group of clinical cases of dogs that suffered from ANP. This study includes histological and immunohistochemical data from 21 dogs that died or were euthanized with a diagnosis of ANP between the years of 2000-2013. The data show that although only 4/21(19%) dogs with ANP presented clear clinical evidence of pulmonary complications, most of ANP dogs showed histological signs of lung inflammation. In addition, immunohistochemical analyses showed significant infiltration of mononuclear phagocytes in the alveolar septa of the lungs of dogs suffering from ANP, which suggested that PIMs are induced in dogs suffering from ANP. Furthermore, increased levels of TLR4 and IL6 in lungs of ANP dogs were associated with the recruitment of PIMs and indicate the presence of acute lung inflammation. There was also induction of iNOS in alveolar macrophages, which may be a protective mechanism occurring during ANP to prevent further lung injury. Finally, this study revealed that lungs of ANP dogs showed evidence of a strong microvascular response indicated by robust staining for vWF in endothelial cells of septal capillaries. The findings reported in this study are valuable as most of the knowledge about lung injury associated with AP comes from rodent models and this is the first time that lung inflammation in spontaneous cases of ANP in dogs is described. Furthermore,

this is the first study investigating the recruitment of PIMs in a large group of dogs presenting with clinical diseases.

3.4.1 Clinical features of ANP dogs

The medical records revealed that ANP dogs included in this study were mostly older dogs (median of 8 years old) of various breeds and with no sex predisposition. All ANP dogs were presented to the emergency with high morbidity and most of them died or were euthanized within 48 hours after presentation. All dogs that had CBC's performed within 48 hours prior to death (n=14) showed inflammatory leukograms indicative of severe inflammatory processes and systemic inflammatory response syndrome. May be due to older age of the patients, we found high incidences of kidney diseases, including glomerulonephritis (38%) and glomerulosclerosis (14%), and liver diseases such as chronic hepatitis (19%) were recorded. Other concomitant conditions present included pre-existing diabetes mellitus (14%), diabetic ketoacidosis (9%) and various types of enteritis (24%). Clinical and pathological findings that could have been complications of ANP included peritonitis (38%), hepatic necrosis (24%), DIC (19%), renal tubular necrosis (9%), and duodenal necrosis (5%).

The incidence of concomitant conditions/complications previously reported in two retrospective studies reviewing the medical records of 61 dogs with AP (2) include: pre-existing diabetes mellitus (6.6%), diabetic ketoacidosis (13%), peritonitis (59%), and coagulation abnormalities including DIC (11.5%), and for the second retrospective study of 80 AP dogs (5): pre-existing diabetes mellitus

(36%), hepatopathy (21%), gastrointestinal disorders (5%) , leukocytosis and/or left shift (>10% band neutrophils) (91%) and DIC (4%). Even if the incidences of each concomitant condition may vary between studies, the main concomitant conditions and complications reported in those two retrospective studies correspond to my findings to suggest that ANP dogs in my study may broadly represent the dogs suffering from AP. The information collected from the medical records of dogs with ANP illustrate that various factors can be involved in the development of pulmonary complications during ANP. Although the influence of other clinical factors on the development of AP makes it challenging to interpret the results, such complexity makes the study stronger compared to rodent models.

As for the clinical signs of pulmonary complications, the previous retrospective studies reported clinical evidence of dyspnea or tachypnea in 4/61 AP dogs (7%) (2) and 18/80 AP dogs (23%) (5). In my study, I recorded that 4/21 (19%) had pulmonary complications including 3 dogs with pleural effusion and one dog with only increased lung sounds upon auscultation. One dog with pleural effusion had dyspnea. The incidence of pulmonary complications reported in my study remains slightly lower than what is published for human patients with severe AP where the incidence of pulmonary complications range between 18-46% (12-15).

3.4.2 Mechanisms of lung inflammation in ANP dogs

The histological evaluation of the lungs of dogs that suffered from ANP revealed that most cases had signs of lung inflammation characterized by significant recruitment of monocytes and macrophages in alveolar septa, which was confirmed with immunohistological staining using MAC387 antibody. Unlike the data from most studies using rodent models of AP (64, 156, 159), the lungs from ANP dogs did not show recruitment of neutrophils in alveolar septa or alveolar spaces. The main purpose of this study was to assess the recruitment of PIMs in the lungs of ANP dogs although, as the MAC387 antibody detects both macrophages and monocytes, I cannot state that all of the MAC387-positive cells are macrophages. Also, the resolution of the light microscope does not lend itself to demarcate the septal interstitium from the septal capillary lumen to distinguish between interstitial versus the intravascular macrophages. However, considering that interstitial macrophages are much fewer in numbers and challenging to observe with a light microscope, I believe that most of the positive cells are PIMs.

PIMs are now established critical regulators of lung inflammation in the species where they are normally present as well as those in which the PIMs are induced through physiological stress such as bacterial infections or liver dysfunction (111, 112). Dogs are one of the species that lack constitutive PIMs (118-120) and there has not been any investigation of PIM recruitment in dogs suffering from clinical diseases. The reason we need to understand whether PIMs are recruited in any systemic condition is the ability of induced PIMs to exacerbate inflammation in the lungs and to increase the mortality following

secondary microbial challenges (111). This is highly relevant regarding ANP patients as secondary gut barrier dysfunction leading to endotoxemia is a known complication in human patients (198, 199) and is often suspected clinically in dogs. Therefore, it is important to investigate the recruitment and function of PIMs in dogs suffering from ANP.

As mentioned previously, lungs from ANP dogs showed reduced amount of neutrophils compared to control dog lungs. There are various explanations possible for this finding. It is possible that neutrophils are being massively recruited and sequestered into the pancreas during the early phase of ANP and therefore are not available to infiltrate the lungs. It is possible that activated cells in the lung during ANP do not produce chemokines such as MIP and IL-8, which attract neutrophils, but rather produce chemokines such as MCP-1 that recruit monocytes and macrophages. Also, ANP dogs may be euthanized after the phase where neutrophils are recruited to the lungs, which would occur in the early phase of ALI. As for the outlier case showing substantial numbers of neutrophils in the lungs it is possible that this case had another cause of ALI independent of ANP.

A second major finding in this study is the robust staining for vWF in the alveolar septal capillaries in all ANP dogs compared to lack of staining in septal capillaries in lungs from control dogs. During inflammation or vascular injury, endothelial cells release the content of Weibel-Palade Bodies, which contain IL-8, P-selectin, and vWF (204, 205). It is known that a portion of the released vWF remains attached to the endothelial cell surface to allow adhesion of platelets

during initiating of the coagulation cascade (206). During ANP, pancreatic proteases including trypsin, elastase, and PLA_2 are released into the blood circulation (149) and are capable of causing vascular injuries (149, 156-158). Therefore, one hypothesis for the presence of vWF in alveolar septal capillaries of ANP dogs would be that circulating pancreatic enzymes could activate and injure the lung microvasculature and induce the synthesis and release of vWF in an attempt to repair the damaged endothelium and prevent hemorrhage or increase in vascular permeability. The granular vWF staining on the capillary endothelial cells may be interpreted as localized accumulation of secreted vWF or clustering of blood-borne vWF. It was previously proposed in our laboratory that this granular vWF staining may be aggregation of platelets containing vWF, but dog platelets do not contain vWF as opposed to other species (207, 208). It is however possible that this type of staining corresponds to vWF-platelet complexes (209). I did not observe vWF staining in alveolar septal capillaries in control dogs possibly because vWF is only synthesized in those blood vessels during inflammation rather than in resting endothelial cells. A similar phenomenon was observed for the presence of IL-8 in Weibel-Palade Bodies where this chemokine was only present during inflammation and not in resting endothelial cells (210, 211).

In addition to being involved in hemostasis, vWF has a direct role in inflammatory processes such as providing binding sites for leukocyte receptors including P-selectin glycoprotein ligand-1 (PSGL-1) and integrin-β2 and therefore promoting rolling and adhesion of leukocytes to the endothelium (212) (213). It

was also reported recently that vWF can bind to the cell receptor named Singlec-5 present in various human immune cells including macrophages, which led to internalization of vWF in early endosomes (214). Although Singlec-5 is not well conserved between species, a similar mechanism could be occurring in dogs with ANP to clear excessive circulating vWF, which needs to be further investigated. This is interesting as intravascular mononuclear phagocytes and alveolar macrophages of a few of the ANP dogs showed cytoplasmic staining for vWF suggesting that vWF was internalized in those cells. Another suggestion that may be investigated to explain this finding could be that alveolar and intravascular macrophages simply bind to extra-cellular secreted vWF. Finally, expression of vWF in the lung microvasculature of ANP dogs may have indirect pro-inflammatory effects as it allows platelets to aggregate in the lungs and various inflammatory roles have now been attributed to platelets including facilitating leukocyte recruitment to the site of inflammation (215). The recruitment of platelets by vWF may also be one of the mechanisms for the recruitment of PIMs in the lungs of ANP dogs.

Since endotoxin or bacterial translocation from the gut is a possible complication during ANP (198) (199), the expression of TLR4 in the lungs of ANP dogs was assessed with immunohistochemical staining. Staining for TLR4 was present in the airway epithelium, vascular endothelium of medium-large blood vessels, and occasional septal monocytes and alveolar macrophages of control dogs. The staining for TLR4 observed in control dogs corresponded to what was previously reported regarding TLR4 staining in normal lungs from cattle, pigs and

horses (216) (86) (134) (98, 217). In lungs of ANP dogs, TLR4 staining was localized in the numerous newly recruited mononuclear phagocytes, mostly PIMs, and alveolar septal capillaries and in alveolar macrophages of some cases. The TLR4 staining in PIMs has been shown in veterinary species including pigs, horses, and cattle (86, 134, 216) and role of PIMs in adding to the total amount of TLR4 mRNA in the lung was demonstrated through significant reduction in TLR4 mRNA amount following depletion of PIMs (134, 135). The recruited septal and alveolar macrophages in dogs with ANP may increase the amount of total TLR4 in the lungs, which would increase the susceptibility for endotoxin-induced lung inflammation as well as contribute to the release of excessive cytokines into circulation. Lungs of rats with acute haemorrhagic necrotizing pancreatitis have increased levels of TLR4 mRNA and protein (174). Interestingly, in contrast to the control dogs, some medium sized blood vessels and airway epithelium in ANP dogs did not show TLR4 staining. Similar observations were also reported in inflamed lungs from *Mannheimia hemolytica*-infected calves and *Pasteurella multocida*-infected Water buffalo (91)(216). The reason for this loss of TLR4 expression in blood vessels and airway epithelium is not clear but could be a protective mechanism to reduce endotoxin-induced inflammtion of the infected lungs.

To further assess the pro-inflammatory response in lungs of ANP dogs, immunohistochemistry for IL6 was performed, which is an important pro-inflammatory cytokine produced during acute inflammation and during SIRS. Similar to the expression of TLR4, increased staining for IL6 was present in lungs

of ANP dogs most likely due to the recruitment of septal macrophages and activation of alveolar macrophages. This corresponds to the report of increased levels of IL6 along with TLR4 in the lungs of rats with acute haemorrhagic necrotizing pancreatitis (174). IL6 staining in septal mononuclear phagocytes suggests that PIMs are pro-inflammatory and participate in the production of pro-inflammatory cytokines released in the systemic circulation during ANP.

Finally, alveolar macrophages showed staining for iNOS in some ANP cases. The staining for iNOS is interesting as the study of the role of NO in ALI associated with experimental AP has led to contradicting results. Indeed, NO has been attributed both pro and anti-inflammatory effects during ALI associated with AP in rodent models (164) (140) (174). Although this is only speculation, the induction of iNOS in lung macrophages may constitute a protective mechanism against lung injury during ANP by promoting vasodilatation and preventing vascular congestion or occlusion of capillaries caused by formation of thrombi secondary to excessive expression of vWF in those blood vessels. However, the possibility that NO could cause oxidative stress and create further lung injury must also be considered.

3.4.3 Correlation between lung inflammation and ANP severity

This study also assessed whether the severity of pancreatitis lesions had an effect on the recruitment of monocytes/PIMs in the lungs during ANP. The results showed that the amount of inflammatory cells infiltrating the pancreas (based on histological scoring) was moderately correlated to infiltration of

monocytes/PIMs in the lungs. Furthermore, the presence of inflammatory cells in the pancreas was correlated more to recruitment of monocytes/PIMs in the lungs than the presence of pancreatic necrosis lesions. This suggests that inflammatory mediators released by inflammatory cells present in the pancreas during ANP are more involved in the pathophysiology leading to lung injury than are the products released in the blood circulation by necrotic acinar cells.

3.4.4 Limitations and flaws

A larger study size for both control dogs and ANP cases could have helped to improve the statistical significance. The sample size for ANP cases was limited for two main reasons. First, not all ANP dogs' owners agreed to perform a post-mortem examination on their dog. Second, not all ANP cases had both lung and pancreas tissues available in PDS. Although, to increase the sample size, 4 external cases were added to this study, but the complete medical records for those dogs were not available. As for control dogs, it was challenging to find healthy dogs with normal lung and pancreas that had to be euthanized. Although control dogs from the SPCA seemed visually healthy, we could not do clinical evaluation than a visual assessment to rule out presence of subclinical conditions in those dogs.

As this study used retrospective clinical cases of ANP in dogs, various clinical factors may have varied among cases influencing the lung results and include the period of time between the ANP onset and death, treatments received during hospitalization such as anti-inflammatory drugs, analgesics,

diuretics and antibiotics and previous history of lung diseases. In addition, the presence of concomitant conditions/complications in the ANP cases was reported in this study but their effect on the lungs could not be assessed.

Also, using tissue samples from retrospective cases brings the issues of variable sampling, fixation, and processing protocols, which can have consequences on the immunohistochemical staining quality causing inconsistent staining intensity among cases and making the interpretation challenging. In addition, since fixation of the lung in a clinical setting does not include instillation of fixative into the airways, the preservation of the lung morphology between cases varied resulting in different levels of atelectasis, which may have influenced the immunohistochemistry to some degree. The study design was also limited by the fact that very few antibodies are available for dog tissues and antibody with mouse or human specificity had to be tried and standardized. I also failed to find a specific antibody for macrophages that does not also bind to monocytes that would have been better to study the presence of PIMs, which however is a minor issue.

3.4.5 Conclusion

Because there has been clinical evidence of pulmonary complications in clinical cases of AP in dogs, we sought to determine recruitment of PIMs in our study, and our data show significant recruitment of septal mononuclear phagocytes, mostly PIMs, in the lungs of dogs that suffered from AP. The interaction between expression of vWF in alveolar septal capillaries and the recruitment/adhesion of PIMs in the microvasculature of ANP dog lungs would be interesting aspect for additional studies. In addition, based on what we know about PIMs in other species, the increase in the number of PIMs along with increased expression of TLR4 in ANP dog lungs would increase their susceptibility for enhanced lung inflammation in response to exposure to further microbes or their products during the course of ANP. This could be one of the explanations for the higher incidence of pulmonary complications in humans than in dogs. Indeed, people with ANP are generally kept alive longer compared to dogs suffering from ANP, which are often euthanized earlier in the course of the disease because of significant abdominal pain or financial issue. Therefore, the longer clinical care of humans with severe AP is more likely to expose them to secondary lung challenges leading to exaggerated lung inflammation and respiratory distress. Overall, dogs suffering from ANP should be closely monitored for signs of respiratory complications, especially if they develop endotoxemia or if they are at risk of being exposed to secondary microbial respiratory challenges during the course of the hospitalisation.

CHAPTER 4: MOUSE MODEL OF ACUTE NECROTIZING PANCREATITIS

4.1 Introduction

Severe acute pancreatitis is a common condition in human patients with an annual incidence of 13-45/100,000 people (1) and also in dogs although the exact incidence is not known. Both people and dogs suffering from severe acute pancreatitis are at high risk of developing systemic inflammatory response syndrome and multiple organ dysfunction syndrome with mortality rates as high as 50% (2-4, 6-9). In human patients suffering from severe AP, it is well established that pulmonary complications are a major cause of death and can be responsible for up to 60% of the mortality occurring in the first week of the disease (10, 11). Furthermore, the incidence of ALI in people with AP varies from 18%-46% (12-15) and clinical signs of respiratory complications in dogs are also reported in the literature (2)(5).Therefore, in the past decades, various studies using rodent models of severe AP have been conducted to attempt to describe the mechanisms involved in the development of ALI during severe AP.

Lung injury reported in rodent models with severe AP mostly corresponds to changes characteristic of ALI including infiltration of neutrophils in the alveolar septa and alveolar spaces, presence of edema and, in some cases, hemorrhage. The cellular response during ALI is strongly modulated by the pulmonary resident macrophages including alveolar macrophages and interstitial macrophages. Thus, there are multiple studies evaluating the roles of alveolar macrophages in the development of lung injury associated with AP but no study to my knowledge assessed the induction of PIMs during experimental acute pancreatitis.

PIMs are highly phagocytic large cells (20-80 μm diameter) with characteristics of mature macrophages and are believed to have pro-inflammatory functions. Some species have constitutive PIMs such as cattle, sheep, goats, horses, and pigs (97-104) (105-107) whereas other species including rats, mice and rabbits don't have constitutive PIMs but have induced PIMs upon physiological stress such as endotoxemia and liver dysfunction(110) (101, 111, 112). Humans and dogs were also not shown to have constitutive PIMs (113, 118-120). Most of the studies show that activation of constitutive or induced PIMs would enhance the host susceptibility to lung injury during subsequent microbial challenges (111).

Rodent models, mostly rats, of AP have been used to study mechanisms of inflammation in the pancreas and other organs associated with AP. ANP in rats and mice is induced through treatment with L-arginine. I observed that PIMs are recruited in the lungs of dogs suffering from ANP. Therefore, to understand the mechanisms of recruitment of PIMs and their contributions to ANP-associated lung inflammation, I decided to establish a mouse model of ANP through injections of L-arginine followed by evaluation of their lungs at various time points. The objective of this study was to first characterize lung inflammation in a mouse model of ANP. The second objective was to determine whether PIMs are induced in a mouse model of AP.

4.2 Materials and methods

4.2.1. Reagents

L-arginine monohydrochloride (cat # 11039-100G) and endotoxin-free saline (S8776) used to make the L-arginine solution were purchased from Sigma-Aldrich. The following reagents used in the MPO assay were from Sigma-aldrich : Cetylthrimethylammonium chloride (CTAC), 3', 5, 5'- tetramethylbenzidine hydrochloride(TMB), myeloperoxidase (MPO) from human leukocytes (M6908-5U). The DC Protein assay kit was from BIO-Rad.

4.2.2. Animals

Six to eight week old male C57BL/6 (19-27g) mice (n=30 for the final experiment, n=11 for the second pilot study and n=8 for the third pilot study) were purchased from Charles River Laboratories (Montréal, Québec, Canada), except for the mice used in the first pilot study (n=9), which were provided by Animal Resources of the University of Saskatchewan. Mice were housed individually in the Animal Care Unit (ACU) of the WCVM in standard shoebox cages in a controlled room with ambient temperature of 23^{o}C +/- 2^{o}C and a 12 hour light-dark cycle. They were fed standard laboratory chow and had water *ad libitum*. The University of Saskatchewan Animal Research Ethics Board approved all procedures involving mice.

4.2.3. L-arginine-induced ANP mouse model pilot studies

Three pilot studies were performed in order to standardize the L-arginine-induced ANP mouse model. The sample size, time points, L-arginine solution concentrations, and posology for each pilot study are summarized in the *Appendix II Table I.* The two first pilot studies performed failed to induce pancreatitis. However, the third pilot study using a new L-arginine monohydrochloride product of higher purity (99.5% instead of 98%) and a different protocol led to the development of ANP. The protocol used in the third pilot study was designed with guidance from Dr. Rajinder Dawra from the Department of Surgery of the University of Minnesota, who generously suggested some modifications for my induction protocol based on his recent findings (not yet published). Dr. Dawra was the first to have used the L-arginine model in mice and has worked with this model since 2007 (175) (218).

4.2.4 Standardized L-arginine-induced ANP mouse model protocol

4.2.4.1 L-arginine monohydrochloride solution preparation

A sterile L-arginine monohydrochloride 9% solution was prepared fresh on the day of the injection. First, 2250 mg of L-arginine monohydrochloride powder was mixed with 23 ml of sterile physiologic saline. The pH was adjusted to 7.0. Then, in a biosafety cabinet, saline was added to have a total volume of 25 ml in order to have a 9% L-arginine solution. The L-arginine solution was filtered with a syringe filter (0.2 µm pore, 25mm diameter) into a 30 ml sterile pharmaceutical sealed glass vial.

4.2.4.2 L-arginine pancreatitis induction protocol

The standardized protocol for the induction of ANP consisted of a first intraperitoneal (IP) injection of L-arginine solution prepared as described above at a dose of 4.5g/kg to each mouse. Mice were returned to their cage with access to food and water for one hour. Then, a second injection of the L-arginine solution was given at the same dose. Control mice received the same injections but with physiological sterile saline. The injections were done with 27G needles and 1 ml syringes.

4.2.5 Experimental design

4.2.5.1 Groups

Mice were randomly divided into the following groups: control (n=9), 24 hours ANP (n=7), 72 hours ANP (n=4) and 120 hours ANP (n=7). Control mice were divided to have three controls per time point. A mouse identification chart was first established to assign a number between 1-26 as follows: mouse #1-7 (24 hour L-arginine group), mouse #8-10 (24 hour control group), mouse #11-14 (72 hour L-arginine group), mouse #15-16 (72 hour control group), mouse #17-23 (120 hour L-arginine group) and mouse #24-26 (120 hour control group). Then, mice were randomly assigned to each group, cage label cards were removed from the cages, numbered from 1-26, mixed as a deck of cards and put back on each cage, which randomly attributed a number to each mouse and therefore determined the treatment group. Only 4 mice were induced in the 72 hour L-arginine treatment group during the final experiment because the results from 3

mice obtained during the pilot study #3 were combined with the data obtained in the final experiment to reduce the number of animals used. For the same reasons as for L-arginine treated mice in the 72 hour time points, only 2 control mice where present in the 72 hour time point group.

4.2.5.2 Experiment timeline

A timeline schematic is represented in the *Appendix II figure 4.1* to facilitate the visualization of the experiment design. As shown in the schematic figure, to alleviate the challenge of handling a large number of animals on the same day, the L-arginine treatments were not done on all the animals on the same day. Furthermore, the L-arginine treatments on a group of mice on the same day were staggered by 35 minutes as it takes about 30 minutes to perform anaesthesia and the necropsy of one mouse on the day of the euthanasia. The mice receiving 2 injections of L-arginine as well as the control mice were also administered 2 injections of sterile physiological saline subcutaneously (SC) to prevent dehydration during the initial morbidity phase associated with the injections of L-arginine. The first injection of saline (1.5-2 ml) was administered in the scruff of the neck at the time of the second injection of L-arginine. Then, 3 hours later (at t=4h) a second SC saline injection was given. An example of schedule followed on an induction day is illustrated in the *Appendix II Table J.*

4.2.5.3 Monitoring of animals

It was noted during the pilot study #3 that significant morbidity and abdominal pain occur after the injections of L-arginine. Therefore, mice were monitored every hour for the first 8 hours following the injections of L-arginine and then, 3 times a day until the time of euthanasia. Briefly, mice were monitored for abdominal pain, weight loss, signs of respiratory distress, and lethargy. Mice were weighed every day to detect weight loss and a daily mean was calculated with the weight of every mouse present in each time point group to create a graph illustrating the weight loss pattern. No analgesic was used because of their potential effect on inflammation and development of pancreatitis (219) (220).The detailed monitoring parameters assessed are indicated in the Humane Intervention Point chart, *Appendix II, Table K.*

4.2.6 Sampling and processing

4.2.6.1 Blood collection and euthanasia

Mice were first anaesthetized with an intraperitoneal injection of a ketamine/xylazine mix (10:1) at the dose of 1-2% of body weight (0.3-0.6 ml for a 30g mouse) followed by intra-cardiac puncture with a 25G needle to collect blood sample in a pre-heparinized (0.05 ml of heparin) 1ml syringe. Blood collection induced the death of the mice. Blood samples were kept on ice in an Eppendorf tube containing another 0.05 ml of heparin until they were sent to PDS clinical pathology laboratory for plasma amylase analysis and a CBC. Blood could not be taken from one mouse belonging to the 24 hours L-arginine group as this mouse had coagulopathy at the time of euthanasia. In addition, the blood sample

from 2 mice (one in the control group and one in the 24 hour L-arginine group) clotted and could not be used for CBC, however plasma amylase activity could still be analysed.

4.2.6.2 Sampling of Pancreas

After the mouse euthanasia, a laparotomy was performed to collect the pancreas rapidly to reduce the possibility of autolysis. The right lobe of the pancreas and the duodenum adjacent to it were kept in 4% paraformaldehyde overnight (16-20 hours) for paraffin embedding (see *Appendix II Table L,* for the complete protocol*).* At the same time, the other abdominal organs including the liver, kidneys, spleen, reproductive tract, bladder, stomach, and intestine were grossly evaluated for presence of abnormalities. The peritoneal cavity was also evaluated for evidence of peritonitis. The left lobe of the pancreas was snap-frozen in liquid nitrogen for future experiments.

4.2.6.3 Bronchoalveolar lavage (BAL)

The BAL was performed only in the left lung. After thoracotomy and isolation of trachea, the right primary bronchus was ligated. Using small surgical scissors, a hole was made in the trachea to insert a small flexible cannula up to the tracheal bifurcation. The lavage was performed using 0.5 ml of cold sterile PBS pH 7.4 in a 1 ml syringe. The lavage was done 3 times in total. WBC count and cytospin for differential count was performed quickly after the BAL fluid was obtained. The remaining BAL supernatant was kept at -80^{o}C for further analysis.

4.2.6.4 Lung sampling

Before collecting the lungs, the left lung was perfused with 1 ml of 4% paraformaldehyde by gravity using a cannula inserted in the trachea. The right lung remained ligated to prevent entry of paraformaldehyde into it. The left lung was kept in 4% paraformaldehyde overnight (16-21h) for paraffin embedding. The processing protocol for paraffin embedding was the same as the one used to process the pancreas. The right lung was snap-frozen in liquid nitrogen to perform the lung MPO activity assay.

.

4.2.7 Pancreas histology grading

In order to confirm the induction of ANP in the L-arginine treated mice, 5 µm thick H&E stained sections of pancreas from all the mice were blindly evaluated and graded for pancreatitis lesions by an ACVP board-certified pathologist from the Department of Veterinary Pathology of the WCVM. The grading criteria were: 1) pancreatic necrosis 2) infiltration of inflammatory cells in the pancreas and 3) pancreatic edema. The type of inflammatory cells infiltrating the pancreas was also recorded. The scoring system is described in *Table M*. The summation of the scores obtained for each three grading criteria listed above generated the histology score.

Table M: Grading system used to evaluate mouse pancreas histology

Grading criteria	Score	Description
Pancreas necrosis	0	Absence of pancreas necrosis
	1	Loss of zymogen granules only
	2	Necrosis in <10% of the pancreas parenchyma
	3	Necrosis in 10-25 % of the pancreas parenchyma
	4	Necrosis in 25-50 % of the pancreas parenchyma
	5	Diffuse pancreas necrosis; >50% of the pancreas parenchyma
Pancreas edema	0	Absence of pancreas edema
	1	Focally increased space between lobules
	2	Diffusely increased space between lobules
	3	Pancreatic acini disrupted and separated
Infiltration of inflammatory cell in the pancreas	0	Absence of inflammatory cell infiltration in the pancreas
	1	Rare inflammatory cell or only around ductal margins
	2	Inflammatory cell infiltration in the pancreas parenchyma (<50% of the lobules)
	3	Inflammatory cell infiltration in the pancreas parenchyma (>50% of the lobules)
Type of inflammation	Neutrophilic, monocytic, lymphocytic, mixed	

4.2.8 Lung histology grading

Lung sections from all the mice were graded for signs of inflammation by the same board-certified veterinary pathologist, who evaluated the pancreas. The evaluator was blinded as to the identity of the samples. Scores were attributed for 1) alveolar septa thickening and 2) the presence of lung edema. The type of inflammatory cells infiltrating the lungs was also recorded. The same scoring system as the one used to evaluate the lungs from AP dogs was used (*Table C* in Chapter 3). The summation of the scores obtained from both grading criteria provided the histology score.

4.2.9 Lung immunohistochemistry for vWF and CD68

The IHC was performed on mouse tissues following the same protocol as the one used on dog tissues (See section 3.2.7). The sections were incubated with pepsin to unmask antigens in the tissues. The following primary antibodies and dilutions were used: a polyclonal rabbit anti-human von Willebrand Factor antibody (P0448) (1:400 dilution in BSA1%) from DAKO and a polyclonal rabbit anti-human CD68 (Sc-9139) (1:25 dilution in BSA 1%) from Santa Cruz Biothechnology. The appropriate HRP-conjugated secondary antibody was diluted at 1:300 for the vWF staining and 1:100 for the CD68 staining. The color was developed for 3 minutes and the methyl green added to the slides for only 3 seconds.

4.2.10 Lung CD68 cell count

To assess the recruitment of monocytes/macrophages in the lungs of mice with ANP, lung sections from all the mice were stained with a CD68 antibody and the number of positive cells was counted in 10 fields of view at 400X following a consistent counting pattern. A field of view was considered appropriate for counting if more than 50% of the view was occupied by lung parenchyma. Fields of view where more than 50% of the area was occupied with airways (bronchiole) or blood vessels were ignored moving to the next field of view. Then, an average of the counts for the various groups (control, 24 hour, 72 hour and 120 hour) was done.

4.2.11 Myeloperoxidase activity in mice lungs

Lung samples equivalent to the size of 1/4th of a complete lung were homogenized in 0.5ml 50mM HEPES buffer solution at a pH of 8.0 in 2 ml homogenizing tubes containing 4 metallic beads (5mm diameter). Tissue samples were homogenized for 40 seconds in a tissue homogenizer. The homogenized samples were centrifuged at 1062g (10,000 rpm) for 20 minutes at 4°C and the supernatants were discarded. The pellets were suspended in 0.5 ml 0.5% cetylthrimethylammonium chloride (CTAC) and then homogenized and centrifuged again as described before. The supernatants were kept on ice until the MPO experiment was ready to be performed. For the standard MPO curve, 6 twofold dilutions were prepared using MPO from human leukocytes diluted in 50mM HEPES buffer solution, the same buffer used for the lung samples. The

standard curve was made with the following dilutions: 0.5 U/ml, 0.25 U/ml, 0.125U/ml, 0.063 U/ml, 0.031 U/ml, and 0.016 U/ml. The lung sample supernatants were diluted 10x in phosphate citrate buffer in order to be included in the standard curve. MPO standards and lung samples were added to a 96-wells plate with a peroxidase color substrate (TMB) for 2 minutes after which the reaction was stopped using 1M sulphuric acid. The optical density was measured using an optical reader at a wavelength of 450nm. After performing the MPO assay, a protein concentration assay was performed using the same samples that were used for the MPO assay. The protein assay was done using the BIO-Rad DC Protein assay kit following the manufacture's instruction. The results from the MPO experiment (U/ml) were divided by the samples' protein concentrations (mg/ml) in order to have the final MPO results expressed in U/mg of protein.

4.2.12 Statistical analysis

Statistical analysis was performed using statistical software (GraphPad Prism, Version 5.04 for Windows, GraphPad Software, San Diego California USA). To detect differences among means of plasma amylase activity, a One-way ANOVA on the ranked data was performed because of unequal variances (Bartlett) among groups. Then, Tukey's multiple comparison was used as post-hoc test. Histologic grading scores were expressed in medians with range and the comparison of medians among the 4 groups of mice was done by the non-parametric test Kruskal-Wallis followed by Dunn's Multiple Comparison test as

post-hoc test. Results from the CD68 cell counts, CBC, BAL WBC and MPO are expressed in means ± standard error of the mean (SEM) and comparison of means among groups was done with One-way ANOVA (One-way analysis of variance) followed by Tukey's multiple comparison as post-hoc test.

4.3. Results

4.3.1 Clinical signs in mice treated with L-arginine

Immediately after receiving the first intraperitoneal injection of L-arginine, mice showed signs of acute abdominal discomfort (reduced mobility, rounded back, compulsively licking the abdomen, almond-shaped eyes, and ears flattened). After the second L-arginine injection, mice became more morbid and showed signs of tachypnea with superficial breathing and stayed morbid until the second subcutaneous injection of saline (3 hours after the second injection of L-arginine) after which they began to recover slowly. It took at least 8-12 hours for the mice to become asymptomatic. After the initial morbidity period and recovery, mice did not show signs of abdominal discomfort or signs of respiratory disease for the rest of the experiment up to the 120 hour time point. However, mice receiving L-arginine injections lost weight in the first 48 hours after which they began to regain weight but never regained their initial weight (Figure 4.2). The weight loss corresponded to approximately 5% of body weight (bw) in the first 24 hours and to an additional 4% of bw between 24-48 hours. Control mice did not show any signs of abdominal discomfort, respiratory distress, and did not loose weight following the saline injections.

There was no unexpected mortality during this experiment. However one mouse in the 24 hour time point group never recovered fully and was hypothermic, had abdominal hemorrhagic effusion, and blood in the bladder at the time of necropsy. As pancreatitis was not severe at this time point, this complication was probably not related to pancreatitis but to an adverse reaction to L-arginine resembling a coagulopathy.

4.3.2 ANP confirmation in L-arginine treated mice

The mean values for the plasma amylase activity in each group of mice are as follows: control mice (1483 ± 48 U/L), 24 hour ANP mice (5528 ± 1210 U/L), 72 hour ANP mice (6547 ± 1275 U/L) and 120 hour ANP mice (1399 ± 62 U/L) *(Figure 4.3).* Compared to the normal plasma amylase values (obtained in the control mice), plasma amylase increased significantly 24 and 72 hours following the injection with L-arginine ($p < 0.001$). There were no differences in the plasma amylase activity in control mice and the 120 hour treatment group.

The second indication of the presence of pancreatitis was the evaluation of the gross pathology of the pancreas at the time of the necropsy. Morphological changes were noted in the pancreas at each time point of the experiment (Figure 4.4). Compared to the pancreas from the control mice, mice euthanized 24 hours post-L-arginine treatment showed an edematous and enlarged pancreas. At 72 hour, the pancreas was discoloured (grey instead of pink) and enlarged with visually evident separations between pancreatic lobules whereas at 120 hour the

pancreas was atrophic allowing visualization of the left kidney, which is usually covered by the left lobe of the pancreas.

The definitive diagnosis of ANP in mice injected with L-arginine was made with histological evaluation of the pancreas. Representative images of pancreatic histology are shown in *Figure 4.4*. The histological evaluation of the pancreas of control mice resulted in scores of ''0'' for every scoring category leading to a total pancreas histology score of ''0'' for every control mouse (*n*=9). After 24 hours of the treatment, the pancreas showed a loss of zymogen granules in acinar cells but this did not lead to a statistical difference in total histology scores for this time point compared to the control group. The highest histology scores were obtained in the 72 hour treatment group where acinar cell necrosis affected greater than 50% of the pancreas parenchyma. In addition, there was a massive infiltration of neutrophils between pancreatic lobules covering >50% of the parenchyma and pancreatic edema causing separation and disruption of acinar cells. All the observations made in the 72 hour group were significantly different from the control group ($p<0.0001$). The 120 hour group showed lesions similar to the 72 hour group with no statistical differences between the histology scores obtained for these 2 groups. However, the presence of pancreatic edema in the 120 hour group was not statistically different from the control group. In addition, mostly lymphocytes instead of neutrophils were observed in the pancreas at 120 hour. The scores for each grading criteria and for each group of mice are summarised in *Table N* and illustrated in *Figure 4.5.*

As an indication for systemic inflammation, a CBC was performed on each mouse. The results for the CBCs are illustrated in Figure 4.6. White blood cell counts in control mice ranged from 2.8-7.9 x 10^9 /L (median 4.9 x 10^9 /L). Compared to the control WBC counts, there were no statistical differences with WBC counts for the various L-arginine groups using One-way ANOVA. However, there was a significant difference ($p < 0.05$) between WBC counts for the 24 hour and 120 hour groups. In control mice, differential blood counts for neutrophils ranged from 0.2240-2.044 x 10^9 /L, and monocytes ranged from 0.0280 - 0.1720 x 10^9 /L. There were no significant differences between the differential blood counts for monocytes or neutrophils in L-arginine groups and the control group. However, it is interesting to note that one mouse in the 24 hour L-arginine group showed neutrophilia whereas two mice in the 24 hour group and one mouse in the 72 hour group showed monocytosis, when compared to the other animals present in the respective groups *(figure 4.6).*

4.3.3. Lung histology grading

The lung histologic evaluation (*Figure 4.7*) revealed infiltration of mononuclear phagocytes in the lungs of mice in the 72 hour group only, which was significantly different ($p < 0.001$) compared to the control lungs. There were no noticeable histology changes in the 24 hour and 120 hour groups compared to the control mice lung histology.

4.3.4 Lung immunohistochemistry for vWF and CD68

The vWF staining was used as a positive immunohistochemical control as well as a marker of inflammation. Based on the qualitative evaluation, vWF staining was apparently increased in the lungs of L-arginine mice compared to control mice, as there was presence of granular staining in the alveolar septal capillaries of some ANP mice. Representative images of the vWF staining are shown in *Figure 4.8.*

Representative images of the immunohistochemical staining with a CD68 antibody and CD68 cell counts are shown in Figure 4.9. The CD68 counts (median; range) are as follows: for control mice (81; 55-147), for the L-arginine 24 hour group (150; 115-190), for the L-arginine 72 hour group (190; 118-200) and for the L-arginine 120 hour group (135; 97-194). There was a significant increase in the number of CD68 cells in all mice treated with L-arginine ($p < 0.01$). However, there were no differences in the counts between the various L-arginine groups. Interestingly, it was noted in some mice that the staining for CD68 was located in the nucleus in addition to cytoplasms or only in the nucleus without cytoplasmic staining. For the purpose of counting positive cells, the cells were not differentiated for nuclear and cytoplasmic staining. However, qualitative evaluation indicated more nuclear staining for CD68 in mononuclear phagocytes in L-arginine treated mice compared to control mice. However, further detailed evaluation of the staining especially with the electron microscope would be necessary to confirm this observation. In addition, staining for CD68 was present in the airway epithelial cells of both control and ANP mice, which was not

expected. Similar to the staining pattern of mononuclear phagocytes, presence of nuclear staining appeared more prominent in epithelial cells in lungs of L-arginine treated mice compared to controls.

4.3.5 WBC counts in BAL fluid and total lung MPO activity

The BAL WBC counts were not significantly different between control mice and the various L-arginine groups ($p=0.08$; Figure 4.10). Cells present in the BAL fluid of all mice, including control and L-arginine treated mice, were mononuclear phagocytes only. The lung MPO activity also did not differ statistically between control and ANP mice ($p=0.07$; Figure 4.10).

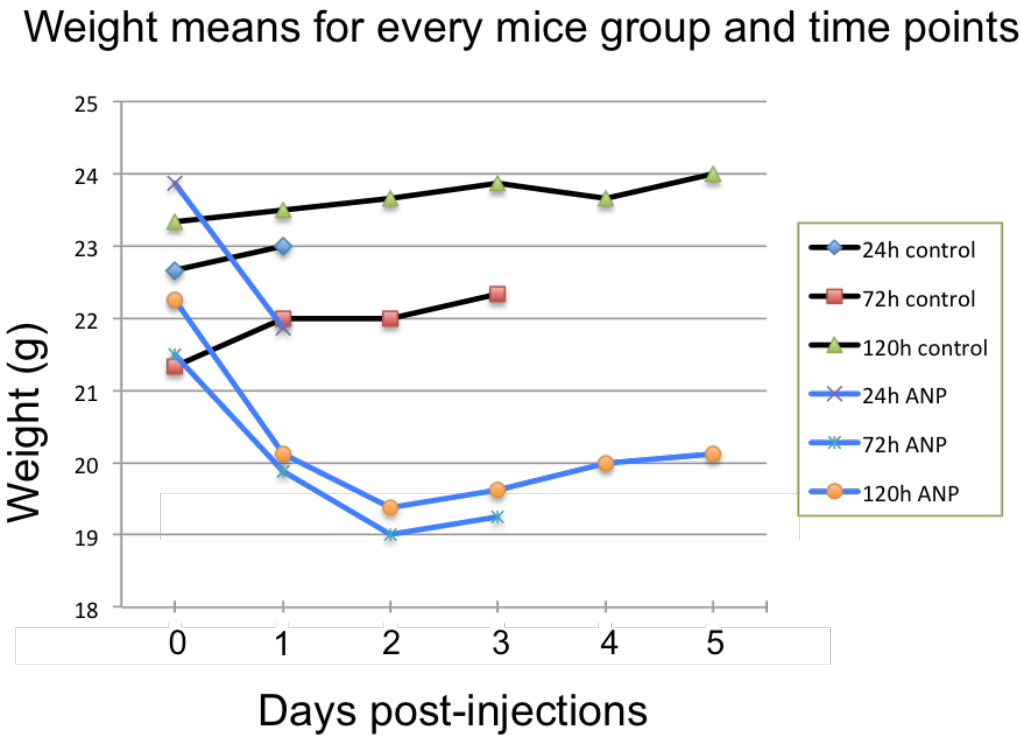

Figure 4.2 **Weight means for each group of mice at 24h post-injection intervals for L-arginine or saline (controls).**

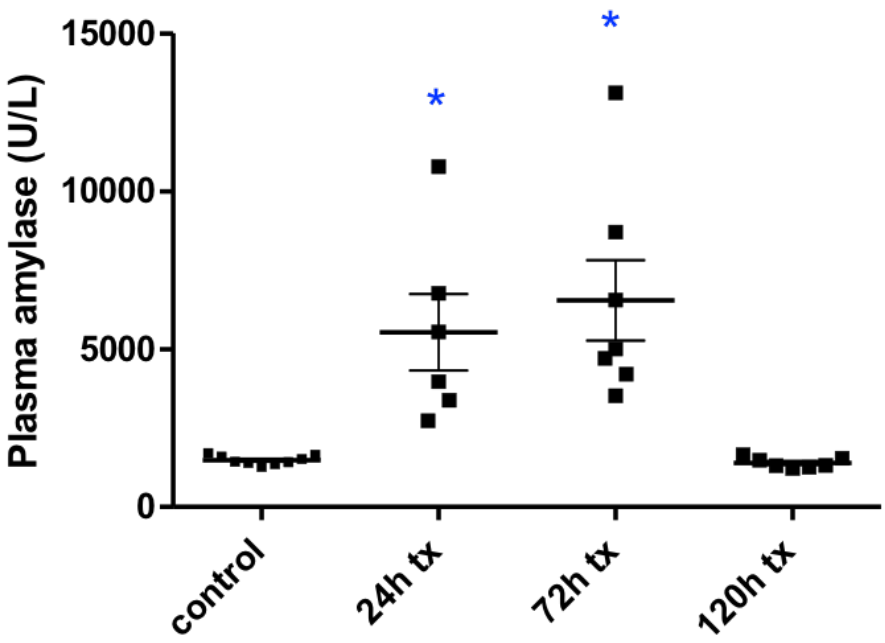

Figure 4.3 **Plasma amylase activity (U/L) in control and L-arginine mice.** There is a significant increase in plasma amylase at 24 and 72 hours following the injections of L-arginine compared to the control. Asterisks indicate significance different at $p < 0.001$. Mean values and SEM represented by horizontal line in graphs.

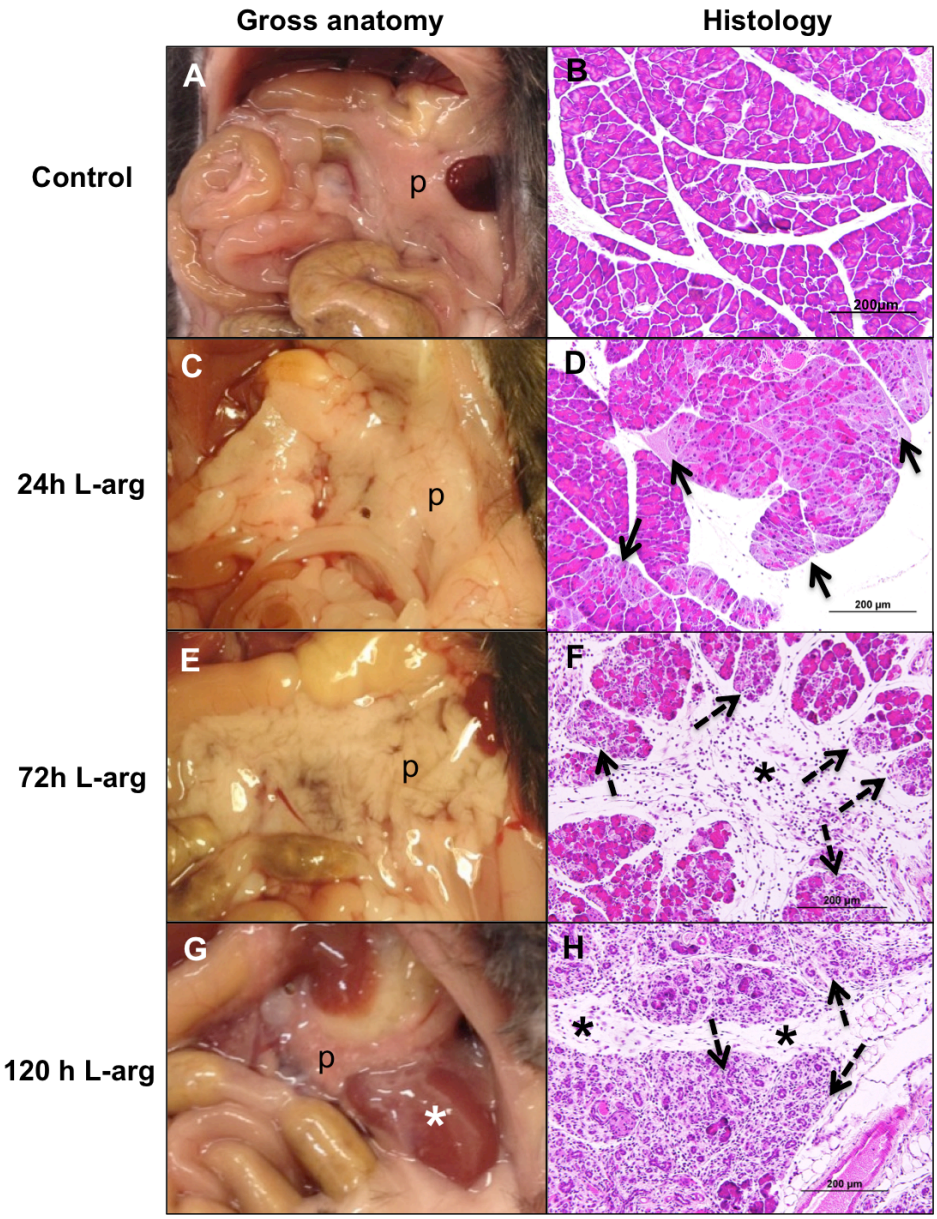

***Figure 4.4* Gross anatomy and histology of the pancreas of control or L-arginine treated mice.** (A-B): Control mice with normal pancreas (P) gross anatomy and histology. (C): Pancreas gross anatomy after 24h and (D): corresponding histology showing a loss of zymogen granules in acinar cells (arrows). (E): Pancreas gross anatomy after 72h and corresponding histology. F shows a massive infiltration of inflammatory cells, mainly neutrophils, between pancreatic lobules (inter-lobular space shown by asterisk) and acinar cell necrosis (dotted tail arrows). (G): After 120h, the pancreas is atrophic and the left kidney (white asterisk) can be visualized. (H): Histology at 120h still shows acinar cell necrosis but lymphocytes and not neutrophils are being recruited in the pancreas.

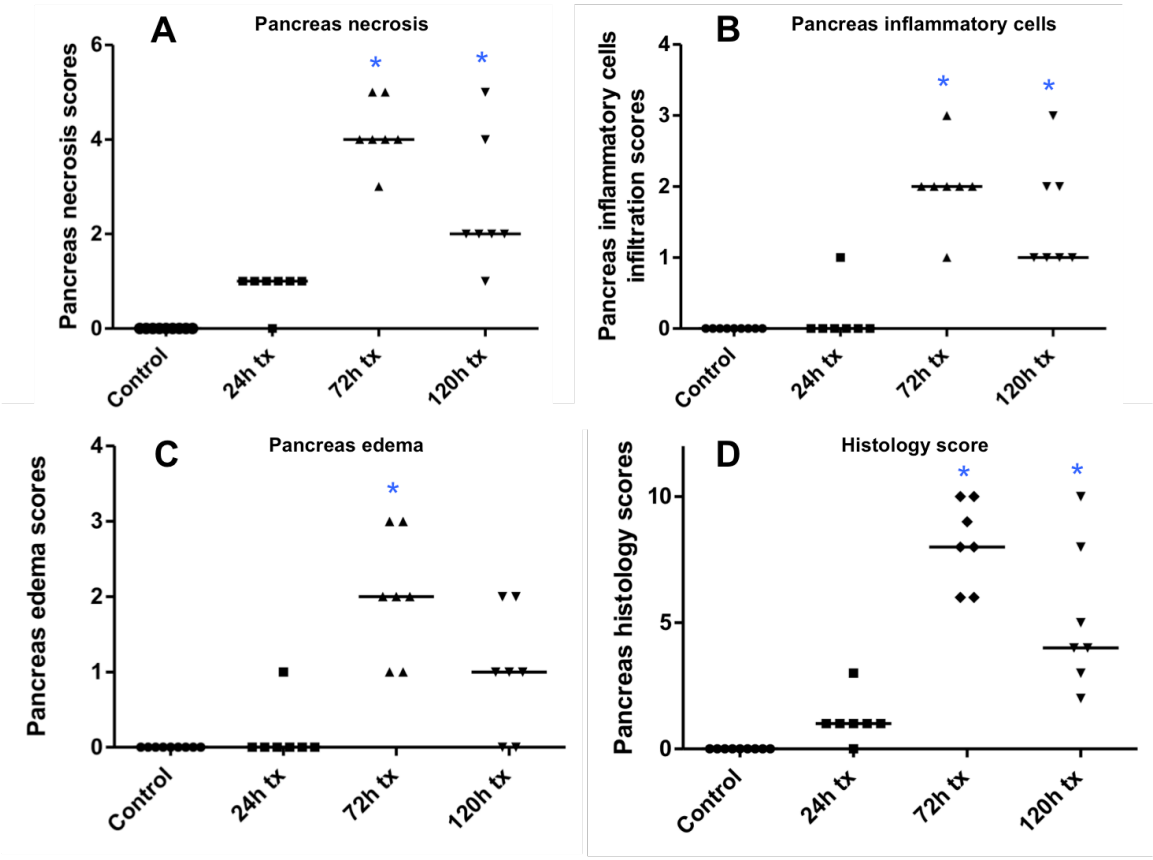

Figure 4.5 **Pancreas histology scores for control and L-arginine.** (A): Scores for pancreas necrosis. (B): Socres for infiltration of inflammatory cells in the pancreas. (C): Scores for pancreas edema. (D): Pancreas histology scores: represent the sum of the 3 different scoring categories. Median values represented by horizontal line in graphs. Significant differences from control mice at $p < 0.0001$ denoted as asterisks (*).

Table N : Pancreas histology scores for the different grading criteria for control and L-arginine treated mice.

	Control	**24h L-arg**	**72h L-arg**	**120h L-arg**
Necrosis	0.0	1 (range 0-1)	4 (range 3-5)*	2 (range 1-5)*
Inflammatory cells	0.0	0 (range 0-1)	2 (range 1-3)*	1 (range 1-3)*
Edema	0.0	0 (range 0-1)	2 (range 1-3)*	1 (range 0-2)
Histology score	0.0	1 (range 0-3)	8 (range 0-3)*	4 (range 2-10)*

Data reported as median with range
An asterisk (*) indicate a statistical difference with the controls at p<0.0001 difference with controls.

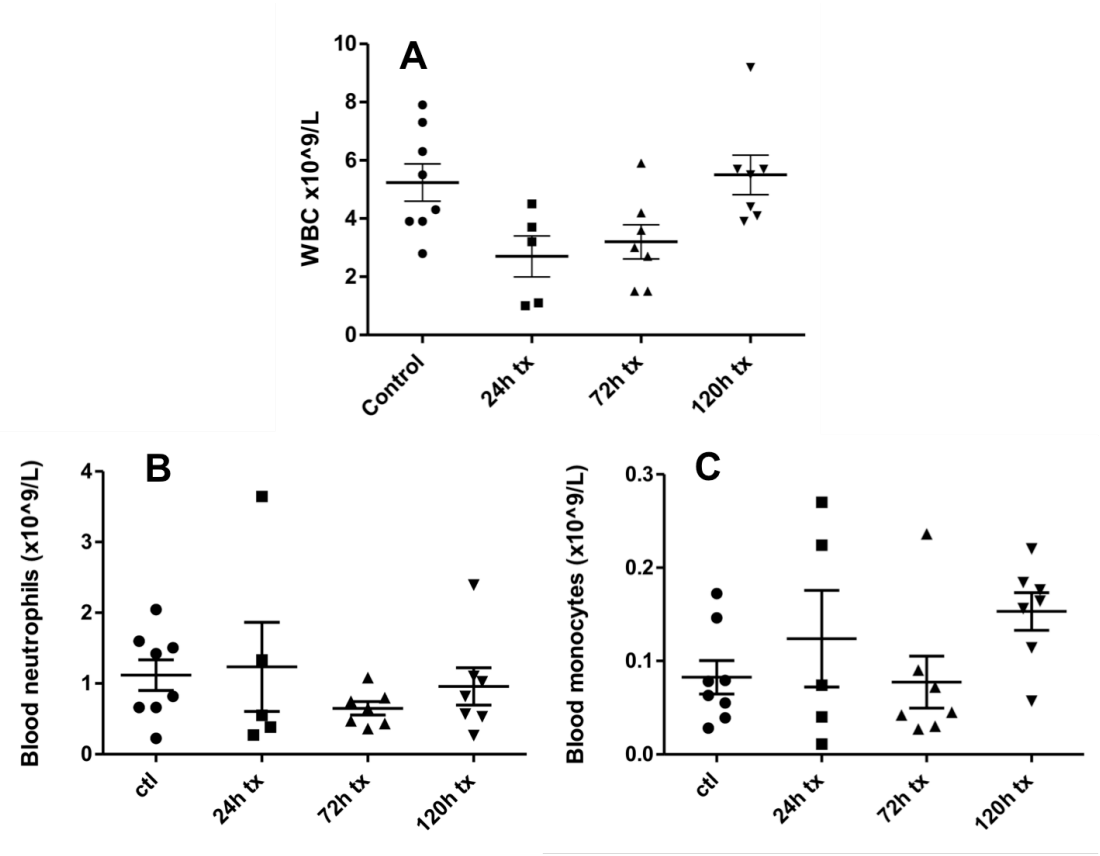

Figure 4.6 **CBCs results from L-arginine and control mice.**
(A): Results from the blood WCB counts. (B): Results from the blood differential counts for neutrophils. (C): Results from the blood differential counts for monocytes. There were no statistical differences between the L-arginine groups and control group. However, the WBC count at 24h and 120h were statistically different.

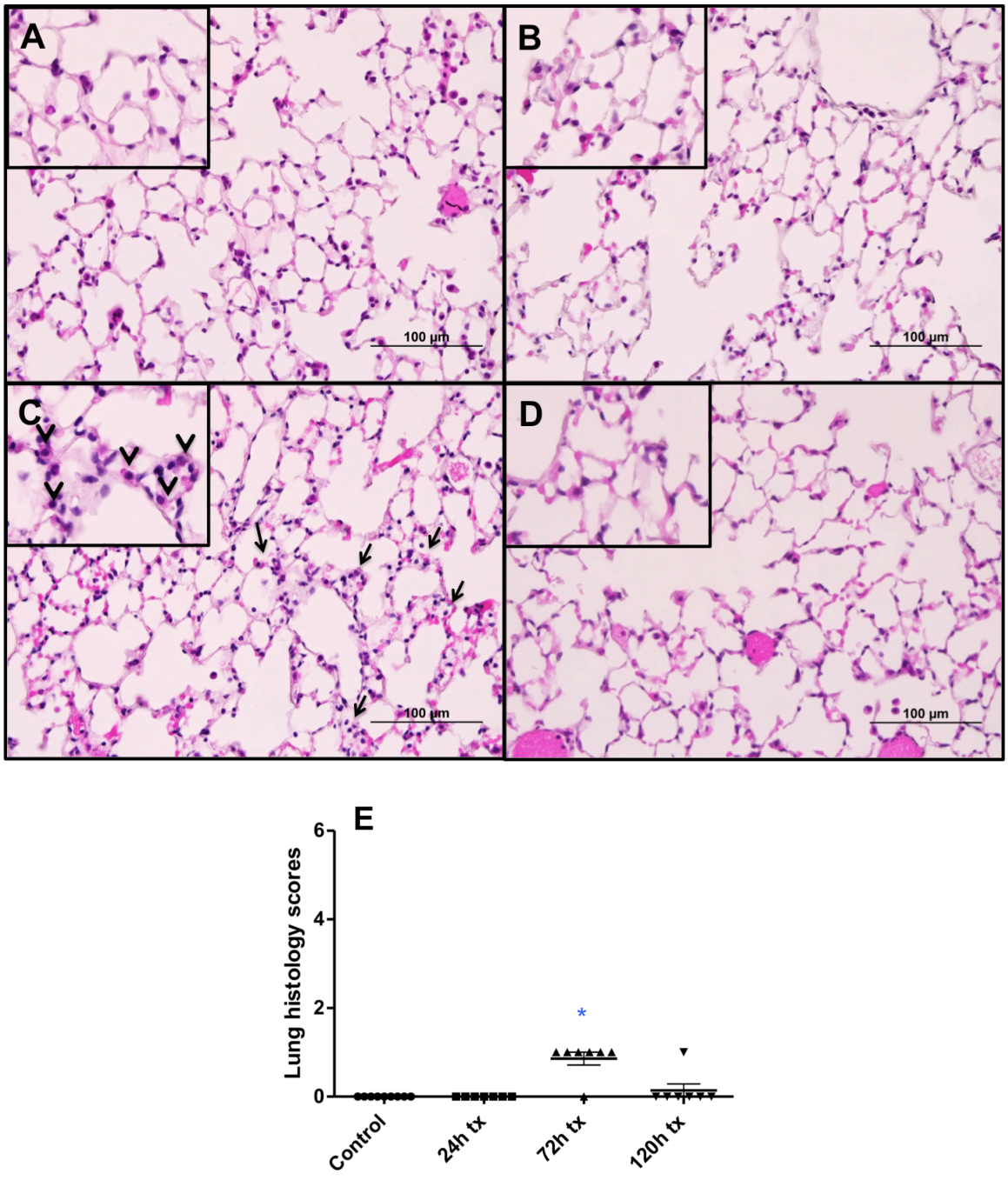

Figure 4.7 **Lung histology and histology scores of control and ANP mice.** (A): Lung sections from control mice showing normal histology. (B): Lung sections from 24 hour ANP mice with no significant changes. (C): 72h ANP mouse lungs showing increased cellularity (arrows) corresponding to the infiltration of mononuclear phagocyte cells in the alveolar septa (arrowheads) (D): 120h ANP mice with no significant changes. (E): Corresponding lung histology scores representing the sum of lung edema scores and alveolar septa thickening scores .(*) indicates $p < 0.001$.

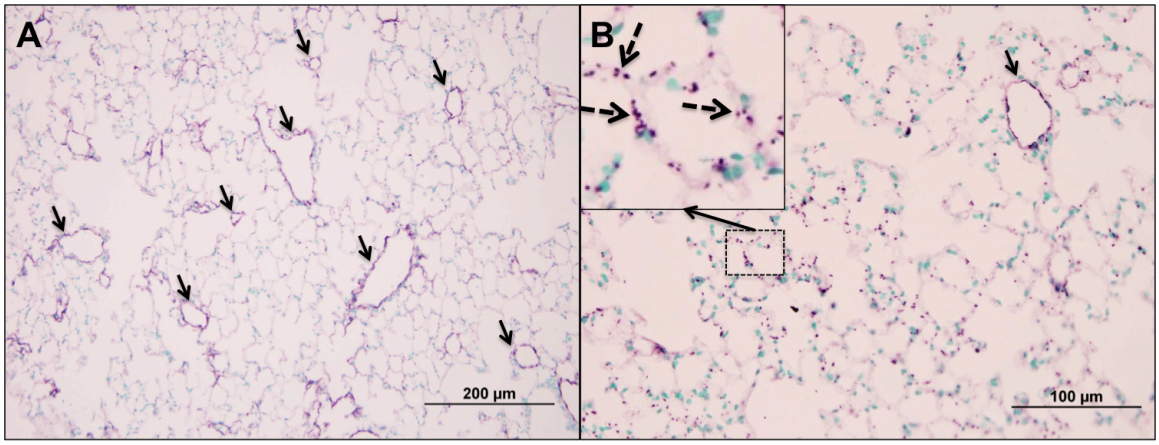

***Figure 4.8* vWF staining of mice lungs.** (A): Representative image of vWF staining of sections of control mouse lung showing specific staining of blood vessels (arrows). (B): Lung sections from L-arginine mice showing granular staining in the alveolar septa (dotted tail arrows).

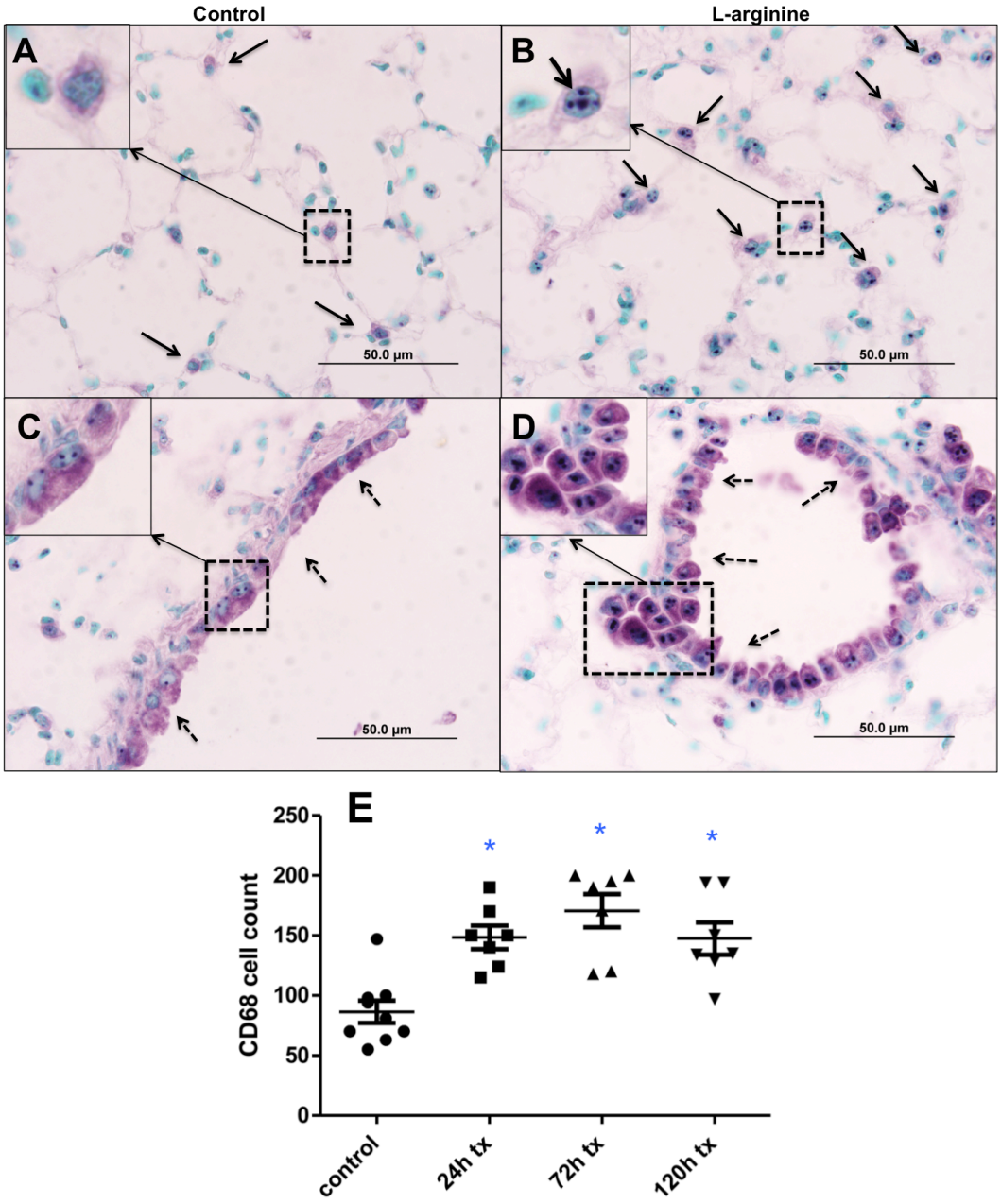

***Figure 4.9* CD68 staining in control and ANP mice.** (A): Lung section from a control mouse showing cytoplasmic staining of mononuclear phagocytes (arrows). Notice the absence of nuclear staining. (B): Staining of the lung section from a L-arginine treated mouse where mononuclear phagocytes show CD68 staining in the cytoplasm but also in the nucleus (broken tail arrow) (C): CD68 staining present in airway epithelial cells of control mice showing cytoplasmic staining and rare nuclear staining (D): CD68 staining present in airway epithelial cells of L-arginine mice showing cytoplasmic staining but also multiple epithelial cells with nuclear staining (E): Results from the CD68 positive cell counts for every mice group. (*) Indicates $p < 0.01$.

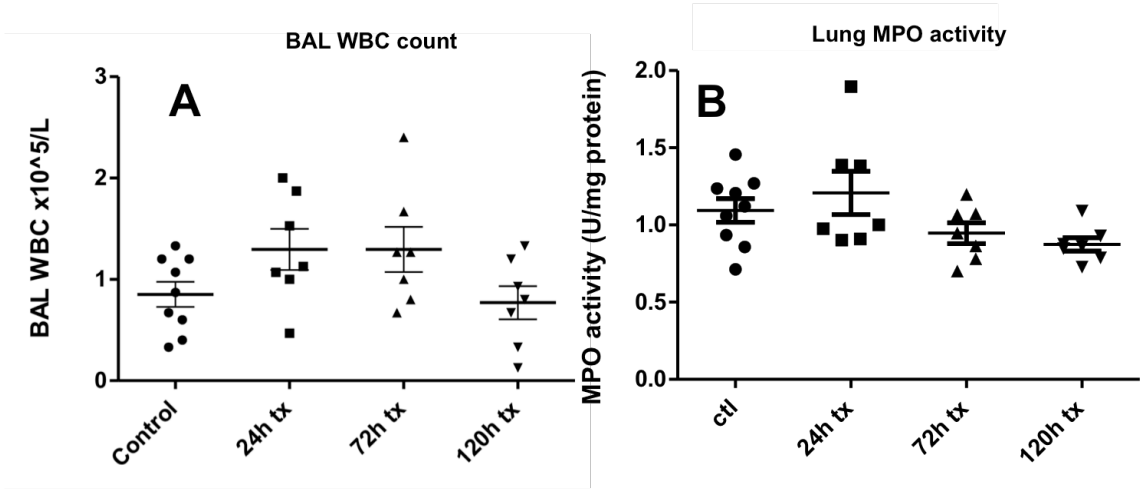

Figure 4.10 **Total WBC counts in BAL and lung MPO activity in control and ANP mice.** (A): Results from the total WBC count present in the BAL fluid of control mice and mice in the different time point of ANP. (B): Results from lung MPO activity of control mice and mice in the different time point of ANP. The results from both assays were not statistically different compare to the controls.

4.4. Discussion

I previously observed that septal mononuclear phagocytes, mostly PIMs, are increased in lungs of dogs that have died due to ANP. Since mice do not have constitutive PIMs similar to dogs, I decided to use a mouse model of ANP to examine the recruitment of PIMs during ANP in order to use the model to further understand the development of lung inflammation associated with this condition.

Although rodent models, especially rats and not mouse, have been used to study ANP, it required three pilot studies to optimise the mouse model of ANP in our laboratory. The pilot studies were to establish an optimal protocol to induce ANP with intraperitoneal treatments of a L-arginine solution. The first pilot was based on the posology used in the rats (40) and failed to induce ANP in mice. However, the second pilot study was based on the L-arginine-induced mice ANP protocol standardized by Dawra and colleagues (181) but did not lead to ANP in mice used in my experiment. The third pilot was based on personal communication with Dr. Dawra and resulted in ANP in my group of mice. The reasons for the failure to induce ANP in the second pilot study even after meticulously replicating every aspect of the published protocol including using the same strain of mice (C57BL/6) are unknown. One possibility is that L-arginine has been mainly used in rats to induce ANP and has only been used in mice recently and therefore it may require further standardization in mice.

Clinically, mice treated with L-arginine only showed abdominal discomfort and lethargy in the first 12 hours following the injections of L-arginine. After this

period, mice did not show signs of discomfort or evidence of pulmonary complications even at the 72 hours time point, which is the period where more severe ALI has been reported in other studies using this model in mice (181, 184, 185). The abdominal discomfort observed following the L-arginine injections may not be due to pancreatitis since only mild pancreatic lesions were present at 24 hour post-injections. One hypothesis for the initial morbidity could include the rise in blood ammonia levels generated from the L-arginine catabolism following injections of L-arginine. Indeed, high levels of ammonia in the blood of rats receiving intraperitoneal injections of L-arginine were detected in the first 8 hours following L-arginine treatments (221). In addition, metabolic acidosis occurs following intraperitoneal administration of chloride salts of L-arginine reaching the most acidic urine sample values (pH=5.5-6.0) at 24 and 48 hours. Weight loss was noted during the first 48 hours following L-arginine, which could be associated with the initial morbidity period where food intake was significantly reduced. After the first 2 days, mice slowly regained weight suggesting that they were feeding normally again and had reduced physiological stress. CBC was performed on every mouse as an indicator for systemic inflammation. Although this was not statistically significant, the graph for the WBC counts suggested that leukopenia may occurs at 24 hours and 72 hours after receiving L-arginine injections, which suggest a systemic inflammatory response. A larger sample size may have increased the statistical significance for those results. It is also interesting to note that the blood neutrophils differential counts in the 72 hour L-arginine group all corresponded to the lower-end values of the range for normal

neutrophils counts (based on the control neutrophils differential values) and is associated with the time point where massive infiltration of neutrophils occur in the pancreas. In addition, monocyte counts after 120 hours following L-arginine injections appeared to increase, but not significantly, and therefore it would be interesting to assess the recruitment of those cells in the lungs past this time point to see if more PIMs would be present in the lungs.

The criterion used to confirm ANP in my experiments including plasma amylase levels and grading of pancreatic histology corresponded to the data published in other studies using the L-arginine induced ANP in mice (175)(184, 185, 222). Although ANP was induced in the mice, there was a lack of neutrophil infiltration into the lungs based on histological evaluation and MPO activity assay. Lung inflammation characterized by neutrophils accumulation in ANP models has been reported previously (175)(184, 185, 222). The reasons for this discrepancy are not clear. One of the reasons could be that if L-arginine treatment induced ALI, I may have missed the optimal time point to detect the increase in neutrophils in the lungs. However, the peak of neutrophil infiltration reported in other studies using this mouse ANP model was at 72 hours (181, 184, 185), which was a time point included in my study design, therefore suggesting that neutrophils were simply not recruited into the lungs of L-arginine mice in my experiments. This creates a discrepancy, which needs to be resolved with further studies focusing on the recruitment of neutrophils in the lungs of animals suffering from ANP. It is interesting that the evaluation of lungs from ANP dogs also showed lack of neutrophil accumulation.

In addition to the quantification of neutrophil accumulation in the lungs, I also used vWF staining as a marker of vascular inflammation. The expression of vWF was increased in the mice in the L-arginine group as shown by more staining present in the alveolar septal capillaries. Similar to observations in lungs of ANP dogs stained for vWF, ANP mice showed granular staining in alveolar septa. As mentioned for the dog study, increased inflammation or vascular injury can lead to activation of endothelial cells and to the release the content of Weibel-Palade Bodies, which contain vWF. (204, 205). In another study, plasma levels of trypsin increased as early as 24 hours after the L-arginine treatments and continued to increase till 120 hours of the treatments (181). Therefore, since trypsin has been shown to cause vascular injury to various organs during AP including the lungs (156, 157), it is possible that this pancreatic enzyme injured vascular endothelium and increased expression of vWF in my study. The granular pattern of vWF staining on the capillaries endothelial cells may be due to focal accumulation after its secretion by the endothelium or clustering vWF present in the capillaries lumen. This staining could also be platelets containing vWF as mouse platelets contains vWF in their α-granules (223). The role of vWF in lung inflammation associated with ANP in mice or in dog patients is not clear however it could promote leukocytes adhesion, including PIMs, as both vWF alone or vWF-platelet aggregation on endothelial cells were shown to facilitate leukocytes recruitment to the site of inflammation (212, 213, 215).

The main focus of my study was to evaluate whether L-arginine treatment would induce PIMs to make an argument for their use to study the role of PIMs in

ANP-induced lung inflammation and systemic pathophysiology. My data showed accumulation of CD68+ monocytes/macrophages in mice treated with L-arginine compared to the control mice at all the L-arginine treatment time points. However, there were no differences in the PIMs numbers between each of the L-arginine groups. CD68 recognizes a lysosomal-associate membrane protein, which is more prominently expressed in differentiated macrophages (224). Therefore, CD68 provides cytoplasmic staining in reactive macrophages. However, I was intrigued by the nuclear staining for CD68 not only in septal macrophages but also in the airway epithelium, which also intensely reacted with the CD68 antibody. The staining of the epithelial cells in various organs has been reported previously but the significance of such staining is not known (224). While the significance of nuclear staining for CD68 is not known, the staining appeared to be more prominent in L-arginine-treated mice compared to the controls. Nevertheless, the data show significant recruitment of CD68 septal macrophages, suggesting they are PIMs.

4.4.1 Limitations and flaws

The use of the L-arginine ANP model to assess the mechanisms involved in lung inflammation associated with this disease can raise some questions. As mentioned previously, L-arginine is a precursor for the production of NO by iNOS, which can be induced in alveolar macrophages (164, 171, 173). Therefore, in theory, L-arginine reaching the lungs via the systemic circulation could have direct protective or detrimental effects on the lungs via the production of NO by

alveolar macrophages. However, the reported half-life of 1-2 hours for L-arginine in mice (175) and its direct effect would likely lead to histological changes in the lungs earlier than 72 hours after the injections of L-arginine; however, that was not the case in my experiments. This observation combined with the fact that injury to abdominal organs other than the pancreas was not present in previous studies using the L-arginine model (180-182) argue in favour of selective and direct actions of L-arginine on the pancreas.

The mice receiving L-arginine developed ANP but did not show clinical sign or mortality associated with ANP. This is at variance with the clinical disease where dogs and people suffering from ANP show high mortality and morbidity. Therefore, the mouse model despite its usefulness to evaluate the basic mechanisms of ANP may not model the real clinical disease.

A larger sample size in each group could have improved the statistical significance of most results. Because inducing ANP in a group of 30 mice on the same day is technically impossible with the induction schedule that I followed, I had to induce ANP on three days. Therefore, the L-arginine solution had to be made three times and therefore the solution could have varied in concentration and pH slightly.

4.5. Conclusions

Taken together, L-arginine induced ANP in mice and was associated with vascular inflammation in the lungs of affected mice as indicated by increased expression of vWF and accumulation of PIMs. The absence of neutrophils infiltration in the lungs of L-arginine mice as opposed to findings from other studies using this model is intriguing and questions the reproducibility of this model. Nevertheless, the lung changes observed in this mouse model of ANP corresponded well to the findings of recruitment of PIMs but not neutrophils and increased vascular expression of vWF in ANP dogs. Also, the use of L-arginine to induce PIMs in mouse provides a non-invasive and progressive method to study the recruitment of PIMs and the lung changes associated with ANP.

CHAPTER 5: GENERAL DISCUSSION AND FUTURE WORK

I report the first detailed investigation of the lung inflammation in clinical cases of ANP in dogs and conducted the first study assessing the induction of PIMs in a mouse model of ANP. The results showed that clinical cases of ANP in dogs develop lung inflammation during the disease. In addition, my work to establish a mouse model of ANP provides the first model to study the role of PIMs in ANP-associated lung inflammation and systemic pathophysiology in humans and dogs. The findings from this study show vascular inflammation and induction of PIMs in the lungs of animals suffering from ANP. Both dogs and mice are species lacking constitutive PIMs and therefore the mechanisms leading to their induction and adhesion to the lung microvasculature will be important to further characterize and understand. This study also brings the hypothesis that the activated pulmonary microvasculature through vWF expression could provide a favourable environment for PIMs to be induced and to adhere to the vascular endothelial cells.

The appearance of PIMs as central characters in the pathogenesis of lung inflammation is changing the way we understand lung disease. While alveolar macrophages have been traditionally attributed the role of an conductor of pro-inflammatory signals in the lung, the recent novel study of direct visualization of the role of alveolar macrophages in an isolated lung casts a serious doubt on such a rule (90). It is possible that while PIMs are induced and take over the pro-inflammatory role, the alveolar macrophages provide signals to dampen the inflammation and take over the clearance of cell debris. The role of induced PIMs

has only been studied in the context of liver dysfunction through the use of rodent models of bile-duct ligation (111) or in septic rats (112). Those data suggested that PIMs make the host already suffering from liver dysfunction or sepsis more susceptible to endotoxin-induced lung inflammation and mortality(111). The possibility that induced PIMs in humans and dogs with severe AP could increase their susceptibility to subsequent respiratory challenges may be a key explanation for the respiratory distress occurring during the course of this disease. This is relevant as patients suffering from ANP are at risk of being exposed to further respiratory challenges either from air-born infections associated with hospitalization conditions or via the blood systemic circulation if gut barrier dysfunction occurs causing endotoxemia or septicemia. Therefore, a special attention should be made to prevent secondary microbial insults in patients with ANP during the course of the hospitalization.

As for the future work, the mouse ANP model provides us a tool to study lung response to a secondary challenge following the onset of ANP through administration of endotoxins or bacteria, which would simulate what happens in clinical cases of AP complicated with dysfunction of the gut barrier. In addition, the role of PIMs in ANP-associated lung pathophysiology could be assessed through their depletion with gadolinium chloride or by the use of specific gene-knockouts to study the molecular mechanisms such as the role of MCP-1 in the induction of PIMs. Finally, evaluating the lungs from human patients that suffered from severe AP in comparison to the findings in ANP dogs' lungs would be very intriguing.

APPENDIX I

Table A : Paraffin embedding protocol for dog's lung and pancreas tissue.

Solution	Time period
70 % ethanol, 37°C	1 h
70 % ethanol, 37°C	1 h
80 % ethanol, 37°C	1 h
95 % ethanol, 37°C	1 h
100 % ethanol, 37°C	1 h
100 % ethanol, 37°C	1 h
100 % ethanol, 37°C	1 h
Xylene, 37°C	45 min
Xylene, 37°C	45 min
Paraffin, 60°C	30 min
Paraffin, 60°C	10 min
Paraffin, 60°C	10 min

APPENDIX II

Table I: Summary of the mouse L-arginine ANP model pilot study experimental designs

	Sample size	**Time points**	**L-arginine solution**	**Posology**
Pilot #1	**L-arginine group:** • 2 mice per time point • Total of 8 mice **Control group:** n=1	6h 48h 72h 120h	L-arginine monohydrochloride in saline 10 % pH 7.4 Product: A5131 Sigma Aldrich (purity 98%)	1 IP injection Dose: 5g/kg
Pilot #2	**L-arginine group:** • 2 mice per time point • Total of 8 mice **Control group:** n=3	6h 24h 72h 120h	L-arginine monohydrochloride in saline 8 % pH 7.4 Product: A5131 Sigma Aldrich (purity 98%)	2 IP injections, 1hour apart Dose: 4g/kg
Pilot #3	**L-arginine group:** n=4 **Control group:** n=4	72h	L-arginine monohydrochloride in saline 9 % pH 7.0 Product: 11039 Sigma Aldrich (purity 99.5%)	2 IP injections, 1hour apart Dose: 4.5g/kg

Figure 4.1: L-arginine ANP mouse model experimental design

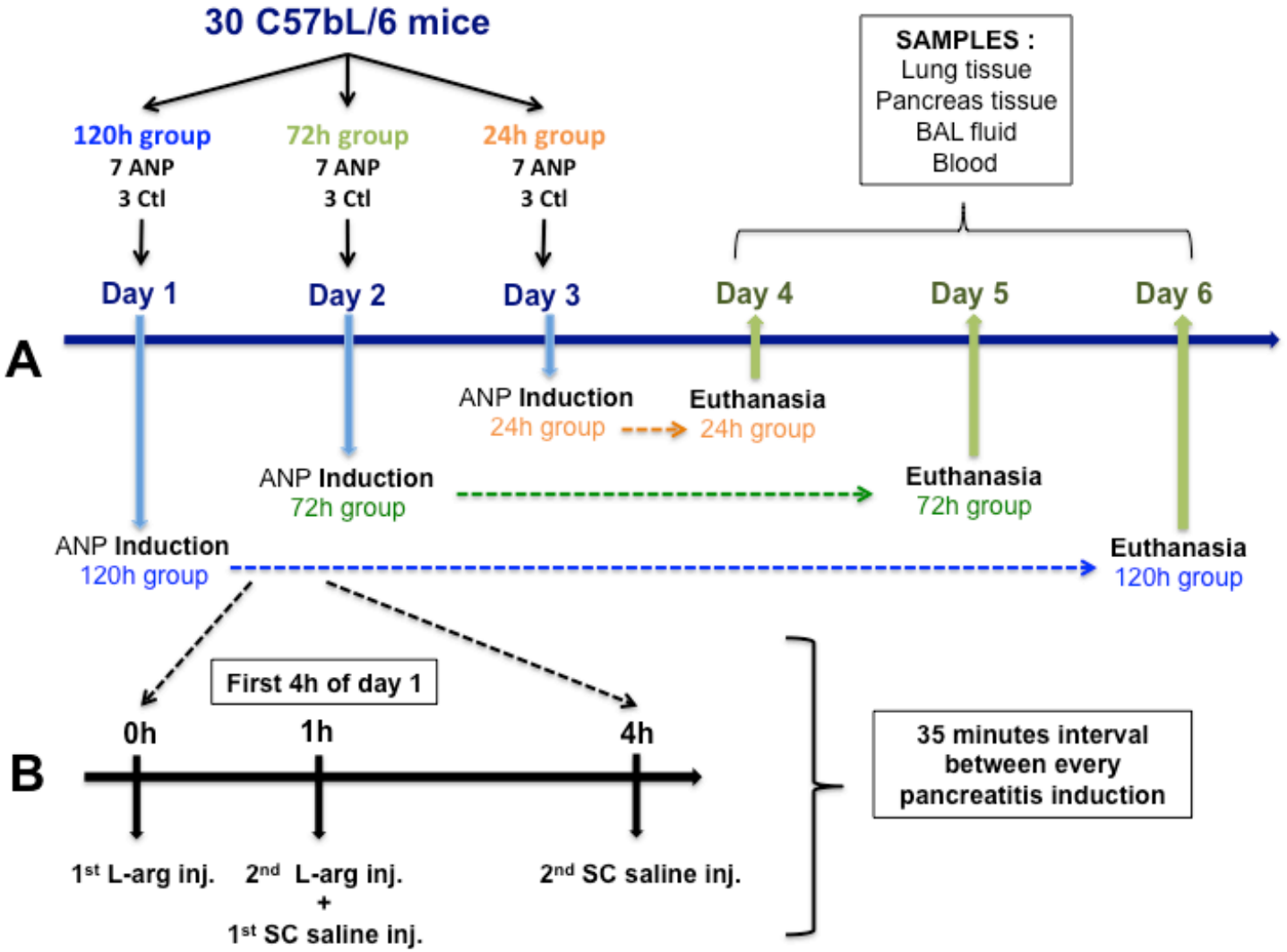

TABLE J: Example of the L-arginine ANP induction schedule for one day

Mouse #	tx	Time 1st injection	Time 2nd injection + SALINE S.C.	Time of 2nd SALINE S.C.
1	L-arg	7h05	8h05	11h05
2	L-arg	7h40	8h40	11h40
3	L-arg	8h15	9h15	12h15
4	L-arg	8h50	9h50	12h50
5	L-arg	9h25	10h25	13h25
6	L-arg	10h00	11h00	14h00
7	L-arg	10h35	11h35	14h35
8	SALINE	11h10	12h10	15h10
9	SALINE	11h45	12h45	15h10
10	SALINE	12h20	13h20	15h10

Table K: Human Intervention Point monitoring parameters used to monitor ANP mice

Humane Intervention Point Monitoring Parameters

Protocol 20100090: Lung inflammation associated with acute pancreatitis

Mice will be observed every hour during the first 8-10 hours after the second injection of L-Arginine. Thereafter, mice will be observed 3 times a day until euthanasia
Time points : 24h, 72h, 120h

Humane Intervention Point Monitoring Parameters

Body Weight – weight the mice every 12 hours
Score 0 Normal
1 <10% of loss of weight
2 10-15% of loss of weight
3 >15% of loss of weight
Physical Appearance
Score 0 Normal
1 Lack of Grooming, Orbital tightening: moderate, Ear position: moderately back
2 Rough Coat, Orbital tightening: severe, Ear position: severely back, round back
3 Very Rough Coat, grimace scale: severe, decubitus (ventral or lateral)
Unprovoked Behaviour
Score 0 Normal
1 Minor Changes :
2 Reduced Mobility, Decreased Alertness, ataxia
3 Self Mutilation, Immobility, Comatose
Respitory pattern
Score 0 Normal
1 increased respiratory rate, superficial
2 decreased respiratory rate and amplitude
3 intense respiratory efforts

- An individual score of 2 in any category: Re-check variables every 2 hours.
- If more than 2 categories are scored at 2 (or more): Consultation with Vet. is advised.*

- An individual score of 3 in any category: Euthanize animal.**

Table L: Paraffin embedding protocol for mice lung and pancreas tissue.

Solution	Time period
70 % ethanol, 37°C	1 h
70 % ethanol, 37°C	1 h
70 % ethanol, 37°C	1 h
80 % ethanol, 37°C	1 h
95 % ethanol, 37°C	1 h
100 % ethanol, 37°C	1 h
100 % ethanol, 37°C	1 h
100 % ethanol, 37°C	1 h
Xylene, 37°C	30 min
Xylene, 37°C	1.5 h
Paraffin, 60°C	30 min
Paraffin, 60°C	1 h
Paraffin, 60°C	2.5 h

LIST OF REFERENCES

1. Yadav D, Lowenfels AB. The epidemiology of pancreatitis and pancreatic cancer. Gastroenterology. 2013;144(6):1252-61.
2. Mansfield CS, James FE, Robertson ID. Development of a clinical severity index for dogs with acute pancreatitis. Journal of the American Veterinary Medical Association. 2008;233(6):936-44.
3. Mansfield C. Acute pancreatitis in dogs: advances in understanding, diagnostics, and treatment. Topics in companion animal medicine. 2012;27(3):123-32.
4. Cook AK, Breitschwerdt EB, Levine JF, Bunch SE, Linn LO. Risk factors associated with acute pancreatitis in dogs: 101 cases (1985-1990). Journal of the American Veterinary Medical Association. 1993;203(5):673-9.
5. Papa K, Mathe A, Abonyi-Toth Z, Sterczer A, Psader R, Hetyey C, et al. Occurrence, clinical features and outcome of canine pancreatitis (80 cases). Acta veterinaria Hungarica. 2011;59(1):37-52.
6. Brisinda G, Vanella S, Crocco A, Mazzari A, Tomaiuolo P, Santullo F, et al. Severe acute pancreatitis: advances and insights in assessment of severity and management. European journal of gastroenterology & hepatology. 2011;23(7):541-51.
7. Buter A, Imrie CW, Carter CR, Evans S, McKay CJ. Dynamic nature of early organ dysfunction determines outcome in acute pancreatitis. The British journal of surgery. 2002;89(3):298-302.
8. Johnson CD, Abu-Hilal M. Persistent organ failure during the first week as a marker of fatal outcome in acute pancreatitis. Gut. 2004;53(9):1340-4.

9. Petrov MS, Shanbhag S, Chakraborty M, Phillips AR, Windsor JA. Organ failure and infection of pancreatic necrosis as determinants of mortality in patients with acute pancreatitis. Gastroenterology. 2010;139(3):813-20.

10. Renner IG, Savage WT, 3rd, Pantoja JL, Renner VJ. Death due to acute pancreatitis. A retrospective analysis of 405 autopsy cases. Digestive diseases and sciences. 1985;30(10):1005-18.

11. Sarr MG, Banks PA, Bollen TL, Dervenis C, Gooszen HG, Johnson CD, et al. The new revised classification of acute pancreatitis 2012. The Surgical clinics of North America. 2013;93(3):549-62.

12. Interiano B, Stuard ID, Hyde RW. Acute respiratory distress syndrome in pancreatitis. Annals of internal medicine. 1972;77(6):923-6.

13. Talamini G, Uomo G, Pezzilli R, Rabitti PG, Billi P, Bassi C, et al. Serum creatinine and chest radiographs in the early assessment of acute pancreatitis. American journal of surgery. 1999;177(1):7-14.

14. Lei H, Minghao W, Xiaonan Y, Ping X, Ziqi L, Qing X. Acute lung injury in patients with severe acute pancreatitis. The Turkish journal of gastroenterology : the official journal of Turkish Society of Gastroenterology. 2013;24(5):502-7.

15. Gong ZY, Tang YQ. Onset time of complications in patients with severe acute pancreatitis receiving nonoperative therapy. Hepatobiliary & pancreatic diseases international : HBPD INT. 2002;1(1):143-5.

16. Lopez A, Lane IF, Hanna P. Adult respiratory distress syndrome in a dog with necrotizing pancreatitis. The Canadian veterinary journal La revue veterinaire canadienne. 1995;36(4):240-1.

17. Whitcomb DC, Lowe ME. Human pancreatic digestive enzymes. Digestive diseases and sciences. 2007;52(1):1-17.

18. Sah RP, Dawra RK, Saluja AK. New insights into the pathogenesis of pancreatitis. Current opinion in gastroenterology. 2013;29(5):523-30.

19. Banks PA, Bollen TL, Dervenis C, Gooszen HG, Johnson CD, Sarr MG, et al. Classification of acute pancreatitis--2012: revision of the Atlanta classification and definitions by international consensus. Gut. 2013;62(1):102-11.

20. Sarr MG. 2012 revision of the Atlanta classification of acute pancreatitis. Polskie Archiwum Medycyny Wewnetrznej. 2013;123(3):118-24.

21. van Santvoort HC, Bakker OJ, Bollen TL, Besselink MG, Ahmed Ali U, Schrijver AM, et al. A conservative and minimally invasive approach to necrotizing pancreatitis improves outcome. Gastroenterology. 2011;141(4):1254-63.

22. Yago MD, Martinez-Victoria E, Huertas JR, Manas M. Effects of the amount and type of dietary fat on exocrine pancreatic secretion in dogs after different periods of adaptation. Archives of physiology and biochemistry. 1997;105(1):78-85.

23. Lem KY, Fosgate GT, Norby B, Steiner JM. Associations between dietary factors and pancreatitis in dogs. Journal of the American Veterinary Medical Association. 2008;233(9):1425-31.

24. Whitcomb DC. Genetic aspects of pancreatitis. Annual review of medicine. 2010;61:413-24.

25. Joergensen MT, Brusgaard K, Cruger DG, Gerdes AM, Schaffalitzky de Muckadell OB. Genetic, epidemiological, and clinical aspects of hereditary pancreatitis: a

population-based cohort study in Denmark. The American journal of gastroenterology. 2010;105(8):1876-83.

26. Teich N, Rosendahl J, Toth M, Mossner J, Sahin-Toth M. Mutations of human cationic trypsinogen (PRSS1) and chronic pancreatitis. Human mutation. 2006;27(8):721-30.

27. Ohmuraya M, Sugano A, Hirota M, Takaoka Y, Yamamura K. Role of Intrapancreatic SPINK1/Spink3 Expression in the Development of Pancreatitis. Frontiers in physiology. 2012;3:126.

28. Paliwal S, Bhaskar S, Mani KR, Reddy DN, Rao GV, Singh SP, et al. Comprehensive screening of chymotrypsin C (CTRC) gene in tropical calcific pancreatitis identifies novel variants. Gut. 2013;62(11):1602-6.

29. Bishop MA, Xenoulis PG, Levinski MD, Suchodolski JS, Steiner JM. Identification of variants of the SPINK1 gene and their association with pancreatitis in Miniature Schnauzers. American journal of veterinary research. 2010;71(5):527-33.

30. Xenoulis PG, Levinski MD, Suchodolski JS, Steiner JM. Serum triglyceride concentrations in Miniature Schnauzers with and without a history of probable pancreatitis. Journal of veterinary internal medicine / American College of Veterinary Internal Medicine. 2011;25(1):20-5.

31. Haworth MD, Hosgood G, Swindells KL, Mansfield CS. Diagnostic accuracy of the SNAP and Spec canine pancreatic lipase tests for pancreatitis in dogs presenting with clinical signs of acute abdominal disease. J Vet Emerg Crit Care (San Antonio). 2014;24(2):135-43.

32. Williams DA, Batt RM. Sensitivity and specificity of radioimmunoassay of serum trypsin-like immunoreactivity for the diagnosis of canine exocrine pancreatic

insufficiency. Journal of the American Veterinary Medical Association. 1988;192(2):195-201.

33. Ruaux CG, Atwell RB. Levels of total alpha-macroglobulin and trypsin-like immunoreactivity are poor indicators of clinical severity in spontaneous canine acute pancreatitis. Research in veterinary science. 1999;67(1):83-7.

34. Mansfield CS, Jones BR. Plasma and urinary trypsinogen activation peptide in healthy dogs, dogs with pancreatitis and dogs with other systemic diseases. Australian veterinary journal. 2000;78(6):416-22.

35. Trivedi S, Marks SL, Kass PH, Luff JA, Keller SM, Johnson EG, et al. Sensitivity and specificity of canine pancreas-specific lipase (cPL) and other markers for pancreatitis in 70 dogs with and without histopathologic evidence of pancreatitis. Journal of veterinary internal medicine / American College of Veterinary Internal Medicine. 2011;25(6):1241-7.

36. Neilson-Carley SC, Robertson JE, Newman SJ, Kutchmarick D, Relford R, Woosley K, et al. Specificity of a canine pancreas-specific lipase assay for diagnosing pancreatitis in dogs without clinical or histologic evidence of the disease. American journal of veterinary research. 2011;72(3):302-7.

37. Newman SJ, Steiner JM, Woosley K, Williams DA, Barton L. Histologic assessment and grading of the exocrine pancreas in the dog. Journal of veterinary diagnostic investigation : official publication of the American Association of Veterinary Laboratory Diagnosticians, Inc. 2006;18(1):115-8.

38. Lim SY, Nakamura K, Morishita K, Sasaki N, Murakami M, Osuga T, et al. Qualitative and quantitative contrast-enhanced ultrasonographic assessment of cerulein-

induced acute pancreatitis in dogs. Journal of veterinary internal medicine / American College of Veterinary Internal Medicine. 2014;28(2):496-503.

39. Mansfield C. Pathophysiology of acute pancreatitis: potential application from experimental models and human medicine to dogs. Journal of veterinary internal medicine / American College of Veterinary Internal Medicine. 2012;26(4):875-87.

40. Su KH, Cuthbertson C, Christophi C. Review of experimental animal models of acute pancreatitis. HPB : the official journal of the International Hepato Pancreato Biliary Association. 2006;8(4):264-86.

41. Rinderknecht H. Activation of pancreatic zymogens. Normal activation, premature intrapancreatic activation, protective mechanisms against inappropriate activation. Digestive diseases and sciences. 1986;31(3):314-21.

42. Dawra R, Sah RP, Dudeja V, Rishi L, Talukdar R, Garg P, et al. Intra-acinar trypsinogen activation mediates early stages of pancreatic injury but not inflammation in mice with acute pancreatitis. Gastroenterology. 2011;141(6):2210-7 e2.

43. Hofbauer B, Saluja AK, Lerch MM, Bhagat L, Bhatia M, Lee HS, et al. Intra-acinar cell activation of trypsinogen during caerulein-induced pancreatitis in rats. The American journal of physiology. 1998;275(2 Pt 1):G352-62.

44. Lerch MM, Gorelick FS. Early trypsinogen activation in acute pancreatitis. The Medical clinics of North America. 2000;84(3):549-63, viii.

45. Grady T, Mah'Moud M, Otani T, Rhee S, Lerch MM, Gorelick FS. Zymogen proteolysis within the pancreatic acinar cell is associated with cellular injury. The American journal of physiology. 1998;275(5 Pt 1):G1010-7.

46. Saluja A, Saluja M, Villa A, Leli U, Rutledge P, Meldolesi J, et al. Pancreatic duct obstruction in rabbits causes digestive zymogen and lysosomal enzyme colocalization. The Journal of clinical investigation. 1989;84(4):1260-6.

47. Saluja AK, Bhagat L, Lee HS, Bhatia M, Frossard JL, Steer ML. Secretagogue-induced digestive enzyme activation and cell injury in rat pancreatic acini. The American journal of physiology. 1999;276(4 Pt 1):G835-42.

48. Kloppel G, Dreyer T, Willemer S, Kern HF, Adler G. Human acute pancreatitis: its pathogenesis in the light of immunocytochemical and ultrastructural findings in acinar cells. Virchows Archiv A, Pathological anatomy and histopathology. 1986;409(6):791-803.

49. Willemer S, Kloppel G, Kern HF, Adler G. Immunocytochemical and morphometric analysis of acinar zymogen granules in human acute pancreatitis. Virchows Archiv A, Pathological anatomy and histopathology. 1989;415(2):115-23.

50. Saluja AK, Steer MLP. Pathophysiology of pancreatitis. Role of cytokines and other mediators of inflammation. Digestion. 1999;60 Suppl 1:27-33.

51. Halangk W, Lerch MM, Brandt-Nedelev B, Roth W, Ruthenbuerger M, Reinheckel T, et al. Role of cathepsin B in intracellular trypsinogen activation and the onset of acute pancreatitis. The Journal of clinical investigation. 2000;106(6):773-81.

52. Simon P, Weiss FU, Sahin-Toth M, Parry M, Nayler O, Lenfers B, et al. Hereditary pancreatitis caused by a novel PRSS1 mutation (Arg-122 --> Cys) that alters autoactivation and autodegradation of cationic trypsinogen. The Journal of biological chemistry. 2002;277(7):5404-10.

53. Kukor Z, Mayerle J, Kruger B, Toth M, Steed PM, Halangk W, et al. Presence of cathepsin B in the human pancreatic secretory pathway and its role in trypsinogen activation during hereditary pancreatitis. The Journal of biological chemistry. 2002;277(24):21389-96.

54. Wartmann T, Mayerle J, Kahne T, Sahin-Toth M, Ruthenburger M, Matthias R, et al. Cathepsin L inactivates human trypsinogen, whereas cathepsin L-deletion reduces the severity of pancreatitis in mice. Gastroenterology. 2010;138(2):726-37.

55. Halangk W, Kruger B, Ruthenburger M, Sturzebecher J, Albrecht E, Lippert H, et al. Trypsin activity is not involved in premature, intrapancreatic trypsinogen activation. American journal of physiology Gastrointestinal and liver physiology. 2002;282(2):G367-74.

56. Han B, Ji B, Logsdon CD. CCK independently activates intracellular trypsinogen and NF-kappaB in rat pancreatic acinar cells. American journal of physiology Cell physiology. 2001;280(3):C465-72.

57. Hietaranta AJ, Saluja AK, Bhagat L, Singh VP, Song AM, Steer ML. Relationship between NF-kappaB and trypsinogen activation in rat pancreas after supramaximal caerulein stimulation. Biochemical and biophysical research communications. 2001;280(1):388-95.

58. Norman JG, Fink GW, Denham W, Yang J, Carter G, Sexton C, et al. Tissue-specific cytokine production during experimental acute pancreatitis. A probable mechanism for distant organ dysfunction. Digestive diseases and sciences. 1997;42(8):1783-8.

59. Norman JG, Fink GW, Franz MG. Acute pancreatitis induces intrapancreatic tumor necrosis factor gene expression. Archives of surgery. 1995;130(9):966-70.

60. Makhija R, Kingsnorth AN. Cytokine storm in acute pancreatitis. Journal of hepato-biliary-pancreatic surgery. 2002;9(4):401-10.

61. Fink GW, Norman JG. Specific changes in the pancreatic expression of the interleukin 1 family of genes during experimental acute pancreatitis. Cytokine. 1997;9(12):1023-7.

62. Pezzilli R, Billi P, Miniero R, Fiocchi M, Cappelletti O, Morselli-Labate AM, et al. Serum interleukin-6, interleukin-8, and beta 2-microglobulin in early assessment of severity of acute pancreatitis. Comparison with serum C-reactive protein. Digestive diseases and sciences. 1995;40(11):2341-8.

63. de Beaux AC, Goldie AS, Ross JA, Carter DC, Fearon KC. Serum concentrations of inflammatory mediators related to organ failure in patients with acute pancreatitis. The British journal of surgery. 1996;83(3):349-53.

64. Bhatia M, Saluja AK, Hofbauer B, Lee HS, Frossard JL, Steer ML. The effects of neutrophil depletion on a completely noninvasive model of acute pancreatitis-associated lung injury. International journal of pancreatology : official journal of the International Association of Pancreatology. 1998;24(2):77-83.

65. Frossard JL, Pastor CM. Experimental acute pancreatitis: new insights into the pathophysiology. Frontiers in bioscience : a journal and virtual library. 2002;7:d275-87.

66. Keck T, Friebe V, Warshaw AL, Antoniu BA, Waneck G, Benz S, et al. Pancreatic proteases in serum induce leukocyte-endothelial adhesion and pancreatic microcirculatory failure. Pancreatology. 2005;5(2-3):241-50.

67. Frossard JL, Saluja A, Bhagat L, Lee HS, Bhatia M, Hofbauer B, et al. The role of intercellular adhesion molecule 1 and neutrophils in acute pancreatitis and pancreatitis-associated lung injury. Gastroenterology. 1999;116(3):694-701.

68. Sandoval D, Gukovskaya A, Reavey P, Gukovsky S, Sisk A, Braquet P, et al. The role of neutrophils and platelet-activating factor in mediating experimental pancreatitis. Gastroenterology. 1996;111(4):1081-91.

69. Bhatia M, Ramnath RD, Chevali L, Guglielmotti A. Treatment with bindarit, a blocker of MCP-1 synthesis, protects mice against acute pancreatitis. American journal of physiology Gastrointestinal and liver physiology. 2005;288(6):G1259-65.

70. Huang H, Liu Y, Daniluk J, Gaiser S, Chu J, Wang H, et al. Activation of nuclear factor-kappaB in acinar cells increases the severity of pancreatitis in mice. Gastroenterology. 2013;144(1):202-10.

71. Baumann B, Wagner M, Aleksic T, von Wichert G, Weber CK, Adler G, et al. Constitutive IKK2 activation in acinar cells is sufficient to induce pancreatitis in vivo. The Journal of clinical investigation. 2007;117(6):1502-13.

72. DiMagno MJ. Nitric oxide pathways and evidence-based perturbations in acute pancreatitis. Pancreatology. 2007;7(5-6):403-8.

73. Ang AD, Adhikari S, Ng SW, Bhatia M. Expression of nitric oxide synthase isoforms and nitric oxide production in acute pancreatitis and associated lung injury. Pancreatology. 2009;9(1-2):150-9.

74. Dabrowski A, Gabryelewicz A. Nitric oxide contributes to multiorgan oxidative stress in acute experimental pancreatitis. Scandinavian journal of gastroenterology. 1994;29(10):943-8.

75. Lomis TJ, Siffring CW, Chalasani S, Ziegler DW, Lentz KE, Stauffer KE, et al. First place winner of the Conrad Jobst Award in the gold medal paper competition. Nitric oxide synthase inhibitors N-monomethylarginine and aminoguanidine prevent the progressive and severe hypotension associated with a rat model of pancreatitis. The American surgeon. 1995;61(1):7-10.

76. Molero X, Guarner F, Salas A, Mourelle M, Puig V, Malagelada JR. Nitric oxide modulates pancreatic basal secretion and response to cerulein in the rat: effects in acute pancreatitis. Gastroenterology. 1995;108(6):1855-62.

77. Klar E, Rattner DW, Compton C, Stanford G, Chernow B, Warshaw AL. Adverse effect of therapeutic vasoconstrictors in experimental acute pancreatitis. Annals of surgery. 1991;214(2):168-74.

78. Takeda K, Mikami Y, Fukuyama S, Egawa S, Sunamura M, Ishibashi T, et al. Pancreatic ischemia associated with vasospasm in the early phase of human acute necrotizing pancreatitis. Pancreas. 2005;30(1):40-9.

79. Foitzik T, Hotz HG, Schmidt J, Klar E, Warshaw AL, Buhr HJ. Effect of microcirculatory perfusion on distribution of trypsinogen activation peptides in acute experimental pancreatitis. Digestive diseases and sciences. 1995;40(10):2184-8.

80. Que RS, Cao LP, Ding GP, Hu JA, Mao KJ, Wang GF. Correlation of nitric oxide and other free radicals with the severity of acute pancreatitis and complicated systemic inflammatory response syndrome. Pancreas. 2010;39(4):536-40.

81. Bernard GR, Artigas A, Brigham KL, Carlet J, Falke K, Hudson L, et al. The American-European Consensus Conference on ARDS. Definitions, mechanisms, relevant

outcomes, and clinical trial coordination. American journal of respiratory and critical care medicine. 1994;149(3 Pt 1):818-24.

82. Wheeler AP, Bernard GR. Acute lung injury and the acute respiratory distress syndrome: a clinical review. Lancet. 2007;369(9572):1553-64.

83. Suratt BT, Parsons PE. Mechanisms of acute lung injury/acute respiratory distress syndrome. Clinics in chest medicine. 2006;27(4):579-89; abstract viii.

84. Tsushima K, King LS, Aggarwal NR, De Gorordo A, D'Alessio FR, Kubo K. Acute lung injury review. Intern Med. 2009;48(9):621-30.

85. Ashbaugh DG, Bigelow DB, Petty TL, Levine BE. Acute respiratory distress in adults. Lancet. 1967;2(7511):319-23.

86. Schneberger D, Aharonson-Raz K, Singh B. Monocyte and macrophage heterogeneity and Toll-like receptors in the lung. Cell and tissue research. 2011;343(1):97-106.

87. Aharonson-Raz K, Singh B. Pulmonary intravascular macrophages and endotoxin-induced pulmonary pathophysiology in horses. Canadian journal of veterinary research = Revue canadienne de recherche veterinaire. 2010;74(1):45-9.

88. Martinez FO, Sica A, Mantovani A, Locati M. Macrophage activation and polarization. Frontiers in bioscience : a journal and virtual library. 2008;13:453-61.

89. Mosser DM, Edwards JP. Exploring the full spectrum of macrophage activation. Nature reviews Immunology. 2008;8(12):958-69.

90. Westphalen K, Gusarova GA, Islam MN, Subramanian M, Cohen TS, Prince AS, et al. Sessile alveolar macrophages communicate with alveolar epithelium to modulate immunity. Nature. 2014;506(7489):503-6.

91. Krausgruber T, Blazek K, Smallie T, Alzabin S, Lockstone H, Sahgal N, et al. IRF5 promotes inflammatory macrophage polarization and TH1-TH17 responses. Nature immunology. 2011;12(3):231-8.

92. Biswas SK, Mantovani A. Macrophage plasticity and interaction with lymphocyte subsets: cancer as a paradigm. Nature immunology. 2010;11(10):889-96.

93. Juarez E, Nunez C, Sada E, Ellner JJ, Schwander SK, Torres M. Differential expression of Toll-like receptors on human alveolar macrophages and autologous peripheral monocytes. Respiratory research. 2010;11:2.

94. Bonfield TL, Konstan MW, Burfeind P, Panuska JR, Hilliard JB, Berger M. Normal bronchial epithelial cells constitutively produce the anti-inflammatory cytokine interleukin-10, which is downregulated in cystic fibrosis. American journal of respiratory cell and molecular biology. 1995;13(3):257-61.

95. Bedoret D, Wallemacq H, Marichal T, Desmet C, Quesada Calvo F, Henry E, et al. Lung interstitial macrophages alter dendritic cell functions to prevent airway allergy in mice. The Journal of clinical investigation. 2009;119(12):3723-38.

96. Horiguchi T, Enzan K, Kawamura K, Suzuki M. Pulmonary responses to heparin-protamine complexes: the effects of age and species. Journal of applied physiology. 1996;80(1):56-61.

97. Warner AE, Barry BE, Brain JD. Pulmonary intravascular macrophages in sheep. Morphology and function of a novel constituent of the mononuclear phagocyte system. Laboratory investigation; a journal of technical methods and pathology. 1986;55(3):276-88.

98. Sethi RS, Brar RS, Singh O, Singh B. Immunolocalization of pulmonary intravascular macrophages, TLR4, TLR9 and IL-8 in normal and Pasteurella multocida-infected lungs of water buffalo (Bubalus bubalis). Journal of comparative pathology. 2011;144(2-3):135-44.

99. Winkler GC. Pulmonary intravascular macrophages in domestic animal species: review of structural and functional properties. The American journal of anatomy. 1988;181(3):217-34.

100. Brain JD. Mechanisms, measurement, and significance of lung macrophage function. Environmental health perspectives. 1992;97:5-10.

101. Brain JD, Molina RM, DeCamp MM, Warner AE. Pulmonary intravascular macrophages: their contribution to the mononuclear phagocyte system in 13 species. The American journal of physiology. 1999;276(1 Pt 1):L146-54.

102. Longworth KE, Albertine KH, Staub NC. Ultrastructural quantification of pulmonary intravascular macrophages in newborn and 2-week-old lambs. The Anatomical record. 1996;246(2):238-44.

103. Winkler GC, Cheville NF. Postnatal colonization of porcine lung capillaries by intravascular macrophages: an ultrastructural, morphometric analysis. Microvascular research. 1987;33(2):224-32.

104. Staub NC. Pulmonary intravascular macrophages. Annual review of physiology. 1994;56:47-67.

105. Atwal OS, Singh B, Staempfli H, Minhas K. Presence of pulmonary intravascular macrophages in the equine lung: some structuro-functional properties. The Anatomical record. 1992;234(4):530-40.

106. Parbhakar OP, Duke T, Townsend HG, Singh B. Immunophenotypic characterization and depletion of pulmonary intravascular macrophages of horses. Veterinary research. 2004;35(1):39-51.

107. Longworth KE, Jarvis KA, Tyler WS, Steffey EP, Staub NC. Pulmonary intravascular macrophages in horses and ponies. American journal of veterinary research. 1994;55(3):382-8.

108. Kawashima M, Kuwamura M, Takeya M, Yamate J. Morphologic characteristics of pulmonary macrophages in cetaceans: particular reference to pulmonary intravascular macrophages as a newly identified type. Veterinary pathology. 2004;41(6):682-6.

109. Molina RM, Brain JD. In vivo comparison of cat alveolar and pulmonary intravascular macrophages: phagocytosis, particle clearance, and cytoplasmic motility. Experimental lung research. 2007;33(2):53-70.

110. Chang SW, Ohara N. Chronic biliary obstruction induces pulmonary intravascular phagocytosis and endotoxin sensitivity in rats. The Journal of clinical investigation. 1994;94(5):2009-19.

111. Gill SS, Suri SS, Janardhan KS, Caldwell S, Duke T, Singh B. Role of pulmonary intravascular macrophages in endotoxin-induced lung inflammation and mortality in a rat model. Respiratory research. 2008;9:69.

112. Singh B, Doane KJ, Niehaus GD. Ultrastructural and cytochemical evaluation of sepsis-induced changes in the rat pulmonary intravascular mononuclear phagocytes. Journal of anatomy. 1998;192 (Pt 1):13-23.

113. Dehring DJ, Wismar BL. Intravascular macrophages in pulmonary capillaries of humans. The American review of respiratory disease. 1989;139(4):1027-9.

114. Klingensmith WC, 3rd, Yang SL, Wagner HN, Jr. Lung uptake of Tc-99m sulfur colloid in liver and spleen imaging. Journal of nuclear medicine : official publication, Society of Nuclear Medicine. 1978;19(1):31-5.

115. Klingensmith WC, 3rd, Tsan MF, Wagner HN, Jr. Factors affecting the uptake of 99mTc-sulfur colloid by the lung and kidney. Journal of nuclear medicine : official publication, Society of Nuclear Medicine. 1976;17(8):681-4.

116. Klingensmith WC, 3rd, Ryerson TW. Lung uptake of 99m Tc-sulfur colloid. Journal of nuclear medicine : official publication, Society of Nuclear Medicine. 1973;14(4):201-4.

117. Shih WJ, Domstad PA, Friedman B, DeLand FH. Intrathoracic abnormalities demonstrated by technetium-99m sulfur colloid imaging. Clinical nuclear medicine. 1986;11(11):792-6.

118. Crocker SH, Eddy DO, Obenauf RN, Wismar BL, Lowery BD. Bacteremia: host-specific lung clearance and pulmonary failure. The Journal of trauma. 1981;21(3):215-20.

119. Dillon AR, Warner AE, Brawner W, Hudson J, Tillson M. Activity of pulmonary intravascular macrophages in cats and dogs with and without adult Dirofilaria immitis. Veterinary parasitology. 2008;158(3):171-6.

120. Schneberger D, Lewis D, Caldwell S, Singh B. Expression of toll-like receptor 9 in lungs of pigs, dogs and cattle. International journal of experimental pathology. 2011;92(1):1-7.

121. Atwal OS, Saldanha KA. Erythrophagocytosis in alveolar capillaries of goat lung: ultrastructural properties of blood monocytes. Acta anatomica. 1985;124(3-4):245-54.

122. Smith JS, Tian J, Lozier JN, Byrnes AP. Severe pulmonary pathology after intravenous administration of vectors in cirrhotic rats. Molecular therapy : the journal of the American Society of Gene Therapy. 2004;9(6):932-41.

123. DeCamp MM, Warner AE, Molina RM, Brain JD. Hepatic versus pulmonary uptake of particles injected into the portal circulation in sheep. Endotoxin escapes hepatic clearance causing pulmonary inflammation. The American review of respiratory disease. 1992;146(1):224-31.

124. Singh B, Atwal OS. Ultrastructural and immunocytochemical study of the pulmonary intravascular macrophages of Escherichia coli lipopolysaccharide-treated sheep. The Anatomical record. 1997;247(2):214-24.

125. Singh B, Minhas KJ, Atwal OS. Ultracytochemical study of multiple dose effect of monastral blue uptake by equine pulmonary intravascular macrophages (PIMs). Journal of submicroscopic cytology and pathology. 1994;26(2):235-43.

126. Warner AE, Molina RM, Brain JD. Uptake of bloodborne bacteria by pulmonary intravascular macrophages and consequent inflammatory responses in sheep. The American review of respiratory disease. 1987;136(3):683-90.

127. Warner AE, Brain JD. The cell biology and pathogenic role of pulmonary intravascular macrophages. The American journal of physiology. 1990;258(2 Pt 1):L1-12.

128. Parbhakar OP, Duke T, Townsend HG, Singh B. Depletion of pulmonary intravascular macrophages partially inhibits lipopolysaccharide-induced lung inflammation in horses. Veterinary research. 2005;36(4):557-69.

129. Singh B, de la Concha-Bermejillo A. Gadolinium chloride removes pulmonary intravascular macrophages and curtails the degree of ovine lentivirus-induced lymphoid interstitial pneumonia. International journal of experimental pathology. 1998;79(3):151-62.

130. Singh B, Pearce JW, Gamage LN, Janardhan K, Caldwell S. Depletion of pulmonary intravascular macrophages inhibits acute lung inflammation. American journal of physiology Lung cellular and molecular physiology. 2004;286(2):L363-72.

131. Sone Y, Serikov VB, Staub NC, Sr. Intravascular macrophage depletion attenuates endotoxin lung injury in anesthetized sheep. Journal of applied physiology. 1999;87(4):1354-9.

132. Thenappan T, Goel A, Marsboom G, Fang YH, Toth PT, Zhang HJ, et al. A central role for CD68(+) macrophages in hepatopulmonary syndrome. Reversal by macrophage depletion. American journal of respiratory and critical care medicine. 2011;183(8):1080-91.

133. Chen ZT, Li SL, Cai EQ, Wu WL, Jin JS, Zhu B. LPS induces pulmonary intravascular macrophages producing inflammatory mediators via activating NF-kappaB. Journal of cellular biochemistry. 2003;89(6):1206-14.

134. Singh Suri S, Janardhan KS, Parbhakar O, Caldwell S, Appleyard G, Singh B. Expression of toll-like receptor 4 and 2 in horse lungs. Veterinary research. 2006;37(4):541-51.

135. Schneberger D, Caldwell S, Suri SS, Singh B. Expression of toll-like receptor 9 in horse lungs. Anatomical record. 2009;292(7):1068-77.

136. Carrasco L, Nunez A, Salguero FJ, Diaz San Segundo F, Sanchez-Cordon P, Gomez-Villamandos JC, et al. African swine fever: Expression of interleukin-1 alpha and tumour necrosis factor-alpha by pulmonary intravascular macrophages. Journal of comparative pathology. 2002;126(2-3):194-201.

137. Charavaryamath C, Janardhan KS, Caldwell S, Singh B. Pulmonary intravascular monocytes/macrophages in a rat model of sepsis. The anatomical record Part A, Discoveries in molecular, cellular, and evolutionary biology. 2006;288(12):1259-71.

138. Chitko-McKown CG, Chapes SK, Brown RE, Phillips RM, McKown RD, Blecha F. Porcine alveolar and pulmonary intravascular macrophages: comparison of immune functions. Journal of leukocyte biology. 1991;50(4):364-72.

139. Sutherland DE, Gruessner RW, Gruessner AC. Pancreas transplantation for treatment of diabetes mellitus. World journal of surgery. 2001;25(4):487-96.

140. Fernandez-Cruz L, Sabater L, Gilabert R, Ricart MJ, Saenz A, Astudillo E. Native and graft pancreatitis following combined pancreas-renal transplantation. The British journal of surgery. 1993;80(11):1429-32.

141. Closa D, Bardaji M, Hotter G, Prats N, Gelpi E, Fernandez-Cruz L, et al. Hepatic involvement in pancreatitis-induced lung damage. The American journal of physiology. 1996;270(1 Pt 1):G6-13.

142. Murr MM, Yang J, Fier A, Kaylor P, Mastorides S, Norman JG. Pancreatic elastase induces liver injury by activating cytokine production within Kupffer cells via

nuclear factor-Kappa B. Journal of gastrointestinal surgery : official journal of the Society for Surgery of the Alimentary Tract. 2002;6(3):474-80.

143. Hoyos S, Granell S, Heredia N, Bulbena O, Closa D, Fernandez-Cruz L. Influence of portal blood on the development of systemic inflammation associated with experimental acute pancreatitis. Surgery. 2005;137(2):186-91.

144. Folch E, Prats N, Hotter G, Lopez S, Gelpi E, Rosello-Catafau J, et al. P-selectin expression and Kupffer cell activation in rat acute pancreatitis. Digestive diseases and sciences. 2000;45(8):1535-44.

145. Gloor B, Blinman TA, Rigberg DA, Todd KE, Lane JS, Hines OJ, et al. Kupffer cell blockade reduces hepatic and systemic cytokine levels and lung injury in hemorrhagic pancreatitis in rats. Pancreas. 2000;21(4):414-20.

146. Liu HB, Cui NQ, Li DH, Chen C. Role of Kupffer cells in acute hemorrhagic necrotizing pancreatitis-associated lung injury of rats. World journal of gastroenterology : WJG. 2006;12(3):403-7.

147. Closa D, Sabater L, Fernandez-Cruz L, Prats N, Gelpi E, Rosello-Catafau J. Activation of alveolar macrophages in lung injury associated with experimental acute pancreatitis is mediated by the liver. Annals of surgery. 1999;229(2):230-6.

148. Mikami Y, Takeda K, Shibuya K, Qiu-Feng H, Egawa S, Sunamura M, et al. Peritoneal inflammatory cells in acute pancreatitis: Relationship of infiltration dynamics and cytokine production with severity of illness. Surgery. 2002;132(1):86-92.

149. Borgstrom A, Ohlsson K. Immunoreactive trypsin in serum and peritoneal fluid in acute pancreatitis. Hoppe-Seyler's Zeitschrift fur physiologische Chemie. 1978;359(6):677-81.

150. Heath DI, Wilson C, Gudgeon AM, Jehanli A, Shenkin A, Imrie CW. Trypsinogen activation peptides (TAP) concentrations in the peritoneal fluid of patients with acute pancreatitis and their relation to the presence of histologically confirmed pancreatic necrosis. Gut. 1994;35(9):1311-5.

151. Lundberg AH, Eubanks JW, 3rd, Henry J, Sabek O, Kotb M, Gaber L, et al. Trypsin stimulates production of cytokines from peritoneal macrophages in vitro and in vivo. Pancreas. 2000;21(1):41-51.

152. Chen HM, Shyr MH, Chen MF. Gabexate mesilate improves pancreatic microcirculation and reduces lung edema in a rat model of acute pancreatitis. Journal of the Formosan Medical Association = Taiwan yi zhi. 1997;96(9):704-9.

153. Souza LJ, Coelho AM, Sampietre SN, Martins JO, Cunha JE, Machado MC. Anti-inflammatory effects of peritoneal lavage in acute pancreatitis. Pancreas. 2010;39(8):1180-4.

154. Mikami Y, Takeda K, Shibuya K, Qiu-Feng H, Shimamura H, Yamauchi J, et al. Do peritoneal macrophages play an essential role in the progression of acute pancreatitis in rats? Pancreas. 2003;27(3):253-60.

155. Satoh A, Shimosegawa T, Kimura K, Moriizumi S, Masamune A, Koizumi M, et al. Nitric oxide is overproduced by peritoneal macrophages in rat taurocholate pancreatitis: the mechanism of inducible nitric oxide synthase expression. Pancreas. 1998;17(4):402-11.

156. Tahamont MV, Barie PS, Blumenstock FA, Hussain MH, Malik AB. Increased lung vascular permeability after pancreatitis and trypsin infusion. The American journal of pathology. 1982;109(1):15-26.

157. Foitzik T, Eibl G, Hotz B, Hotz H, Kahrau S, Kasten C, et al. Persistent multiple organ microcirculatory disorders in severe acute pancreatitis: experimental findings and clinical implications. Digestive diseases and sciences. 2002;47(1):130-8.

158. Pastor CM, Matthay MA, Frossard JL. Pancreatitis-associated acute lung injury: new insights. Chest. 2003;124(6):2341-51.

159. Guice KS, Oldham KT, Caty MG, Johnson KJ, Ward PA. Neutrophil-dependent, oxygen-radical mediated lung injury associated with acute pancreatitis. Annals of surgery. 1989;210(6):740-7.

160. Inoue S, Nakao A, Kishimoto W, Murakami H, Itoh K, Itoh T, et al. Anti-neutrophil antibody attenuates the severity of acute lung injury in rats with experimental acute pancreatitis. Archives of surgery. 1995;130(1):93-8.

161. Werner J, Z'Graggen K, Fernandez-del Castillo C, Lewandrowski KB, Compton CC, Warshaw AL. Specific therapy for local and systemic complications of acute pancreatitis with monoclonal antibodies against ICAM-1. Annals of surgery. 1999;229(6):834-40; discussion 41-2.

162. Kaufmann P, Tilz GP, Smolle KH, Demel U, Krejs GJ. Increased plasma concentrations of circulating intercellular adhesion molecule-1 (cICAM-1) in patients with necrotizing pancreatitis. Immunobiology. 1996;195(2):209-19.

163. Lundberg AH, Granger N, Russell J, Callicutt S, Gaber LW, Kotb M, et al. Temporal correlation of tumor necrosis factor-alpha release, upregulation of pulmonary ICAM-1 and VCAM-1, neutrophil sequestration, and lung injury in diet-induced pancreatitis. Journal of gastrointestinal surgery : official journal of the Society for Surgery of the Alimentary Tract. 2000;4(3):248-57.

164. Tsukahara Y, Morisaki T, Horita Y, Torisu M, Tanaka M. Phospholipase A2 mediates nitric oxide production by alveolar macrophages and acute lung injury in pancreatitis. Annals of surgery. 1999;229(3):385-92.

165. Nevalainen TJ, Hietaranta AJ, Gronroos JM. Phospholipase A2 in acute pancreatitis: new biochemical and pathological aspects. Hepato-gastroenterology. 1999;46(29):2731-5.

166. Gronroos JM, Nevalainen TJ. Increased concentrations of synovial-type phospholipase A2 in serum and pulmonary and renal complications in acute pancreatitis. Digestion. 1992;52(3-4):232-6.

167. Edelson JD, Vadas P, Villar J, Mullen JB, Pruzanski W. Acute lung injury induced by phospholipase A2. Structural and functional changes. The American review of respiratory disease. 1991;143(5 Pt 1):1102-9.

168. Nordback I, Teerenhovi O, Auvinen O, Koivula T, Thuren T, Kinnunen P, et al. Human pancreatic phospholipase A2 in acute necrotizing pancreatitis. Digestion. 1989;42(3):128-34.

169. Offenstadt G, Pinta P, Masliah J, Alcindor LG, Hericord P, Amstutz P. Phospholipase and prophospholipase activities in bronchoalveolar lavage fluid in severe acute pulmonary disease with or without ARDS. Intensive care medicine. 1981;7(6):285-90.

170. Gea-Sorli S, Guillamat R, Serrano-Mollar A, Closa D. Activation of lung macrophage subpopulations in experimental acute pancreatitis. The Journal of pathology. 2011;223(3):417-24.

171. Sailai Y, Yu X, Baiheti P, Tang H, Li Y, Xu M. Influence of nuclear factor kappaB activation on inflammatory mediators of alveolar macrophages in rats with acute necrotizing pancreatitis. Journal of investigative medicine : the official publication of the American Federation for Clinical Research. 2010;58(1):38-42.

172. Cheng S, Zhao J, He SG, Song MM, Li ZH, Zhang YW. [The role of nitric oxide in lung injury associated with acute necrotizing pancreatitis]. Zhonghua wai ke za zhi [Chinese journal of surgery]. 2003;41(5):336-9.

173. Cheng S, Yan WM, Yang B, Shi JD, Song MM, Zhao Y. A crucial role of nitric oxide in acute lung injury secondary to the acute necrotizing pancreatitis. Human & experimental toxicology. 2010;29(4):329-37.

174. Zhang L, Chen Y, Wang L, Chen XP, Zhang WG, Wang CY, et al. Chloroquine relieves acute lung injury in rats with acute hemorrhagic necrotizing pancreatitis. Journal of Huazhong University of Science and Technology Medical sciences = Hua zhong ke ji da xue xue bao Yi xue Ying De wen ban = Huazhong keji daxue xuebao Yixue Yingdewen ban. 2013;33(3):357-60.

175. Medzhitov R. Toll-like receptors and innate immunity. Nature reviews Immunology. 2001;1(2):135-45.

176. Hoshino K, Takeuchi O, Kawai T, Sanjo H, Ogawa T, Takeda Y, et al. Cutting edge: Toll-like receptor 4 (TLR4)-deficient mice are hyporesponsive to lipopolysaccharide: evidence for TLR4 as the Lps gene product. Journal of immunology. 1999;162(7):3749-52.

177. Poltorak A, He X, Smirnova I, Liu MY, Van Huffel C, Du X, et al. Defective LPS signaling in C3H/HeJ and C57BL/10ScCr mice: mutations in Tlr4 gene. Science. 1998;282(5396):2085-8.

178. Jiang D, Liang J, Fan J, Yu S, Chen S, Luo Y, et al. Regulation of lung injury and repair by Toll-like receptors and hyaluronan. Nature medicine. 2005;11(11):1173-9.

179. Zou N, Ao L, Cleveland JC, Jr., Yang X, Su X, Cai GY, et al. Critical role of extracellular heat shock cognate protein 70 in the myocardial inflammatory response and cardiac dysfunction after global ischemia-reperfusion. American journal of physiology Heart and circulatory physiology. 2008;294(6):H2805-13.

180. Mizunuma T, Kawamura S, Kishino Y. Effects of injecting excess arginine on rat pancreas. The Journal of nutrition. 1984;114(3):467-71.

181. Dawra R, Sharif R, Phillips P, Dudeja V, Dhaulakhandi D, Saluja AK. Development of a new mouse model of acute pancreatitis induced by administration of L-arginine. American journal of physiology Gastrointestinal and liver physiology. 2007;292(4):G1009-18.

182. Weaver C, Bishop AE, Polak JM. Pancreatic changes elicited by chronic administration of excess L-arginine. Experimental and molecular pathology. 1994;60(2):71-87.

183. Shen JQ, Shen J, Wang XP. Expression of insulin-like growth factor binding protein-4 (IGFBP-4) in acute pancreatitis induced by L-arginine in mice. Acta histochemica. 2012;114(4):379-85.

184. Shen J, Wan R, Shen Z, Gao J, Wang X, Qian L, et al. Chemokine receptor CXCR3 is involved in the acute pancreatitis-associated lung injury. Biomedicine & pharmacotherapy = Biomedecine & pharmacotherapie. 2012;66(5):390-6.

185. Shen J, Wan R, Hu G, Wang F, Shen J, Wang X. Involvement of thrombopoietin in acinar cell necrosis in L-arginine-induced acute pancreatitis in mice. Cytokine. 2012;60(1):294-301.

186. Biczo G, Hegyi P, Berczi S, Dosa S, Hracsko Z, Varga IS, et al. Inhibition of arginase activity ameliorates L-arginine-induced acute pancreatitis in rats. Pancreas. 2010;39(6):868-74.

187. Rakonczay Z, Jr., Hegyi P, Dosa S, Ivanyi B, Jarmay K, Biczo G, et al. A new severe acute necrotizing pancreatitis model induced by L-ornithine in rats. Critical care medicine. 2008;36(7):2117-27.

188. Chvanov M, Petersen OH, Tepikin A. Free radicals and the pancreatic acinar cells: role in physiology and pathology. Philosophical transactions of the Royal Society of London Series B, Biological sciences. 2005;360(1464):2273-84.

189. Dobosz M, Hac S, Mionskowska L, Dymecki D, Dobrowolski S, Wajda Z. Organ microcirculatory disturbances in experimental acute pancreatitis. A role of nitric oxide. Physiological research / Academia Scientiarum Bohemoslovaca. 2005;54(4):363-8.

190. DiMagno MJ, Hao Y, Tsunoda Y, Williams JA, Owyang C. Secretagogue-stimulated pancreatic secretion is differentially regulated by constitutive NOS isoforms in mice. American journal of physiology Gastrointestinal and liver physiology. 2004;286(3):G428-36.

191. Takacs T, Rakonczay Z, Jr., Varga IS, Ivanyi B, Mandi Y, Boros I, et al. Comparative effects of water immersion pretreatment on three different acute pancreatitis models in rats. Biochemistry and cell biology = Biochimie et biologie cellulaire. 2002;80(2):241-51.

192. Ayub K, Serracino-Inglott F, Williamson RC, Mathie RT. Expression of inducible nitric oxide synthase contributes to the development of pancreatitis following pancreatic ischaemia and reperfusion. The British journal of surgery. 2001;88(9):1189-93.

193. Konturek SJ, Bilski J, Konturek PK, Cieszkowski M, Pawlik W. Role of endogenous nitric oxide in the control of canine pancreatic secretion and blood flow. Gastroenterology. 1993;104(3):896-902.

194. Hegyi P, Rakonczay Z, Jr., Sari R, Gog C, Lonovics J, Takacs T, et al. L-arginine-induced experimental pancreatitis. World journal of gastroenterology : WJG. 2004;10(14):2003-9.

195. Werner J, Fernandez-del Castillo C, Rivera JA, Kollias N, Lewandrowski KB, Rattner DW, et al. On the protective mechanisms of nitric oxide in acute pancreatitis. Gut. 1998;43(3):401-7.

196. Hardman J, Shields C, Schofield D, McMahon R, Redmond HP, Siriwardena AK. Intravenous antioxidant modulation of end-organ damage in L-arginine-induced experimental acute pancreatitis. Pancreatology. 2005;5(4-5):380-6.

197. Foitzik T, Eibl G, Buhr HJ. Therapy for microcirculatory disorders in severe acute pancreatitis: comparison of delayed therapy with ICAM-1 antibodies and a specific endothelin A receptor antagonist. Journal of gastrointestinal surgery : official journal of the Society for Surgery of the Alimentary Tract. 2000;4(3):240-6; discussion 7.

198. Ammori BJ. Role of the gut in the course of severe acute pancreatitis. Pancreas. 2003;26(2):122-9.

199. Ammori BJ, Leeder PC, King RF, Barclay GR, Martin IG, Larvin M, et al. Early increase in intestinal permeability in patients with severe acute pancreatitis: correlation with endotoxemia, organ failure, and mortality. Journal of gastrointestinal surgery : official journal of the Society for Surgery of the Alimentary Tract. 1999;3(3):252-62.

200. Brandtzaeg P, Jones DB, Flavell DJ, Fagerhol MK. Mac 387 antibody and detection of formalin resistant myelomonocytic L1 antigen. Journal of clinical pathology. 1988;41(9):963-70.

201. Brandtzaeg P. The new monoclonal antibody (Mac 387) that reacts with macrophages on paraffin sections detects the well-known leukocyte L1 antigen. The journal of histochemistry and cytochemistry : official journal of the Histochemistry Society. 1988;36(9):1203-6.

202. Guignard F, Mauel J, Markert M. The monoclonal antibody Mac 387 recognizes three S100 proteins in human neutrophils. Immunology and cell biology. 1996;74(1):105-7.

203. Aulakh GK, Suri SS, Singh B. Angiostatin inhibits acute lung injury in a mouse model. American journal of physiology Lung cellular and molecular physiology. 2014;306(1):L58-68.

204. Weibel ER, Palade GE. New Cytoplasmic Components in Arterial Endothelia. The Journal of cell biology. 1964;23:101-12.

205. van Mourik JA, Romani de Wit T, Voorberg J. Biogenesis and exocytosis of Weibel-Palade bodies. Histochemistry and cell biology. 2002;117(2):113-22.

206. Dong JF, Moake JL, Nolasco L, Bernardo A, Arceneaux W, Shrimpton CN, et al. ADAMTS-13 rapidly cleaves newly secreted ultralarge von Willebrand factor multimers on the endothelial surface under flowing conditions. Blood. 2002;100(12):4033-9.

207. Nichols TC, Bellinger DA, Reddick RL, Smith SV, Koch GG, Davis K, et al. The roles of von Willebrand factor and factor VIII in arterial thrombosis: studies in canine von Willebrand disease and hemophilia A. Blood. 1993;81(10):2644-51.

208. Sanders WE, Jr., Reddick RL, Nichols TC, Brinkhous KM, Read MS. Thrombotic thrombocytopenia induced in dogs and pigs. The role of plasma and platelet vWF in animal models of thrombotic thrombocytopenic purpura. Arteriosclerosis, thrombosis, and vascular biology. 1995;15(6):793-800.

209. Petri B, Broermann A, Li H, Khandoga AG, Zarbock A, Krombach F, et al. von Willebrand factor promotes leukocyte extravasation. Blood. 2010;116(22):4712-9.

210. Wolff B, Burns AR, Middleton J, Rot A. Endothelial cell "memory" of inflammatory stimulation: human venular endothelial cells store interleukin 8 in Weibel-Palade bodies. The Journal of experimental medicine. 1998;188(9):1757-62.

211. Utgaard JO, Jahnsen FL, Bakka A, Brandtzaeg P, Haraldsen G. Rapid secretion of prestored interleukin 8 from Weibel-Palade bodies of microvascular endothelial cells. The Journal of experimental medicine. 1998;188(9):1751-6.

212. Koivunen E, Ranta TM, Annila A, Taube S, Uppala A, Jokinen M, et al. Inhibition of beta(2) integrin-mediated leukocyte cell adhesion by leucine-leucine-glycine motif-containing peptides. The Journal of cell biology. 2001;153(5):905-16.

213. Pendu R, Terraube V, Christophe OD, Gahmberg CG, de Groot PG, Lenting PJ, et al. P-selectin glycoprotein ligand 1 and beta2-integrins cooperate in the adhesion of leukocytes to von Willebrand factor. Blood. 2006;108(12):3746-52.

214. Pegon JN, Kurdi M, Casari C, Odouard S, Denis CV, Christophe OD, et al. Factor VIII and von Willebrand factor are ligands for the carbohydrate-receptor Siglec-5. Haematologica. 2012;97(12):1855-63.

215. Bernardo A, Ball C, Nolasco L, Choi H, Moake JL, Dong JF. Platelets adhered to endothelial cell-bound ultra-large von Willebrand factor strings support leukocyte tethering and rolling under high shear stress. Journal of thrombosis and haemostasis : JTH. 2005;3(3):562-70.

216. Wassef A, Janardhan K, Pearce JW, Singh B. Toll-like receptor 4 in normal and inflamed lungs and other organs of pig, dog and cattle. Histology and histopathology. 2004;19(4):1201-8.

217. Montgomery JB, Hamblin B, Suri SS, Johnson LE, New D, Johnston J, et al. Remote lung injury after experimental intestinal ischemia-reperfusion in horses. Histology and histopathology. 2014;29(3):361-75.

218. Sharif R, Dawra R, Wasiluk K, Phillips P, Dudeja V, Kurt-Jones E, et al. Impact of toll-like receptor 4 on the severity of acute pancreatitis and pancreatitis-associated lung injury in mice. Gut. 2009;58(6):813-9.

219. Ogden JM, Modlin IM, Gorelick FS, Marks IN. Effect of buprenorphine on pancreatic enzyme synthesis and secretion in normal rats and rats with acute edematous pancreatitis. Digestive diseases and sciences. 1994;39(11):2407-15.

220. Kim EH, Hoge SG, Lightner AM, Grady EF, Coelho AM, Kirkwood KS. Activation of nociceptive neurons in T9 and T10 in cerulein pancreatitis. The Journal of surgical research. 2004;117(2):195-201.

221. Bohus E, Coen M, Keun HC, Ebbels TM, Beckonert O, Lindon JC, et al. Temporal metabonomic modeling of l-arginine-induced exocrine pancreatitis. Journal of proteome research. 2008;7(10):4435-45.

222. Chen J, Cai QP, Shen PJ, Yan RL, Wang CM, Yang DJ, et al. Netrin-1 protects against L-Arginine-induced acute pancreatitis in mice. PloS one. 2012;7(9):e46201.

223. Kanaji S, Fahs SA, Shi Q, Haberichter SL, Montgomery RR. Contribution of platelet vs. endothelial VWF to platelet adhesion and hemostasis. Journal of thrombosis and haemostasis : JTH. 2012;10(8):1646-52.

224. Gottfried E, Kunz-Schughart LA, Weber A, Rehli M, Peuker A, Muller A, et al. Expression of CD68 in non-myeloid cell types. Scandinavian journal of immunology. 2008;67(5):453-63.

225. Pamela A. Wilkins, Cynthia M. Otto, James E. Baumgardner, Bettina Dunkel, Daniela Bedenice, et al. Acute lung injury and acute respiratory distress syndromes in veterinary medicine: consensus definitions: The Dorothy Russell Havemeyer Working Group on ALI and ARDS in Veterinary Medicine. Journal of Veterinary Emergency and Critical Care 2007; 17(4):333–339

226. Cohen J. Differences between correlation coefficients. In: Statistical Power Analysis for the Behavioral Sciences. 2nd ed. Mahwah, New Jersey: Lawrence Erlbaum, 1988:109–139

227. MendaneS, Ahmet T, Yüksel A, Sait B, Necmettin K, Kemal D. Acute pancreatitis possibly due to arginine use: A case report. Turk J Gastroenterology 2004; 15(1): 56-58